CO_2 STORAGE CO_2 ATLAS IN COLOMBIA

ANH
AGENCIA NACIONAL DE HIDROCARBUROS

Uptc
Universidad Pedagógica y Tecnológica de Colombia

CO_2 STORAGE ATLAS IN COLOMBIA

ANH
AGENCIA NACIONAL DE HIDROCARBUROS

Uptc®
Universidad Pedagógica y Tecnológica de Colombia

National Hydrocarbons Agency

Orlando Velandia Sepúlveda
President

María Cecilia Ruiz Cardona
Technical Vice President

Carlos Ernesto García Ruiz
Technical Vice-Presidency expert

Pedagogical and Technological University of Colombia
Sogamoso Branch Faculty

Héctor Antonio Fonseca
Dean

Project supervisors:
Oscar García Cabrejo
Luis David Mesa

Director of Subproject 4:
Dr. Gilles Levresse

Teamwork:
Augusto Díaz, Carlos Alberto Tavera, Carolina Sánchez Ruiz, Carlos Perea, César Augusto Duarte Prada, Cristian Manrique, Daniel Rojas, Diana Carolina Pérez, Elizabeth Novoa, Germán Reyes, Jairo Osorio, Katherine León Palma, Libardo Murillo Vallejo, Luis Naranjo, Miguel Farfán Silva, Nelson Pesca, Sindy Judith Parada, William Gómez, Yarithza Quimbayo.

Art direction and design:
Ana Berrio

Senior designer:
Felipe Cortazar

Text style correction:
Alexandra Cano

Photograph:
Jaír Ramírez Cadena

First Edition, December 2024

TABLE OF CONTENTS

1. INTRODUCTION

1. INTRODUCTION

The greenhouse effect is a natural process fundamental to life on Earth, as it regulates the planet's temperature and keeps it within a habitable range. Greenhouse Gases (GHGs), including water vapor (H_2O), carbon dioxide (CO_2), methane (CH_4), nitrogen oxides (NOx), ozone (O_2), and chlorofluorocarbons (CFCs), allow shortwave solar radiation to enter but absorb and re-emit longwave infrared radiation emitted by the Earth's surface, hindering its total escape into outer space. While this process is essential to maintaining a suitable global temperature, the excessive accumulation of GHGs in the atmosphere, mainly due to anthropogenic activities, disrupts the planet's energy balance.

It is estimated that anthropogenic CO_2 emissions, from the onset of the industrial era (circa 1850) to 2022, reached approximately 2,255 ± 205 Gt, significantly contributing to increased atmospheric concentration levels. In 2023, the annual average atmospheric CO_2 concentration reached 419.3 ppm, approximately 50% higher than the pre-industrial period (NOAA, 2024). This increase, driven mainly by fossil fuel combustion and deforestation, accelerates global climate change.

Among the ten companies emitting the most CO_2 in Colombia, eight belong to the hydrocarbons sector, and two are international coal mining companies. This highlights the crucial role that fossil fuel and electric power sectors play in economic and social growth, making fossil fuels indispensable until viable and adequate alternative energy sources are available. Climate change, exacerbated by GHG emissions such as CO_2, represents one of the most urgent and complex challenges of the 21st century.

The National Development Plan 2022–2026, under the slogan "Colombia, World Power of Life," prioritizes transforming Colombia into a global leader in sustainability and environmental protection. Aligned with this ambition, the Colombia 2050 Strategy proposes an integrated approach to decarbonizing the economy and promoting long-term sustainable development.

Under this governmental framework, sustainable development and climate change mitigation become top priorities. Colombia, with its rich biodiversity and abundant geological resources, is strategically positioned to lead innovative initiatives in clean energy and environmental management. To develop this potential, implementing an atlas identifying major GHG emission sources and areas with the highest CO_2 storage capacity is essential. This will enable the application of the most suitable technologies and strategies to meet the country's energy and environmental needs.

This initiative is not only essential for mitigating climate change but also for optimizing the use of Colombia's geological resources. Among the strategies for controlling atmospheric CO_2, Carbon Capture, Utilization, and Storage (CCUS) stands out as one of the most economically viable alternatives for industrial-scale removal of atmospheric CO_2 and emissions from concentrated industrial sources, permanently storing it in large-capacity geological reservoirs.

Globally, the implementation of CCUS projects is still in its initial stages, with an installed capacity of 40 Mt annually as of 2021 and a projected increase to 800 Mt by 2050 to meet the targets of the 2015 Paris Agreement. By 2022, there are 27 large-scale CCUS projects in operation, four under construction, and 102 in development, with capacities ranging between 0.1 and 7 Mt of CO_2 per year (GSSI, 2021; Statista, 2022).

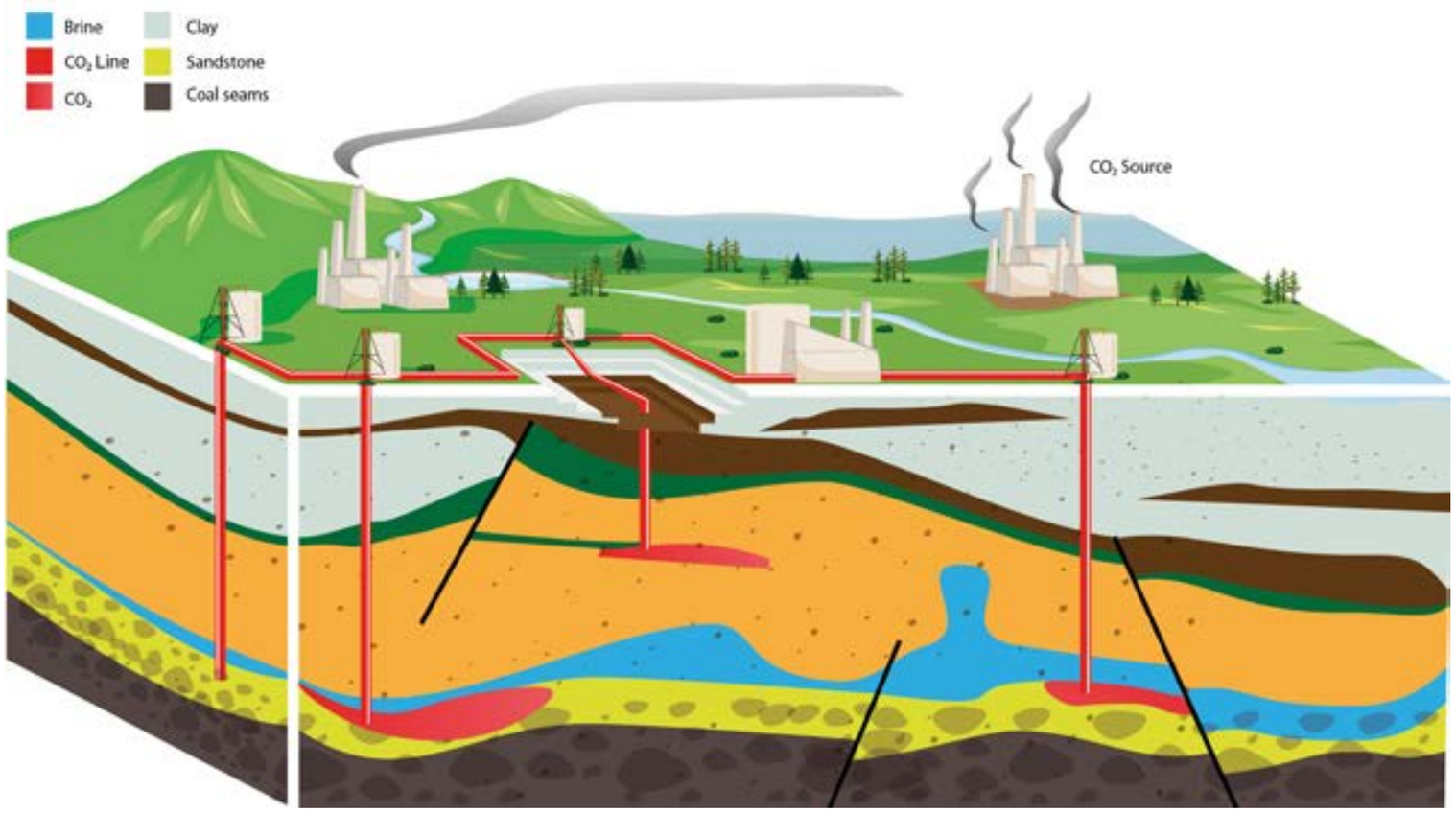

Figure 1. CO_2 Capture, Transport, Utilization, and Storage Technology. Adapted from Bundesanstalt für Geowissenschaften und Rohstoffe website.

This progressive advancement positions CCUS as an essential tool in global efforts to mitigate climate change and transition toward a low-carbon economy. This scenario represents a valuable opportunity for countries like Colombia to boost industrial development, strengthen their economies, and contribute to meeting global climate goals by leveraging the potential of their extensive sedimentary basins.

This document analyzes the identification of volumes and emission sources, as well as emitting activity sectors, at the global, national, and departmental levels in Colombia. Its objective is to assess the country's emissions in comparison with other territories and determine strategic areas for CO_2 capture and future storage. Additionally, it aims to maximize the efficiency in utilizing the country's geological resources, fostering leadership in innovative initiatives related to climate management.

2. OBJECTIVE AND METHODOLOGY

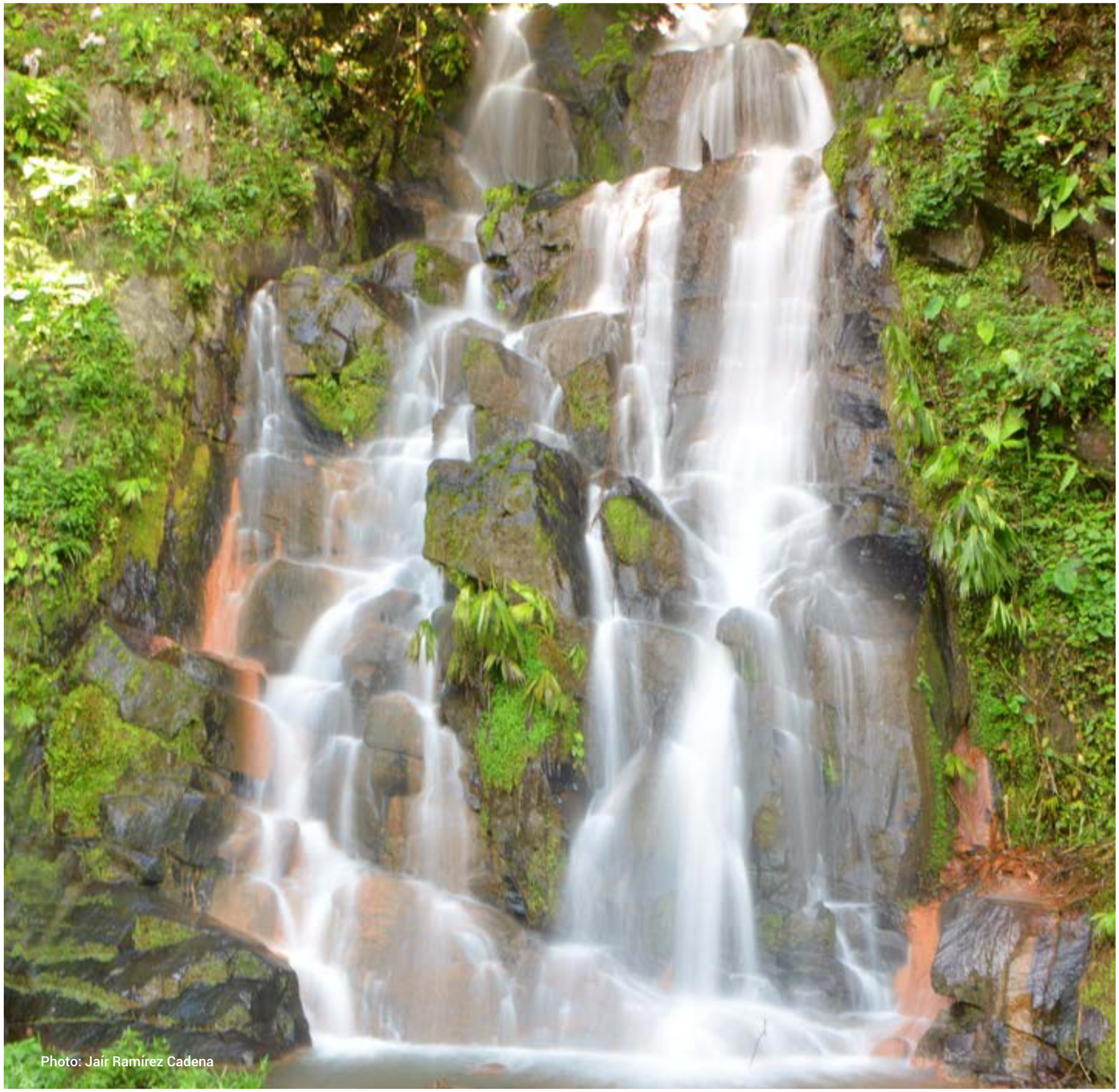

Photo: Jaír Ramírez Cadena

Objective

To develop an atlas that reflects the current state of geological CO_2 storage in Colombia, including the identification of capture points, transportation networks, and storage locations. This atlas will provide a comprehensive database to facilitate the analysis of global and national trends in CO_2 emissions, enabling the evaluation of carbon emission, capture, utilization, and storage potential. In doing so, it will support the formulation of effective strategies for mitigating climate change

The methodological approach focuses on two main aspects:

1.Identification and analysis of relevant and reliable information sources at both national and international levels.

2.Application of specific national and international regulatory criteria for evaluating the various processes associated with Carbon Capture, Transport, and Storage (CCS).

This evaluation not only allows for the collection of data regarding existing and potential infrastructure but also enables a critical analysis of the national regulatory landscape. The integrated information is presented in a unified database, linked to a geographic information system (Annex-1_P1 and Annex-2_P2).

The GDB information model has been structured according to the guidelines established in Annex 4 of the EPIS, ensuring that the thematic data integrated at various stages of the subproject are adequately represented. All referenced information is cited throughout the text and presented in the bibliography section.

The aforementioned annexes, along with the Geological Database (GDB) and other technical information, are available as part of Subproject 4, developed under the framework of inter-administrative contract 419 of 2024, signed between UPTC and ANH.

The cartographic representation of the Atlas uses reference systems based on geographic coordinates with the Magna-SIRGAS datum, as well as planar coordinates with the Magna-SIRGAS National Origin datum.

3.THEORETICAL FRAMEWORK

3.1 CO_2 Capture methods

During the combustion of fossil fuels such as coal, natural gas, or oil, gases composed of a mixture of CO_2, water vapor, oxygen, and other contaminants are generated. These gases must be treated to reduce their environmental impact. CO_2 capture processes can be carried out using four main methods: (1) post-combustion capture, (2) pre-combustion capture, (3) oxy-combustion capture, and (4) direct air capture.

Post-combustion capture uses chemical solvents, with amines being the most common. Amines are organic compounds that chemically react with CO_2 in a process known as absorption. Once the CO_2 is absorbed, the saturated solvent is sent to a regenerator, where it is heated to release the CO_2 from the solvent. The captured CO_2 may require additional purification to remove impurities before transportation.

Pre-combustion capture involves converting fossil fuels into synthesis gas, allowing CO_2 to be separated before combustion. This process is primarily used in power plants and industrial processes that utilize fossil fuels. In this method, the fuel is transformed into syngas, a mixture of hydrogen (H_2) and carbon monoxide (CO), at high temperatures and pressures using a gasifying agent, such as water vapor or carbon dioxide.

Oxy-combustion is an innovative approach to CO_2 capture that employs pure oxygen instead of air, resulting in more efficient combustion. This process primarily produces CO_2 and water vapor (H_2O), with a significant reduction in other pollutants such as nitrogen oxides (NOx). CO_2 capture is simplified as it does not need to be separated from large volumes of other gases. Its high concentration in exhaust gases enhances the efficiency of chemical absorption or adsorption technologies.

Direct Air Capture (DAC) is an emerging technological solution aimed at removing CO_2 capture is simplified as it does not need to be separated fro directly from the atmosphere.

3.2 CO_2 Transportation methods

CO_2 transportation refers to the process by which captured carbon dioxide is moved from emission points to geological storage sites. This process can be carried out through various transportation modes, such as pipelines, trucks, and ships.

The choice of transport mode depends on factors such as the volume of CO_2 to be transported, the distance to be covered, and the geographical conditions of the terrain.

To optimize efficiency and facilitate handling, CO_2 is typically transported in a supercritical state, which increases its density and reduces the required transport volumes.

3.3 CO_2 Storage methods

The primary method of CO_2 storage is injection into geological formations. The goal is to ensure that the injected CO_2 remains securely stored in reservoirs over geological timescales (millions of years) (Bachu, S., 2000).

These formations must meet specific criteria to guarantee the safety and effectiveness of the injection and storage processes (EPRI, 2021; Liu, 2016):

- Reservoir formations must have sufficient porosity to allow CO_2 to be stored within the void spaces between rock particles. This ensures that a significant amount of CO_2 can be injected and stored.
- There must be an effective seal. These sealing layers act as barriers, ensuring that the CO_2 remains confined within the geological reservoir.
- The formations must be sufficiently permeable to allow efficient CO_2 injection while also being capable of retaining the CO_2 once injected.
- The rock chemistry should promote CO_2 mineralization.
- The formations must be geologically stable and not subject to significant seismic activity that could compromise storage integrity.

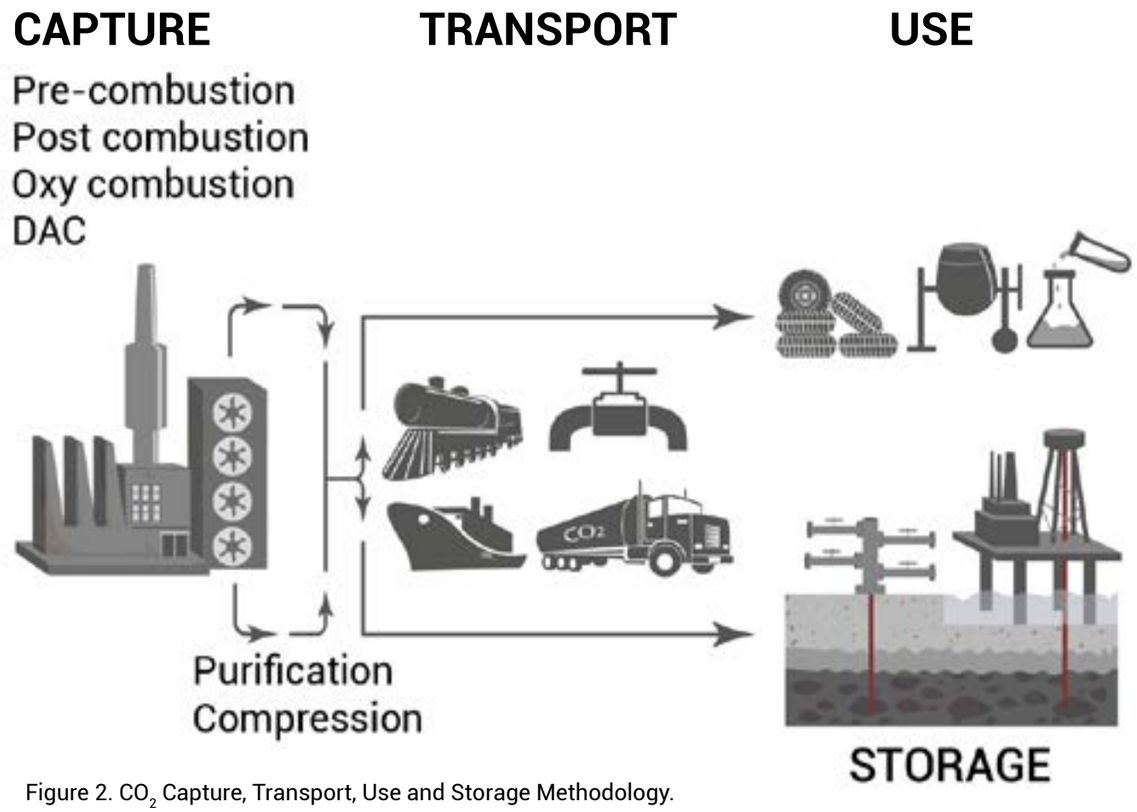

Figure 2. CO_2 Capture, Transport, Use and Storage Methodology.

4. GLOBAL GHG AND CO_2

This chapter explores the major CO_2 storage projects worldwide and the available information on them. Through this review, the goal is to provide a clear overview of the current state of CO_2 storage. Carbon Capture, Utilization, and Storage (CCUS) encompasses technologies that capture CO_2 from industrial sources, transport it, and either store or use it to reduce greenhouse gas (GHG) emissions. Carbon Capture and Storage (CCS), a subset of CCUS, focuses exclusively on capturing and storing CO_2 without its utilization.

Globally, CO_2 capture and storage (CCS) projects have experienced significant growth over the past decade, with more than 30 operational initiatives and several others in development, primarily in North America and Europe. These projects have a combined storage capacity exceeding hundreds of millions of tons of CO_2 annually, making a substantial contribution to reducing industrial and energy-related emissions. However, CO_2 capture still accounts for only a small fraction of global emissions, highlighting the need for broader implementation.

Key challenges include high implementation costs, social acceptance, and the absence of a uniform international regulatory framework. Nonetheless, opportunities lie in investment in research, supportive policies, and integration with renewable energy, which could amplify the impact of these technologies in combating climate change.

The International Energy Agency (IEA) reports that, as of 2024, there are 844 CCS projects at various stages of development (Figure 2; Annex 1): 744 in planning, 44 under construction, 51 in operation, and 5 suspended. These projects are distributed across several countries, with the United States leading with 293 projects, followed by the United Kingdom (92), Canada (74), Australia (33), France (26), and the Netherlands (24).

Of the 51 operational projects, 20 are located in the United States. Regarding the 744 projects in the planning phase, 260 are expected to be developed in the United States; of the 44 under construction, 9 are in the United States; and of the 5 suspended projects, 4 were canceled in the United States. In the United Kingdom, none of the projects are operational; all remain in the planning phase.

4.1 Historical development of CO_2

The injection of CO_2 into oil fields to support or enhance production, known as Enhanced Oil Recovery (EOR), has been conducted in the United States since the 1960s. Chevron pioneered the first large-scale industrial project in 1972 at the Scurry Field in Texas.

The injected CO_2 was sourced from natural CO_2reservoirs in Colorado and transported over 300 km through pipelines. Between 1972 and 2009, an estimated 175 million tons of CO_2 were produced, transported, and injected in the U.S.

From the mid-1990s to the early 2000s, two significant saline aquifer injection projects were launched: the Sleipner Project in the North Sea, Norway, and the Weyburn Project in Saskatchewan, Canada. Both initiatives are scientific projects led by international consortia under the IEA's GHG R&D Programme.

In Europe, the Sleipner Project is operated by the Norwegian oil company Equinor, with support from the Norwegian Government. Since 1995, over 25 million tons of CO_2have been injected into a deep saline aquifer, providing extensive monitoring experience (Torp and Gale, 2003).

The Weyburn Project, on the other hand, is a land-based initiative that has injected more than 35 million tons of CO_2 since 2000. The project is managed by a consortium involving Natural Resources Canada, the U.S. Department of Energy, and several companies.

These projects have demonstrated the technical feasibility of CO_2 storage in saline aquifers. In 2020, the Global CCS Institute established that the minimum storage volume required for a viable industrial project is between 0.8 and 1 million tons of CO_2 per year.

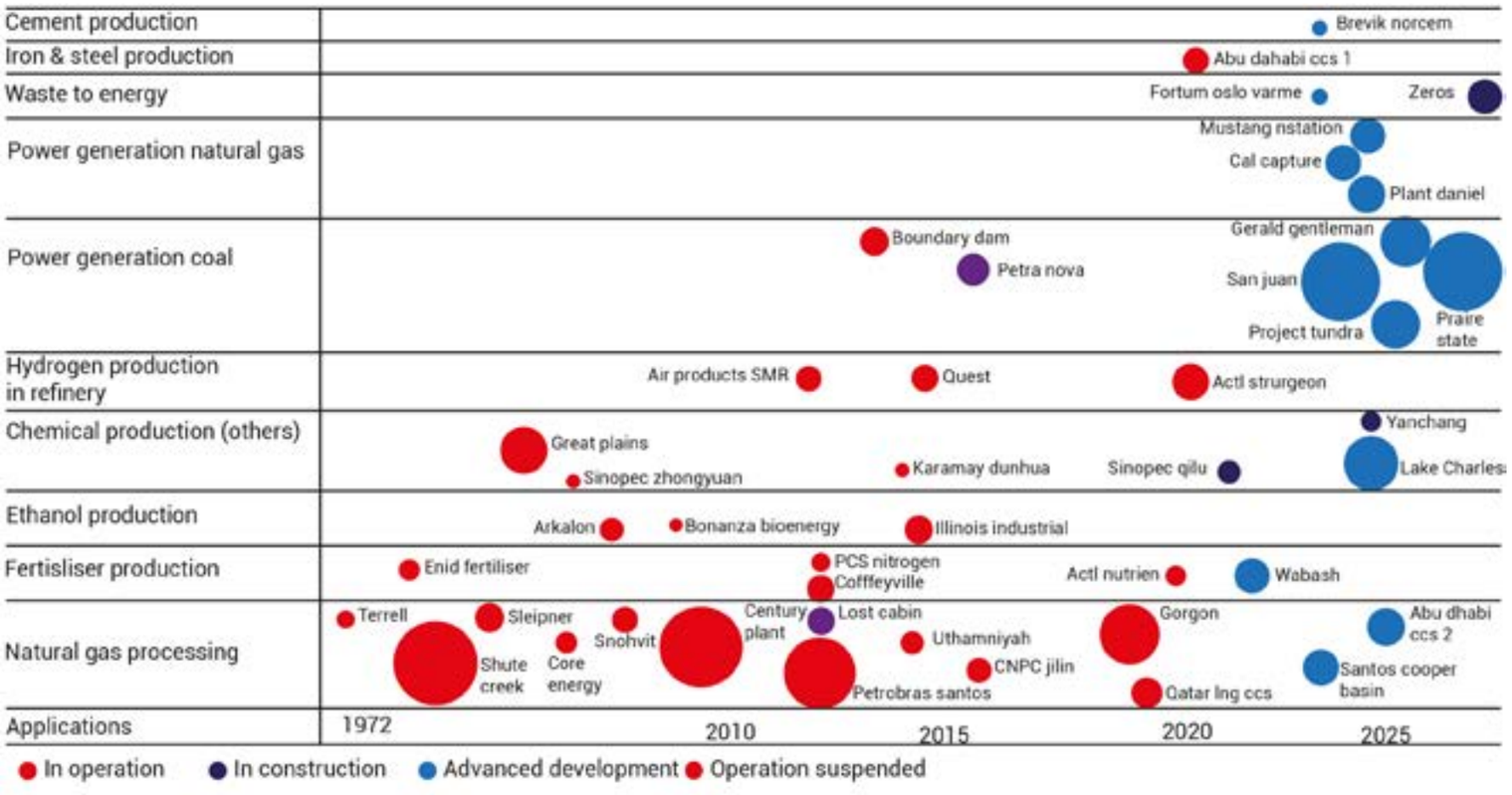

Figure 3. Historical Evolution of Ccs Projects Worldwide. Modified From CO_2 Database, Global Carbon Ccs Institute, 2021.

4.1.1 Global CO_2 emissions map

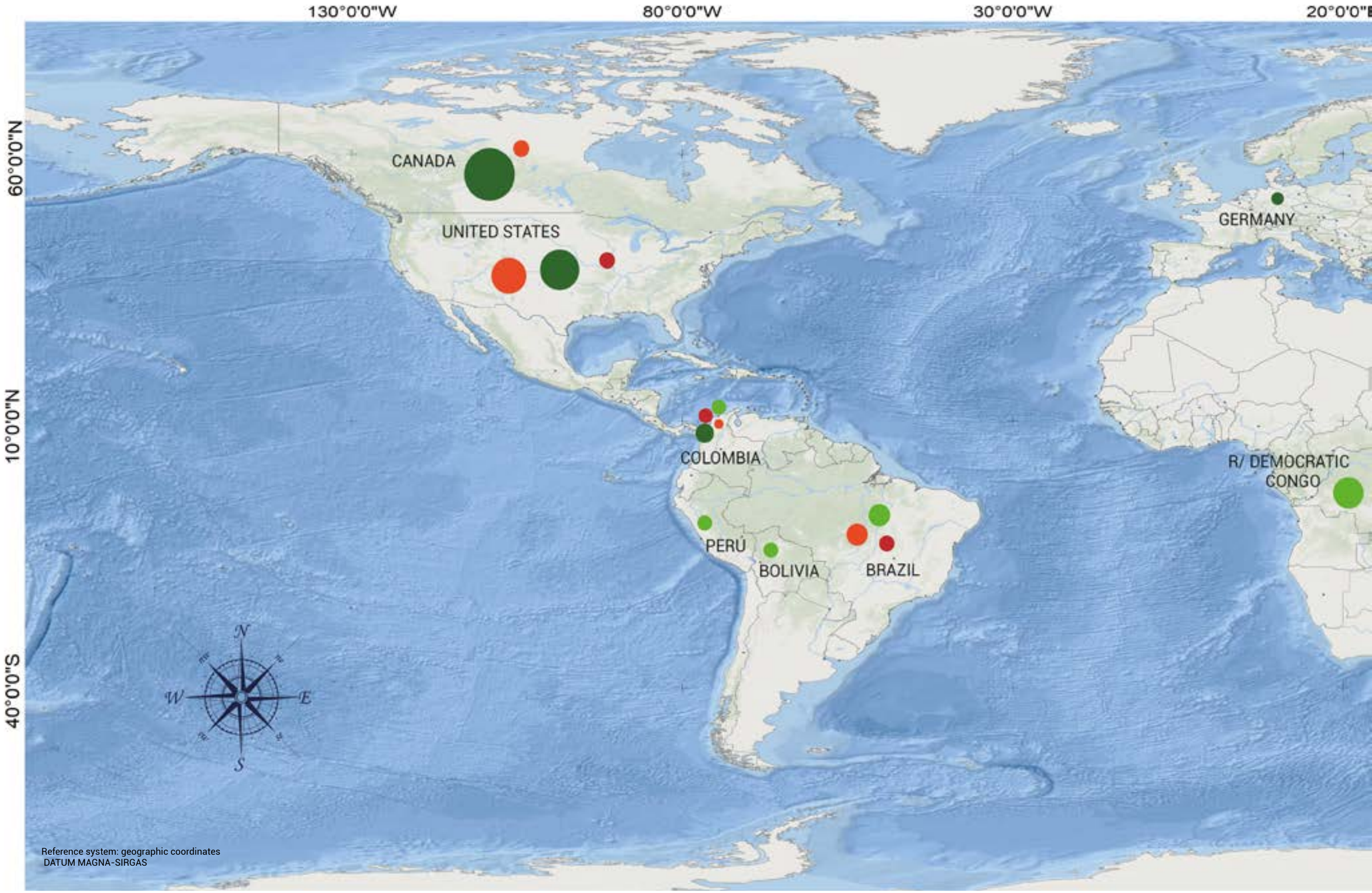

Figure 4. Map of CO_2 emissions worldwide.

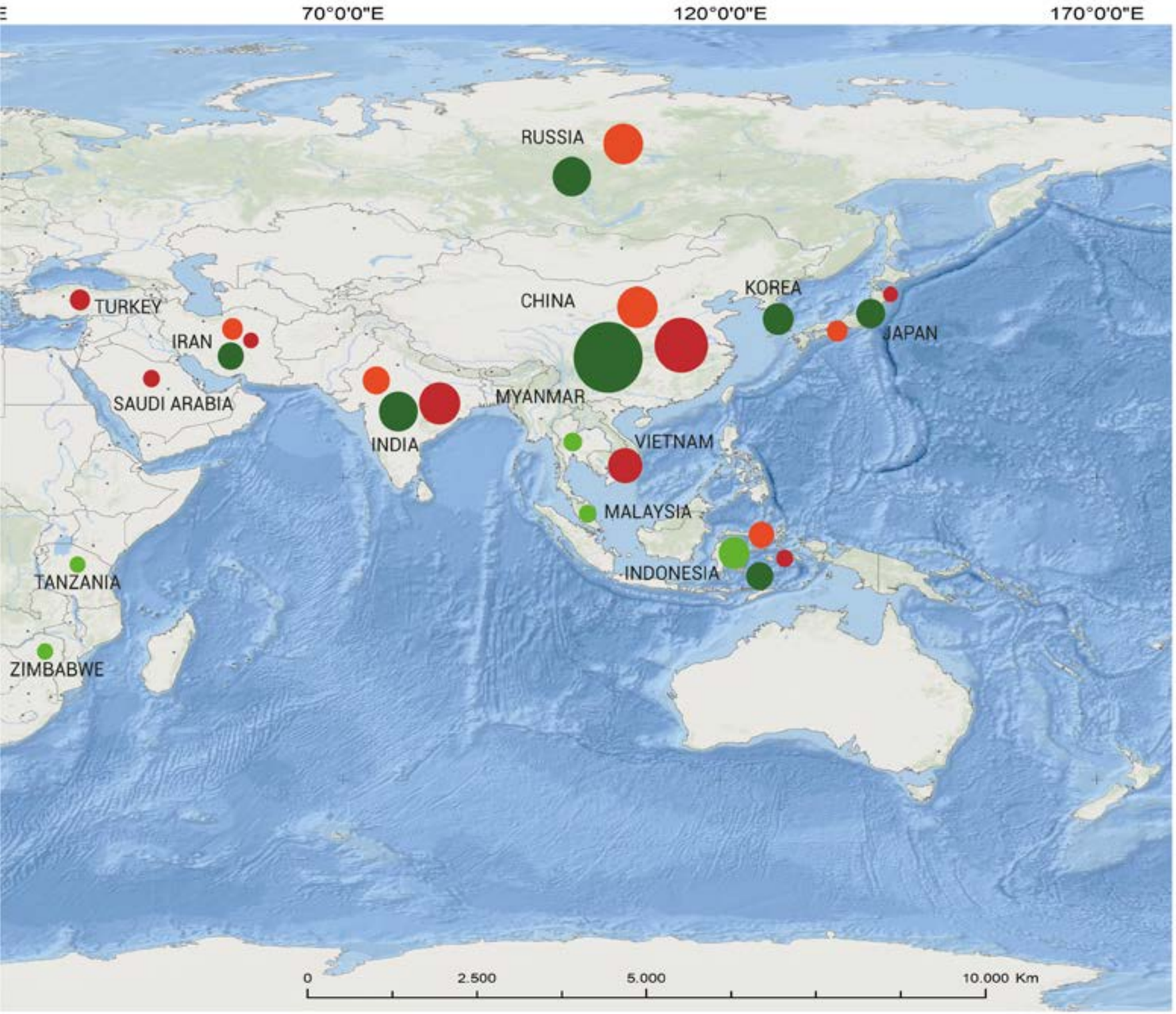

CO_2 Emissions - Land Use and Forestry Changes, 2021

COUNTRY	EMITTED GAS	EMISSIONS MT CO_2 eq
COLOMBIA	GHG	82,88
R/ DEMOCRATIC CONGO	GHG	601,25
INDONESIA	GHG	473,38
BRAZIL	GHG	384,47
MYANMAR	GHG	99,23
PERU	GHG	89,75
ZIMBABWE	GHG	87,16
BOLIVIA	GHG	67,38
MALAYSIA	GHG	66,72
TANZANIA	GHG	63,66

CO_2 GHG Emissions - TRANSPORT 2021

COUNTRY	EMITTED GAS	EMISSIONS MT CO_2 eq
COLOMBIA	GHG	34,57
UNITED STATES	GHG	1.663,66
CHINA	GHG	969,45
INDIA	GHG	295,09
RUSSIA	GHG	253,53
BRAZIL	GHG	209,17
JAPAN	GHG	183,24
CANADA	GHG	156,93
GERMANY	GHG	147,24
INDONESIA	GHG	135,67
IRAN	GHG	134,16

GHG Emissions (IEA) Energy Sector 2022

COUNTRY	EMITTED GAS	EMISSIONS MT CO_2 eq
COLOMBIA	GHG	94,78
CHINA	GHG	11.378,4
UNITED STATES	GHG	5.102,2
INDIA	GHG	2.748,1
RUSSIA	GHG	2.117,3
JAPAN	GHG	985,6
IRAN	GHG	879,9
INDONESIA	GHG	740,2
GERMANY	GHG	624,4
CANADA	GHG	599,1
KOREA	GHG	556,3

CO_2 Emissions - Industrial Processes, 2021

COUNTRY	EMITTED GAS	EMISSIONS MT CO_2 eq
COLOMBIA	GHG	5,07
CHINA	GHG	843,8
INDIA	GHG	149,0
VIETNAM	GHG	52,07
TURKEY	GHG	44,23
UNITED STATES	GHG	41,31
IRAN	GHG	37,42
SAUDI ARABIA	GHG	28,60
INDONESIA	GHG	27,26
BRAZIL	GHG	24,49
JAPAN	GHG	24,4

Figure 5. Infographic of Global CO_2 Emissions Data. Adapted from CO_2 Database, Global. Carbon CCs Institute, 2021.

4.2 CO_2 Worldwide

4.2.1 Carbon storage in the Ocean

Oceanic CO_2 storage involves capturing atmospheric carbon dioxide and injecting it into deep ocean waters or storing it as mineral deposits on the seabed.

Oceans are natural CO_2 sinks, capable of absorbing atmospheric carbon dioxide through natural exchanges between the atmosphere and ocean surface until equilibrium is reached. This process occurs via two mechanisms: physical and biological.

The physical mechanism is driven by the solubility of CO_2 in water. Atmospheric CO_2 naturally dissolves in the ocean, with dissolution enhanced at lower temperatures. Since cold water is denser, it sinks, carrying the dissolved CO_2 to deeper layers. The biological mechanism involves photosynthesis performed by phytoplankton. As a result of these processes, oceans have absorbed approximately 500 of the 1,300 Gt of CO_2 released into the atmosphere from human activities over the past 200 years (do Rosario Vaz Morgado & Pecanha Esteves, 2013).

It is estimated that oceanic processes absorb approximately 7 Gt of CO_2 annually. Most of this CO_2 remains in the ocean's surface layer, where increased acidity has led to a pH reduction of 0.1 (Orr, 2010). However, no significant changes in acidity have been observed in the deeper ocean layers.

Based on these processes, two primary methodologies for oceanic carbon storage have emerged: direct injection into ocean depths and fertilization with iron oxide (FeO) to stimulate phytoplankton growth and enhance photosynthetic CO_2 fixation.

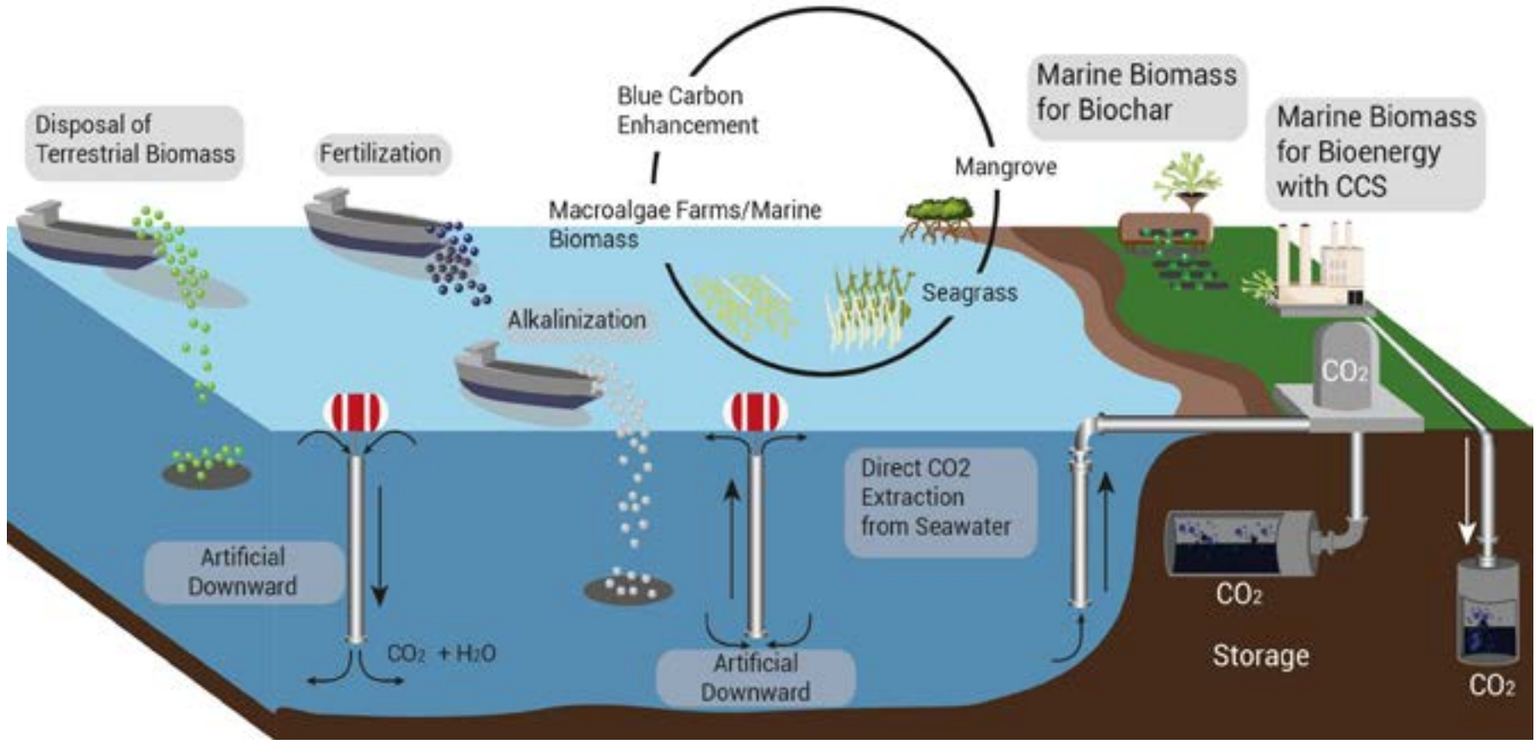

Figure 6. CO_2 Storage Processes in the Ocean. Adapted from de Pryck and Boettcher, 2024.

Direct injection of CO_2

Captured CO_2 could be injected into deep ocean waters, where it would remain isolated from the atmosphere for centuries. This process involves transporting CO_2 to storage sites via pipelines or ships and injecting it into the water column or seabed. Once dissolved and dispersed, it integrates into the global carbon cycle. Potential storage options include forming solid CO_2 hydrates or liquid CO_2 lakes on the seabed. Variations in pH caused by such injections could be counteracted by the dissolution of calcareous and carbonate sediments. However, challenges such as industrial complexity, high costs, physicochemical control mechanisms, and uncertainty over storage duration (ranging from years to centuries) make this option highly demanding.

Biological pump concept

The "biological pump" process has gained attention for its role in oceanic carbon storage. Phytoplankton, the base of the marine food chain, is central to this process. Organic material sinks, sequestering CO_2 and preventing its atmospheric exchange on timescales ranging from months to millennia, depending on where respiration occurs within the water column. Since photosynthesis requires light, phytoplankton grows only in the sunlit surface layer of the ocean, typically to depths of 100 meters. While most of the CO_2 absorbed by phytoplankton is recycled near the surface, a significant fraction (around 30%) sinks to deeper waters before being reconverted into CO_2 by marine bacteria. Only about 0.1% of the absorbed CO_2 reaches the ocean floor to be buried in sediments.

Martin and Fitzwater demonstrated that phytoplankton growth is limited by iron rather than macronutrients. Studies suggest that dispersing iron into oceans—known as "ocean fertilization"—could effectively stimulate CO_2 removal from the atmosphere (Boyd et al., 2007; Yoon et al., 2018).

4.2.2 CO_2 Storage in porous media

The physical properties of geological reservoirs, such as storage capacity, confinement, injectivity, and accessibility, are directly influenced by the characteristics of porous media. These include porosity, permeability, relative permeability, capillarity, pressure, adsorption, wettability, and others.

Geological CO_2 queda confinado físicamente bajo capas de roca imperme storage operates through one or more trapping mechanisms, including structural, solubility, mineral, and adsorption trapping.

- **Structural or stratigraphic trapping**

This occurs when CO_2 is physically confined beneath impermeable rock layers acting as barriers, preventing its migration to the surface.

- **Solubility trapping**

In this mechanism, CO_2 dissolves into the formation fluid, such as brine, and migrates along with it. Over time, dissolved CO_2 can chemically react with minerals in the formation, leading to the creation of solid carbonate compounds in a process known as mineral trapping.

- **Mineral trapping**

This involves chemical reactions between injected CO_2, formation fluids, and the rock matrix, resulting in the precipitation of stable minerals, predominantly carbonates. This is considered the safest storage method, as it immobilizes CO_2 permanently, significantly reducing the risk of atmospheric release.

- **Adsorption trapping**

CO_2 is adsorbed onto surfaces of coal or organic-rich shales, replacing naturally occurring methane. The displaced methane can then be harvested as an energy source in a process known as enhanced coalbed methane recovery.

Each mechanism contributes to the stabilization and long-term storage of CO_2 in the subsurface. The effectiveness and predominance of a particular mechanism depend on the geological properties of the storage site, as well as factors like temperature and pressure.

Solubility trapping in brine

When CO_2 dissolves in formation brine, the solution's density increases by about 1% compared to the original brine. Over time, this density change can induce convective mixing processes, driving the saturated brine downward and away from the free-phase CO_2. This movement allows unsaturated brine to contact the free-phase CO_2, enhancing further dissolution of the gas into the formation fluid (Ennis-King & Paterson, 2001). Convection significantly improves solubility trapping, enabling broader CO_2 distribution within the reservoir and increasing long-term storage potential.

Mineral trapping

This process depends on the availability of metal cations such as calcium, iron, and magnesium, which are required for carbonate formation, and on the rates of geochemical reactions influenced by site-specific temperature, pressure, and salinity conditions. Mineral trapping gains importance over the long term, with timescales ranging from decades to millennia (IPCC, 2005). While the general interaction processes are well understood, uncertainties remain regarding the effects of complex mineralogy and mixing conditions within reservoirs.

Adsorption trapping in coal beds and organic-rich shales

Coal beds exhibit a strong affinity for CO_2, allowing it to displace methane naturally present in the coal and adhere to the coal's surface. This methane can be captured and used as an energy source through enhanced coalbed methane recovery. In deep saline aquifers, adsorption occurs on seal rocks, such as organic-rich shales, where CO_2 adheres to the organic material, providing an additional barrier that limits its migration.

Figure 7. Example of a 3D Model of Porosity in a Geological Sample Defined by Microtomography. Adapted from Denbury Resources Inc. 2024.

4.2.3 Enhanced Oil Recovery (EOR)

In the oil industry, it is estimated that only 30% to 35% of the oil in a reservoir can be recovered using conventional production methods, which include primary and secondary recovery:

- Primary Recovery: Utilizes the natural pressure of the reservoir to push oil to the surface.

- Secondary Recovery: Involves injecting water or gas to maintain reservoir pressure and facilitate extraction (NPC, 2007).

EOR encompasses advanced techniques to access the remaining crude oil after conventional methods. These techniques employ external energy or materials to maximize extraction. The main types of EOR are:

Thermal methods

- Include steam injection, hot water injection, or in-situ combustion.
- Aim to reduce oil viscosity, facilitating its flow to production wells.

Non-thermal methods

- Chemical Injection: Involves surfactants (reducing surface tension between water and oil), polymers (improving injection water mobility and sweep efficiency), and alkalis.

- Miscible Gas Injection: Uses gases like CO_2, which, when mixed with oil, reduce its viscosity, enhance its expandability, and optimize recovery.

Advanced Oil Recovery broadens the spectrum of techniques by combining conventional methods with more complex engineering strategies. These include:

- Using horizontal or multilateral wells to maximize contact with the reservoir.
- Polymer injection for better fluid mobility control.
- Advanced reservoir management, involving detailed characterization, continuous monitoring, and optimized strategies to enhance process efficiency.

CO_2 Storage and EOR

Storage CO_2 in depleted oil reservoirs is preferred over other storage methods due to its economic benefits, particularly in the context of EOR. This approach combines CO_2storage with increased oil production, offering an economically attractive and environmentally significant solution.

Depleted oil and gas reservoirs have favorable geological characteristics for CO_2 storage, as they have proven capable of securely containing hydrocarbons over geological timescales. These formations, often composed of sandstones and carbonates, possess suitable porosity and permeability values for efficient storage.

Injected CO_2can be miscible or non-miscible with the oils present, depending on factors such as oil type and system conditions, including pressure and temperature (Solomon, 2006):

- Miscible CO_2: Mixes completely with the oil, reducing its viscosity and enhancing its flow toward production wells.
-
- Non-Miscible CO_2: Acts as a displacement agent, pushing the oil toward production wells.

CO_2-EOR (Enhanced Oil Recovery with CO_2 injection)

This proven technology was developed in the United States during the 1950s, beginning in the Permian Basin and later expanding to other regions. Today, over 136 commercial CO_2-EOR projects are active in the United States, collectively injecting more than 3 billion cubic feet of CO_2 and producing over 300,000 barrels of oil daily (Kuuskraa and Wallace, 2014).

In 2014, approximately 14 million metric tons of industrial CO_2 were stored using CO_2-EOR (Kuuskraa and Wallace, 2014). This method has proven effective and economically viable for carbon storage in the U.S. (Gozalpour et al., 2005).

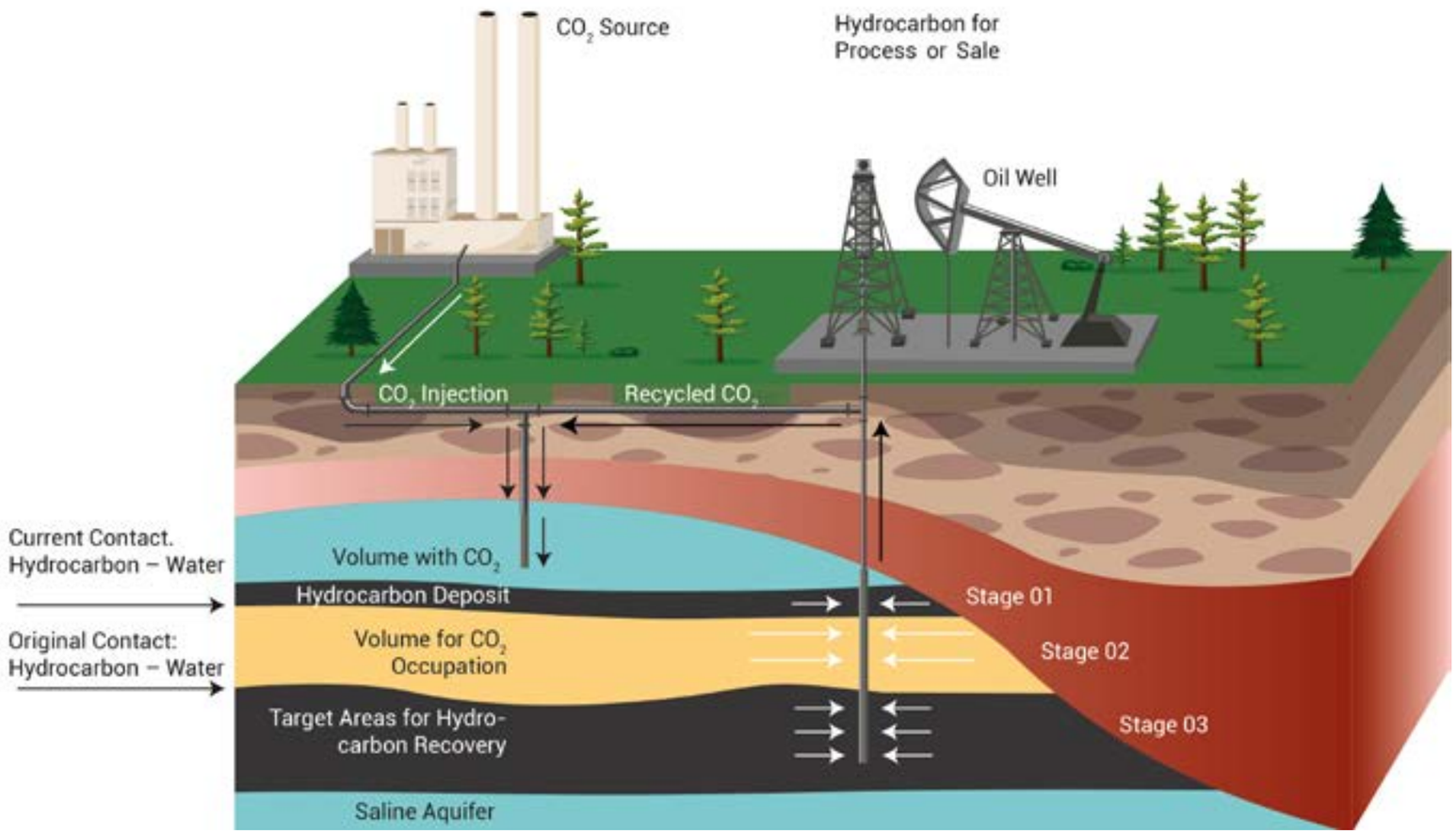

Figure 8. Diagram of the Enhanced Oil Recovery (EOR) Process.

4.2.4 Enhanced Coalbed Methane Recovery (ECBM)

The storage of CO_2 in coal seams is comparable to EOR in terms of objectives and procedures. This method aims to produce methane, known as coalbed methane (CBM) or firedamp, from abandoned or unmineable coal seams. Over the years, several pilot projects have been implemented in countries such as the United States, Canada, Poland, Australia, and Japan. However, none have yet progressed to an industrial phase (Dusar & Verkaeren, 1992).

Coal seams feature highly permeable structures isolated by clay layers, creating an effective seal for storage. Depending on the objective—whether for CO_2 storage and/or methane recovery—and the depth of the seams, CO_2 is injected either in a gaseous or supercritical state.

CO_2 Injection in coal seams

- Flooded areas: CO_2 can be trapped as gas in the porosity, dissolved in formation water, and adsorbed by the coal.
- Non-flooded areas: CO_2 can be injected as pure gas into the coal seams.

The optimal depth range for CO_2 adsorption in coal seams is between 700 and 1,300 meters (Welkenhuysen et al., 2011). Other studies suggest that CO_2 storage in abandoned coal mines should be conducted at depths of at least 500 meters. At greater depths, coal seam permeability may decrease significantly, necessitating engineering interventions to initiate and maintain gas injection (Sarhosis et al., 2016).

Storage in flooded areas

The storage process in flooded areas is similar to that in deep saline aquifers. Generally, the available storage volumes are limited, and the connectivity of the porosity is poor. However, coal proves to be an efficient base for CO_2 and CH_4 fixation through adsorption.

One of the primary challenges of this method is the alteration of coal seams upon contact with CO_2. This interaction leads to a reduction in effective permeability, diminishing CH_4 desorption.

Figure 9. 2-meter Thick Coal Seam, Intercalated with Sandstones and Shales (photo: Germán Reyes).

Consequently, this affects injection rates and increases the risk of leaks due to the formation of localized fractures.

Benefits and limitations

Despite these challenges, available experiences show that storage in flooded areas is relatively simple and low-cost. Under these conditions, high permeability favors elevated injection rates, making them reliable temporary reservoirs, as demonstrated by the injection of natural gas in similar settings. However, permanent CO_2 storage still lacks consolidated experience, particularly regarding suitable monitoring processes.

4.2.5 Salt cavern formation

The storage of CO_2 in large artificial or natural cavities, as well as in mines, has been proposed as a less conventional method. A notable example of salt cavern usage is its application for natural gas storage, designed to meet the increased seasonal cyclic demand (Dusseault et al., 2002; Liu et al., 2024).

Approximately 7% of the total underground natural gas storage capacity is located in salt caverns. In the United States, there are 36 such underground natural gas storage facilities. The most prominent example is the Strategic Petroleum Reserve, which uses these caverns to store the nation's crude oil reserves for national emergencies.

Salt caverns have proven to be an effective medium for hydrocarbon storage because salt acts as a natural sealant, efficiently trapping the contents within the cavern.

These formations are created through a leaching process in which hot water is pumped to dissolve the salt. The resulting brine is extracted through a well that is also used for gas injection and withdrawal.

Currently, the feasibility of using salt caverns for CO_2 storage is under evaluation. However, several technical and safety considerations must be addressed, including the structural integrity of the caverns, pressure management, and the potential for leaks.

Additionally, the economic viability and environmental impact of this technology require a thorough analysis before it can be widely implemented as a storage solution.

A key feature of salt is its near "impermeability" to gases and its ability to deform without fracturing, making salt caverns particularly well-suited for underground storage. Their walls exhibit high resistance to degradation caused by pressure variations or interactions with stored gases.

The creation of salt caverns takes place in salt domes located at depths ranging from 1,000 to 2,500 meters below the surface. This process can take several years to form a cylindrical cavity of suitable dimensions.

These caverns can reach up to 100 meters in diameter and 500 meters in height, with a potential storage capacity of approximately 8 million m³ of CO_2 in a supercritical state.

However, leaching to form these caverns is generally more costly than other underground gas storage methods. Additionally, when used for temporary storage, there is a risk of hydrate formation at the water/gas/hydrocarbon interface. Such formations can reduce transmissibility, block pipeline flow, and even cause ruptures over time.

Due to their unique characteristics, salt caverns are often reserved for strategic purposes, such as storing national crude oil reserves for emergencies, rather than being widely considered a permanent solution for CO_2 storage.

Since salt formations are distributed globally—with notable exceptions around the Pacific Ring of Fire—there are opportunities to use this type of storage in various locations. However, implementing such solutions requires addressing the aforementioned considerations regarding appropriate uses and potential technical challenges.

The technology for CO_2 storage in salt caverns is not considered a permanent storage solution. Although these caverns are already widely used for the seasonal storage of hydrocarbons, this usage directly competes for available space.

Additionally, salt caverns have size limitations compared to other geological storage options, such as depleted oil and gas reservoirs or deep saline aquifers.

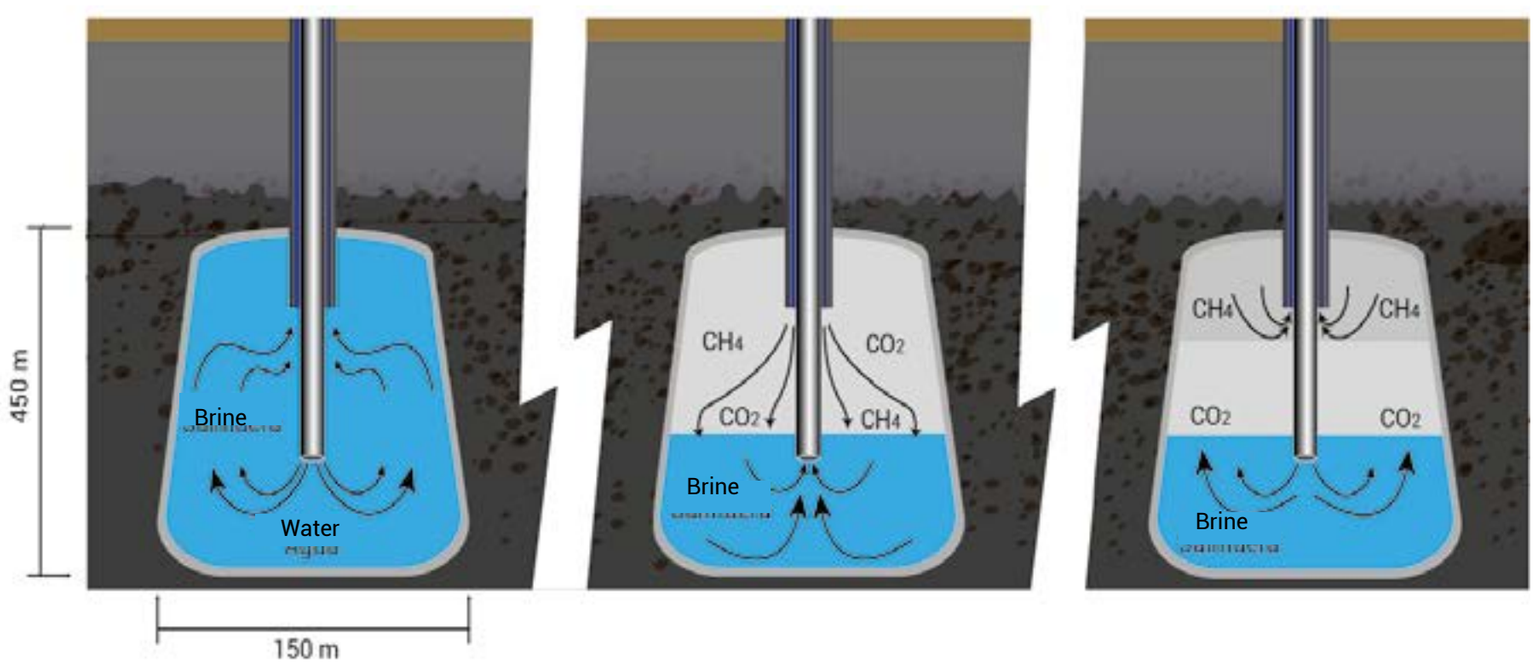

Figure 10. CO_2 Creation and Filling Process in Salt Caverns. Adapted from Research Center for Gas Innovation, 2020.

4.2.6 CO_2 Storage in deep saline aquifers

The storage of CO_2 in deep saline aquifers is one of the most utilized options in industrial projects due to its significant storage capacity compared to oil fields. These aquifers offer considerably greater potential and are not dependent on fluctuations in CO_2 demand by oil companies, which could be influenced by changes in international oil prices.

Furthermore, saline aquifer storage projects typically have a lower net cost of carbon emission reductions compared to EOR. An additional advantage is that they do not require capturing extremely high concentrations of CO_2, simplifying the process and making it more accessible. For these reasons, CO_2 storage in saline aquifers has become one of the main directions for developing CCUS (Carbon Capture, Utilization, and Storage) technologies.

Deep saline aquifers located in sedimentary basins have been the focus of extensive research as part of global efforts to develop economic decarbonization pathways. Currently, there are 65 geological CO_2 storage projects worldwide, 26 of which are operational and collectively store 40 million tons of CO_2 annually.

From a technical perspective, geological storage in saline aquifers is performed by directly injecting CO_2 gas into layers of permeable rocks containing saline fluids in their pore spaces. These formations must be located at depths greater than potable aquifers. Additionally, the salinity of the water must exceed 10,000 ppm, rendering it unsuitable for technical or economic exploitation, including agricultural and industrial uses.

Saline formations located in sedimentary basins worldwide represent one of the most promising options for anthropogenic CO_2 storage. This is due to their large porous volume and wide geographic distribution, making them more likely to be located near significant CO_2 emission sources. However, unlike hydrocarbon reservoirs or freshwater aquifers, these formations have not been studied in the same level of detail. As a result, storage capacity estimates are associated with significant uncertainties, and site selection heavily depends on the available knowledge.

Rocks with the best properties for fluid storage, such as CO_2, are sandstones and limestones due to their high porosity and permeability. However, to ensure safe and long-term storage, the presence of an impermeable overlying layer acting as a barrier is essential to prevent the vertical migration of CO_2.

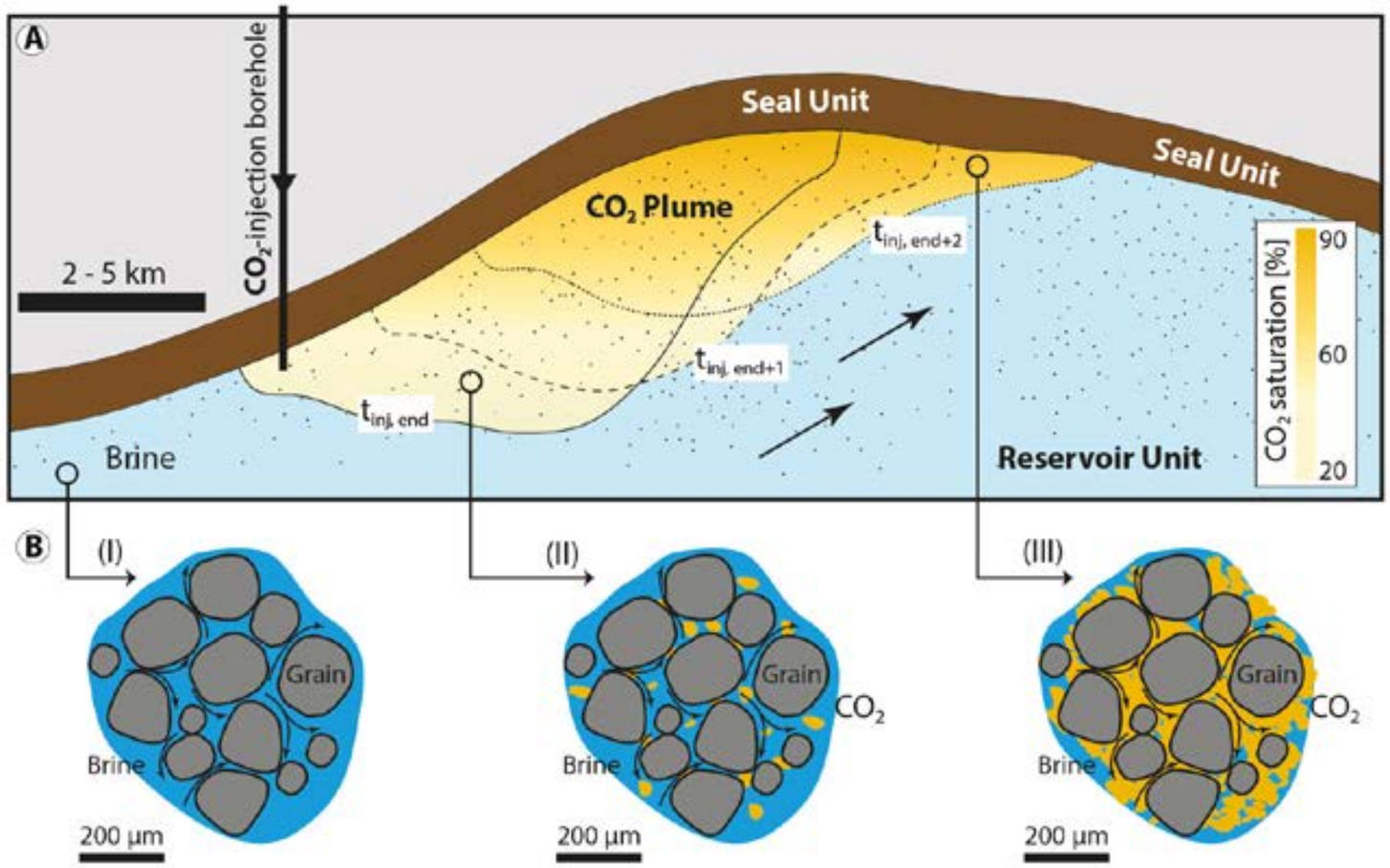

Figure 11. Schematic Diagram of CO2 Storage Processes in Deep Saline Aquifers (Hefny et al., 2020).

When CO_2 is injected into these formations, its higher buoyancy compared to the fluids present in the reservoir causes it to rise to the upper part. The existence of a caprock, typically composed of shales with low permeability, is critical for preventing this vertical migration and ensuring long-term storage safety. This structural trapping mechanism is considered the primary factor for the effective containment of CO_2 in deep saline formations.

For practical and economic reasons, it is recommended to inject CO_2 in a supercritical state, allowing a larger volume to be stored in a smaller space. This state is achieved when CO_2 is at pressures above 7.38 MPa and temperatures exceeding 31.1°C, conditions typically reached at depths of approximately 800 meters in basins with a low geothermal gradient (25°C/km).

In its 2005 report, the IPCC suggested a technical depth limit of 2,500 meters. Beyond this depth, there would be no significant increase in CO_2 density but a notable rise in operational costs, making deeper depths economically inadvisable.

For the storage process to be economically viable, it is estimated that the reservoir must have a minimum capacity of 1 million m³ of CO_2. The mechanisms involved in storage include CO_2 dissolution in water, carbonate precipitation (water/rock interaction), and CO_2 buoyancy at the top of the reservoir.

4.2.7 CO_2 Storage in geothermal reservoirs

CO_2 storage in geothermal reservoirs combines carbon capture with geothermal energy exploitation, offering an integrated solution that fulfills two primary functions:

1. Heat extraction for energy production

In this process, supercritical CO_2 is used as a working fluid in Enhanced Geothermal Systems (EGS) due to its advantageous thermophysical properties. CO_2 is injected into hot, dry rock formations where it absorbs geothermal heat. It is then returned to the surface for conversion into electricity. This technique has demonstrated greater efficiency than using water, increasing heat extraction rates in geothermal reservoirs.

2. Geological sequestration

In addition to heat extraction, a portion of the injected CO_2 can remain permanently trapped in the geothermal reservoir. When introduced into these high-temperature formations, it contributes not only to energy generation but also to geological storage.

Recent studies have shown that the use of supercritical CO_2 could enhance energy generation by approximately 50% compared to traditional water-based methods. This increase is attributed to CO_2's properties, including higher mobility and heat transfer capacity. Furthermore, the geothermal system acts as an efficient reservoir, securely retaining the CO_2 and preventing its release into the atmosphere.

Injected CO_2 is effectively confined by caprock and various geochemical processes, preventing atmospheric leakage and ensuring long-term storage. Over time, the CO_2 can also undergo mineralization, transforming into stable carbonate minerals within the reservoir structure.

This process enhances storage security and makes the system doubly beneficial: mitigating greenhouse gas emissions and boosting geothermal energy generation. As such, CO_2 storage in geothermal reservoirs emerges as a promising alternative in the transition to a more sustainable energy future.

However, this approach requires detailed analysis of specific geological conditions, as well as the potential impacts on reservoir geochemistry and permeability. Originally, CO_2usage for geothermal heat extraction was proposed for systems that, while hot, lacked water (vapor) or had insufficient permeability to sustain traditional water-based methods. With the significant thermal resource of deep, hot rocks exhibiting geothermal gradients above 60°C/km, Enhanced Geothermal Systems aim to leverage techniques like artificial stimulation or hydraulic fracturing.

Nevertheless, the implementation of these techniques has raised social concerns due to the potential for induced seismicity, which could limit public acceptance and consequently restrict the expansion of this technology.

Supercritical CO_2 is injected into the reservoir, where it absorbs heat upon contact with geothermal formations. It is then pumped through a production well to expand in a turbine, generating electricity directly, or transferring its heat to a secondary fluid in an indirect system. In indirect systems, various configurations of Organic Rankine Cycles (ORC) have been studied, including subcritical, superheated, and supercritical cycles, offering significant flexibility to optimize energy efficiency. Additionally, these systems can integrate auxiliary heat sources, such as solar energy, enhancing their applicability and contributing to energy diversification.

In both direct and indirect approaches, a pump can be used to supplement the natural thermosiphon effect, ensuring optimal flow rates that maximize system performance.

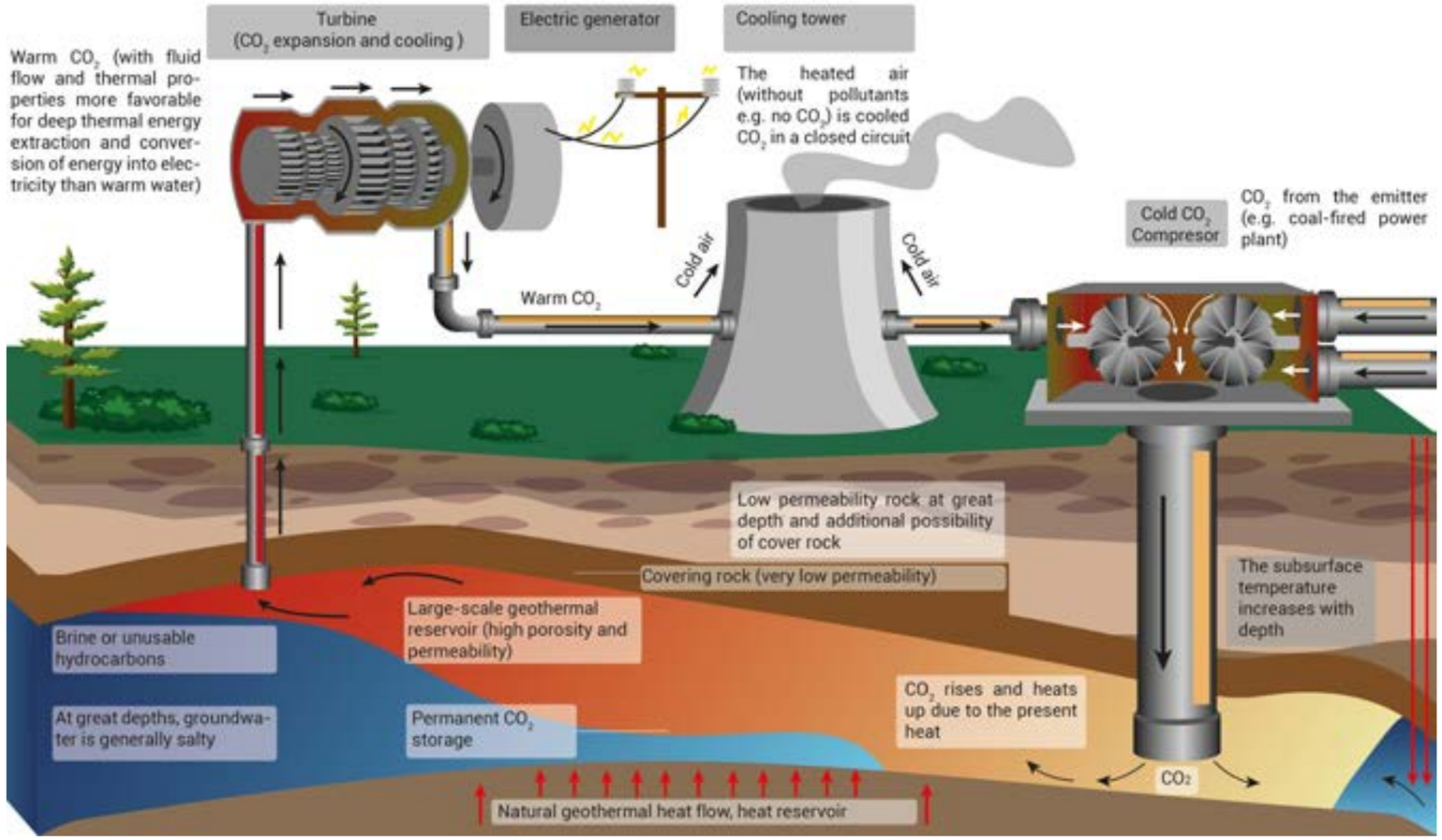

Figure 12. Schematic Diagram of CO_2 Storage Processes in Geothermal Reservoirs. Adapted from Saar et al., CPG Consortium, 2022.

4.2.8 CO_2 storage and mineralization in basalts and serpentinite rocks

There are three notable pilot projects exploring CO_2 injection into basalts: CarbFix in Iceland, Wallula in the United States, and Tomakomai in Japan. The CarbFix and Wallula projects have demonstrated successful results, achieving high percentages of CO_2 fixation and mineralization as well as effective industrial integration. However, the Tomakomai project, while successful in CO_2 injection into sandstone, did not achieve ideal results for basalt storage. This was due to low injectivity and the absence of the high-temperature conditions characteristic of the CarbFix project, resulting in limited mineralization.

Despite the growing interest from countries like India, Australia, Canada, and South Africa in projects such as CarbFix and Wallula, numerous uncertainties persist regarding the feasibility of CO_2 injection and storage in basalt formations. For example, Zakharova et al. noted that basalts in the Newark Basin lack storage potential due to their shallow depth, low temperature, limited permeability, and high likelihood of fault reactivation.

An emerging alternative is the injection of CO_2 into serpentinite rocks, which are widely distributed in oceanic plates. These rocks offer a favorable thermal gradient (70°C and 100 bars) and exhibit faster chemical reactivity than basalts, allowing for higher CO_2 consumption in mineralization reactions. Although offshore injection increases operational costs, it also provides safety advantages, as the ocean acts as a natural dissolution medium in the event of leaks. To reduce uncertainties associated with these methods, the development of CO_2 precipitation plants is proposed. These plants would allow controlled reaction conditions, such as substrate reactivity, pressure, and temperature. Currently, these solutions remain in experimental stages, limited to laboratory research.

The CarbFix pilot project in Iceland is the first fully integrated CCS project globally to store CO_2 in basaltic rocks. This project aims to optimize in situ mineral carbonation in oceanic crust basalt. It encompasses a combined program, including a CO_2 gas separation pilot plant, a pilot injection test, laboratory experiments, studies of natural analogs, and numerical modeling.

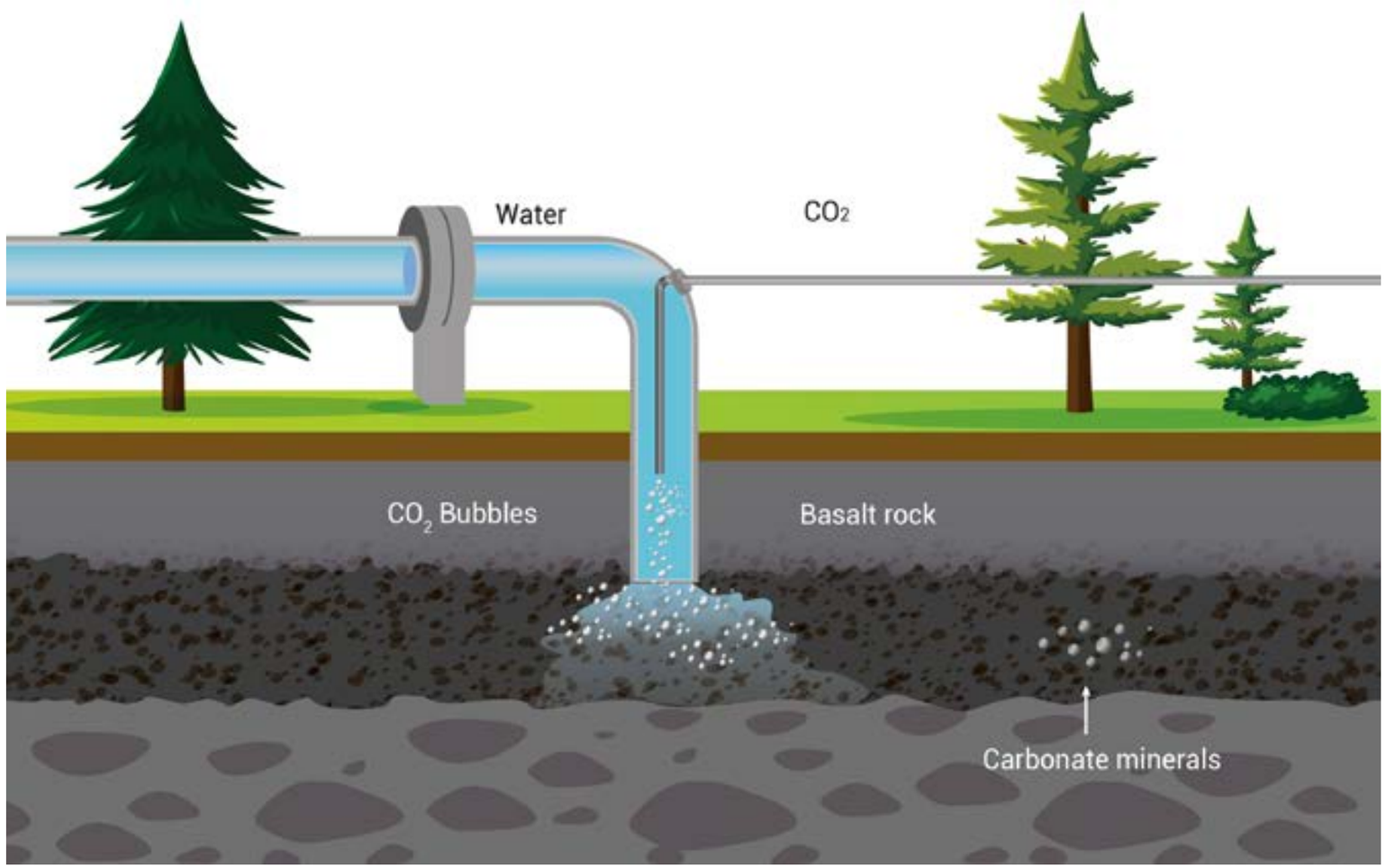

Figure 13. Schematic Diagram of CO_2 Storage Processes in Basalts and Serpentine Rocks. Adapted from Wei et al., 2024.

The main partners in this project are Reykjavik Energy, the University of Iceland, Columbia University in New York, and the Centre National de la Recherche Scientifique/Université Paul Sabatier in France (Matter et al., 2011).

The formation of serpentinite involves the transformation of ultrabasic rocks through processes that incorporate a hydrated phase by interacting with ultramafic rocks. The mineral association and resulting textures from the serpentinization of ultramafic rocks depend on both the original protolith and the system's pressure-temperature regime. Serpentinization is more intense in dunite than in harzburgite and more intense in harzburgite than in lherzolite.

Serpentinites are formed in tectonic contexts associated with ultramafic complexes. Known serpentinites include those related to the fracturing of ocean ridges, where water is introduced into deep zones, as well as serpentinites associated with transform fault systems that also facilitate water infiltration into deep oceanic crust zones, giving rise to so-called ocean-floor serpentinites. Additionally, serpentinization can occur in tectonic settings of subduction and obduction (Barbero, 2012).

5. GHG AND CO_2 IN COLOMBIA

5.1 GHG and CO_2 emissions in Colombia

In Colombia, the national and departmental GHG inventory includes a detailed analysis of emissions from various gases, such as CO_2, CH_2, nitrogen oxides (N_2O), hydrofluorocarbons (HFCs), perfluorocarbons (PFCs), and sulfur hexafluoride (SF_6). These emissions are measured in terms of carbon dioxide equivalent (CO_2eq), estimating their impact using the Global Warming Potential (GWP) specific to each gas. This standardized methodology, established by the 2006 IPCC guidelines, allows for a consistent and comparative evaluation of the impacts of different GHGs on global warming. Conversion to CO_2eq facilitates understanding emissions in terms of their cumulative capacity to contribute to climate change, which is essential for formulating effective mitigation policies and strategies.

According to the 2006 IPCC guidelines, Colombia's national GHG inventory covers four emission modules: IPPU (Industrial Processes and Product Use), AFOLU (Agriculture, Forestry, and Other Land Use), Energy, and Waste. Based on data from the National GHG Inventory, the AFOLU module, which includes agriculture, forestry, and other land uses, accounts for the largest share of emissions at 63.4%. This is followed by the Energy module at 28.4%, the Waste module at 5.3%, and the industry module, contributing the smallest share at 2.9%.

Between 2008 and 2018, the AFOLU module in Colombia recorded an average of 150,086 Kt CO_2eq in emissions.

The lowest emissions were recorded in 2015, with 134,185 Kt CO_2eq, while 2017 saw the highest emissions, reaching 181,323 Kt CO_2eq. This increase aligns with the 2023 IDEAM report, which notes that 2017 registered the highest deforestation rate, with 220,000 hectares cleared, driven primarily by agricultural and livestock expansion (Figure 14).

During the same period, Colombia's Energy module recorded an average emission value of 85,336 Kt CO_2eq. The year with the highest emissions was 2016, at 95,654 Kt CO_2eq, while the lowest emissions were in 2008, at 69,868 Kt CO_2eq.

A progressive increase in emissions between 2008 and 2016 is observed, corresponding to the country's population growth and economic expansion (Figure 14).

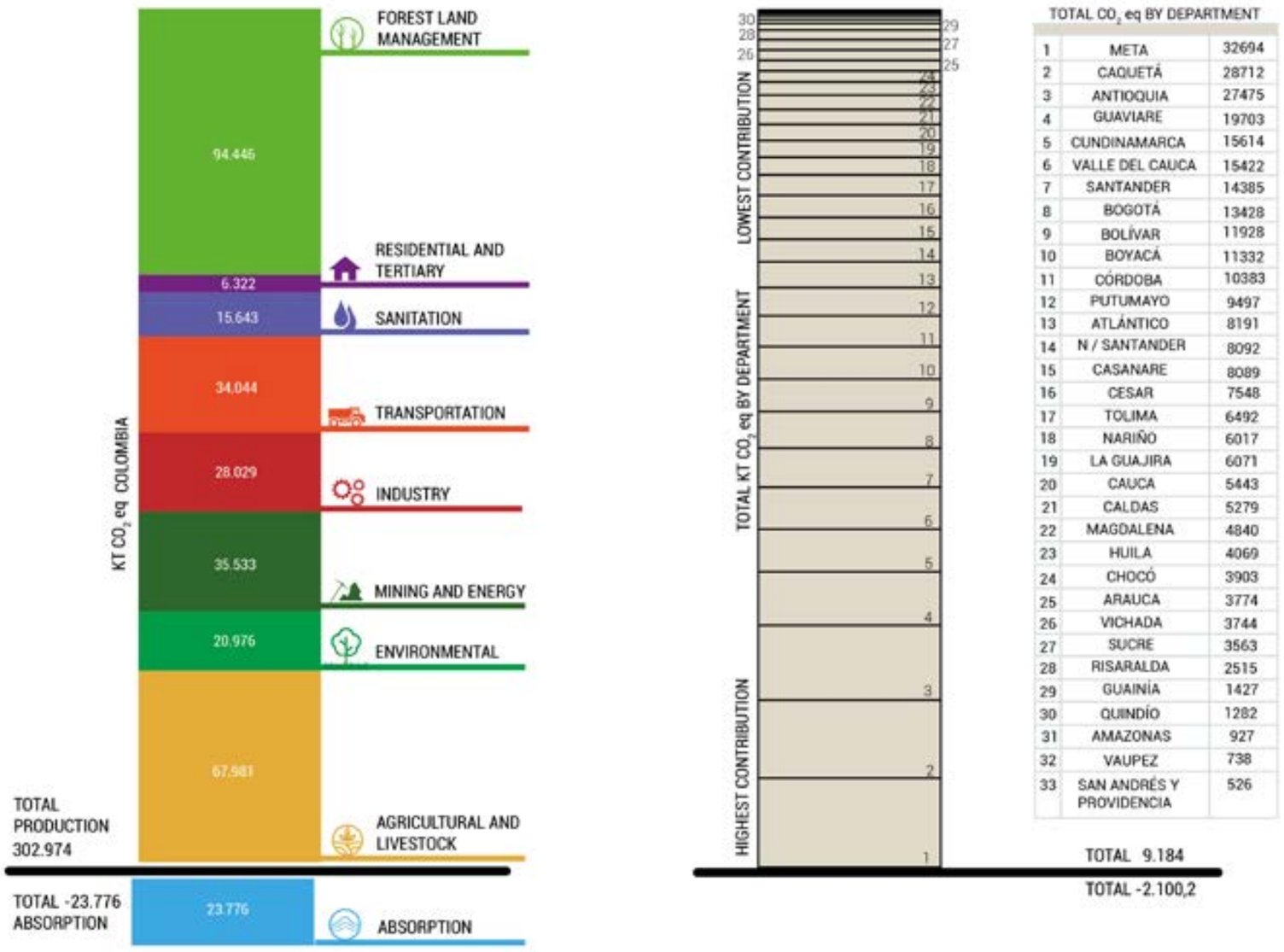

TOTAL CO_2 eq BY DEPARTMENT

1	META	32694
2	CAQUETÁ	28712
3	ANTIOQUIA	27475
4	GUAVIARE	19703
5	CUNDINAMARCA	15614
6	VALLE DEL CAUCA	15422
7	SANTANDER	14385
8	BOGOTÁ	13428
9	BOLÍVAR	11928
10	BOYACÁ	11332
11	CÓRDOBA	10383
12	PUTUMAYO	9497
13	ATLÁNTICO	8191
14	N / SANTANDER	8092
15	CASANARE	8089
16	CESAR	7548
17	TOLIMA	6492
18	NARIÑO	6017
19	LA GUAJIRA	6071
20	CAUCA	5443
21	CALDAS	5279
22	MAGDALENA	4840
23	HUILA	4069
24	CHOCÓ	3903
25	ARAUCA	3774
26	VICHADA	3744
27	SUCRE	3563
28	RISARALDA	2515
29	GUAINÍA	1427
30	QUINDÍO	1282
31	AMAZONAS	927
32	VAUPEZ	738
33	SAN ANDRÉS Y PROVIDENCIA	526

Figure 14. CO_2 Emissions by Sector at the Departmental Level.Inventory (2022).

In the Waste module, the average emissions during the 2008–2018 period were 15,615 Kt CO_2eq, showing an upward trend. The lowest emissions were recorded in 2008, at 15,048 Kt CO_2eq, while the highest values were reached in 2018, at approximately 20,474 Kt CO_2eq. This increase is linked to population and urban growth, which has led to higher waste generation.

For the IPPU module, the average emissions during the same period were 9,009 Kt CO_2eq. The lowest emissions were recorded in 2009, at 7,343 Kt CO_2eq, and the highest in 2018, at approximately 10,495 Kt CO_2eq. This pattern reflects Colombia's economic structure, characterized by a predominance of the agricultural sector and a smaller proportion of emission-intensive industries (Figure 14).

5.2 Emission results in Colombia at the departmental level

At the departmental level, the emissions analysis encompasses activities in the agricultural, environmental, mining and energy, industrial, transportation, housing and sanitation, tertiary residential, and deforestation sectors. According to emission data, the sectors generating the highest emissions are: Agriculture, Transportation and Mining and Energy.

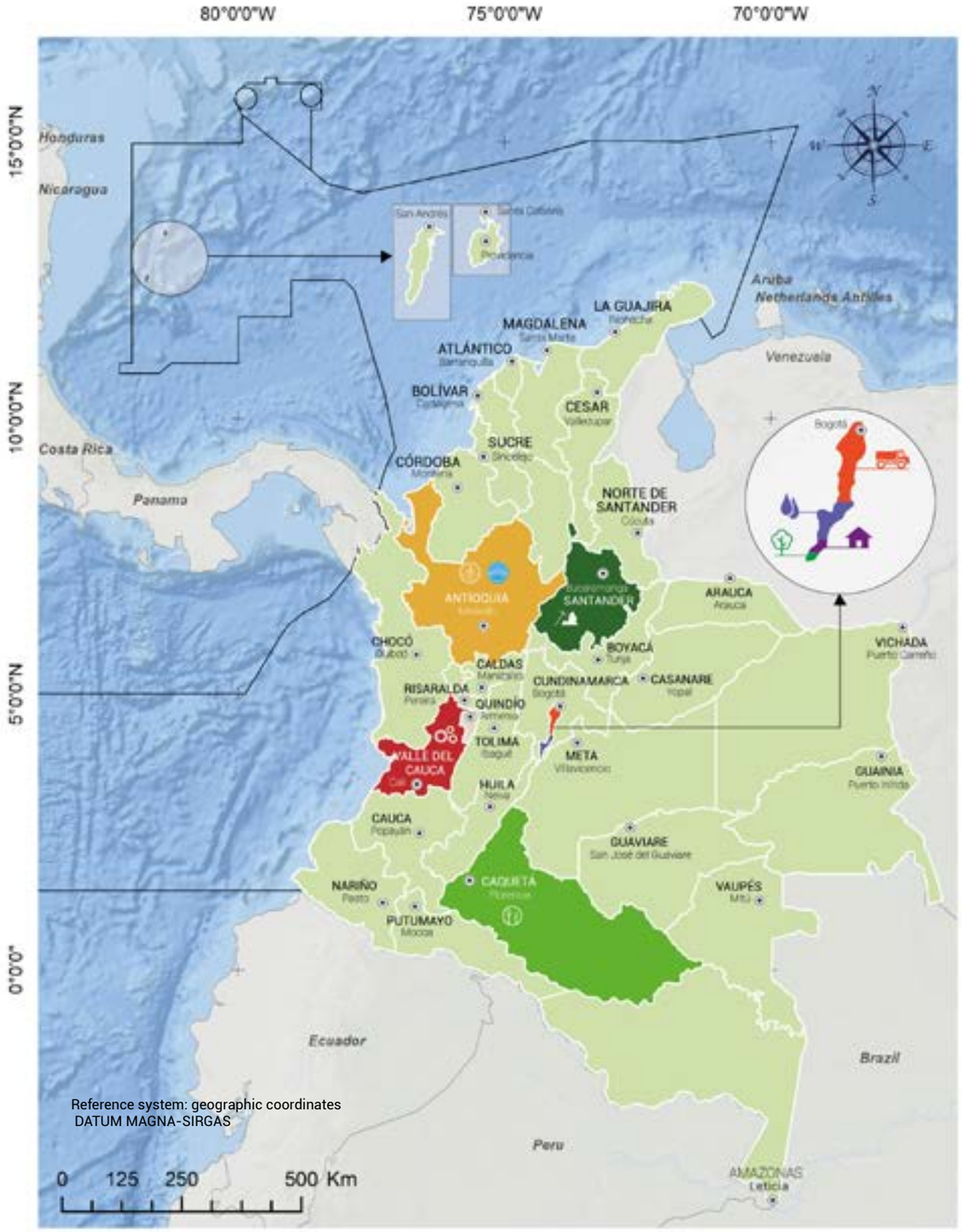

Figure 15. GHG Emissions for Colombia. Note: Adapted from the Departmental Greenhouse Gas Inventory, 2022.

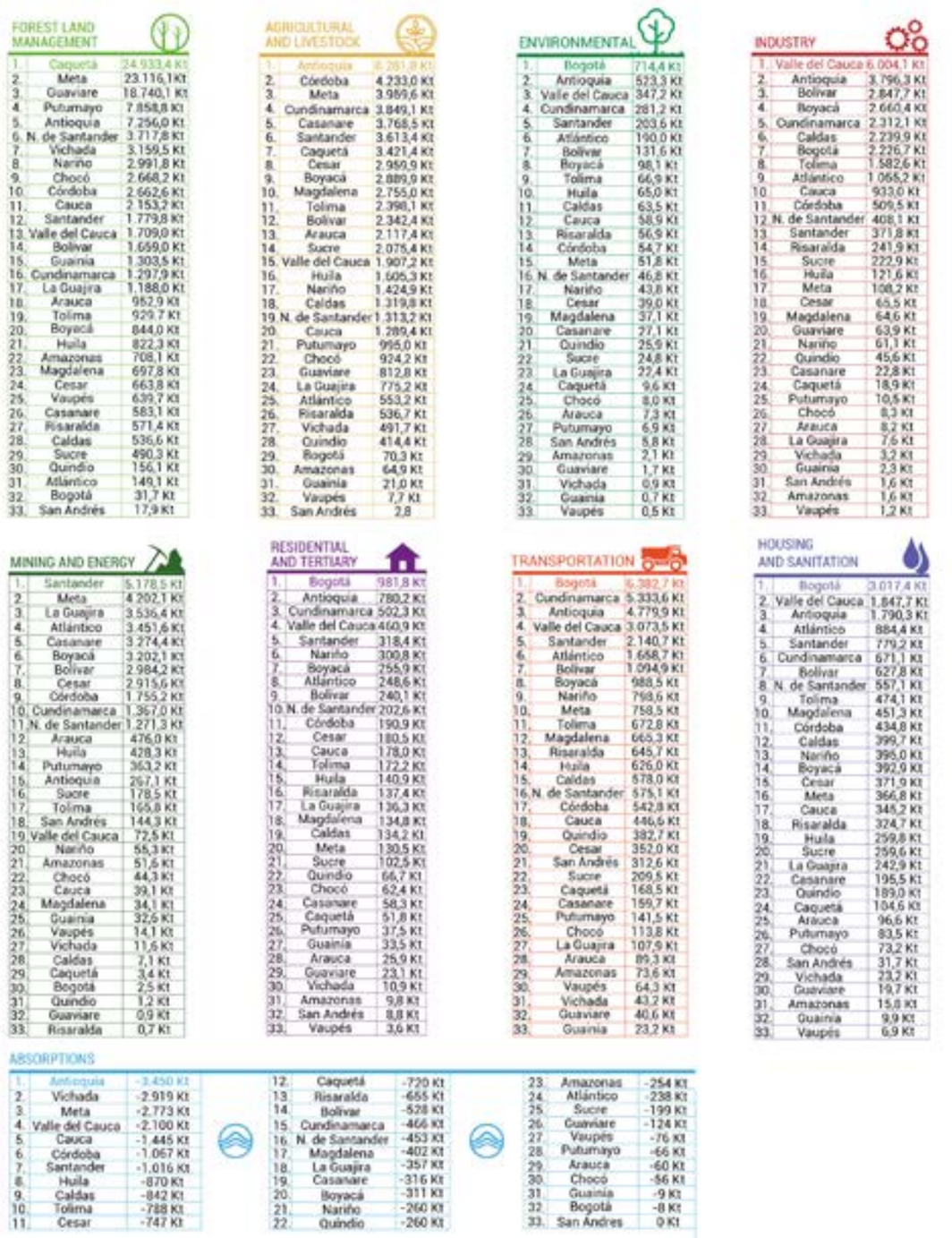

FOREST LAND MANAGEMENT

1.	Caquetá	24.933,4 Kt
2.	Meta	23.116,1 Kt
3.	Guaviare	18.740,1 Kt
4.	Putumayo	7.858,8 Kt
5.	Antioquia	7.256,0 Kt
6.	N. de Santander	3.717,8 Kt
7.	Vichada	3.159,5 Kt
8.	Nariño	2.991,8 Kt
9.	Chocó	2.668,2 Kt
10.	Córdoba	2.662,6 Kt
11.	Cauca	2.153,2 Kt
12.	Santander	1.779,8 Kt
13.	Valle del Cauca	1.709,0 Kt
14.	Bolívar	1.659,0 Kt
15.	Guainía	1.303,5 Kt
16.	Cundinamarca	1.297,9 Kt
17.	La Guajira	1.188,0 Kt
18.	Arauca	952,9 Kt
19.	Tolima	929,7 Kt
20.	Boyacá	844,0 Kt
21.	Huila	822,3 Kt
22.	Amazonas	708,1 Kt
23.	Magdalena	697,8 Kt
24.	Cesar	663,8 Kt
25.	Vaupés	639,7 Kt
26.	Casanare	583,1 Kt
27.	Risaralda	571,4 Kt
28.	Caldas	536,6 Kt
29.	Sucre	490,3 Kt
30.	Quindío	156,1 Kt
31.	Atlántico	149,1 Kt
32.	Bogotá	31,7 Kt
33.	San Andrés	17,9 Kt

AGRICULTURAL AND LIVESTOCK

1.	Antioquia	8.261,8 Kt
2.	Córdoba	4.233,0 Kt
3.	Meta	3.989,6 Kt
4.	Cundinamarca	3.849,1 Kt
5.	Casanare	3.768,5 Kt
6.	Santander	3.613,4 Kt
7.	Caquetá	3.421,4 Kt
8.	Cesar	2.959,9 Kt
9.	Boyacá	2.889,9 Kt
10.	Magdalena	2.755,0 Kt
11.	Tolima	2.398,1 Kt
12.	Bolívar	2.342,4 Kt
13.	Arauca	2.117,4 Kt
14.	Sucre	2.075,4 Kt
15.	Valle del Cauca	1.907,2 Kt
16.	Huila	1.606,3 Kt
17.	Nariño	1.424,9 Kt
18.	Caldas	1.319,8 Kt
19.	N. de Santander	1.313,2 Kt
20.	Cauca	1.289,4 Kt
21.	Putumayo	995,0 Kt
22.	Chocó	924,2 Kt
23.	Guaviare	812,8 Kt
24.	La Guajira	775,2 Kt
25.	Atlántico	553,2 Kt
26.	Risaralda	536,7 Kt
27.	Vichada	491,7 Kt
28.	Quindío	414,4 Kt
29.	Bogotá	70,3 Kt
30.	Amazonas	64,9 Kt
31.	Guainía	21,0 Kt
32.	Vaupés	7,7 Kt
33.	San Andrés	2,8

ENVIRONMENTAL

1.	Bogotá	714,4 Kt
2.	Antioquia	523,3 Kt
3.	Valle del Cauca	347,2 Kt
4.	Cundinamarca	281,2 Kt
5.	Santander	203,6 Kt
6.	Atlántico	190,0 Kt
7.	Bolívar	131,6 Kt
8.	Boyacá	98,1 Kt
9.	Tolima	66,9 Kt
10.	Huila	65,0 Kt
11.	Caldas	63,5 Kt
12.	Cauca	58,9 Kt
13.	Risaralda	56,9 Kt
14.	Córdoba	54,7 Kt
15.	Meta	51,8 Kt
16.	N. de Santander	46,8 Kt
17.	Nariño	43,8 Kt
18.	Cesar	39,0 Kt
19.	Magdalena	37,1 Kt
20.	Casanare	27,1 Kt
21.	Quindío	25,9 Kt
22.	Sucre	24,8 Kt
23.	La Guajira	22,4 Kt
24.	Caquetá	9,6 Kt
25.	Chocó	8,0 Kt
26.	Arauca	7,3 Kt
27.	Putumayo	6,9 Kt
28.	San Andrés	5,8 Kt
29.	Amazonas	2,1 Kt
30.	Guaviare	1,7 Kt
31.	Vichada	0,9 Kt
32.	Guainía	0,7 Kt
33.	Vaupés	0,5 Kt

INDUSTRY

1.	Valle del Cauca	6.004,1 Kt
2.	Antioquia	3.796,3 Kt
3.	Bolívar	2.847,7 Kt
4.	Boyacá	2.660,4 Kt
5.	Cundinamarca	2.312,1 Kt
6.	Caldas	2.239,9 Kt
7.	Bogotá	2.226,7 Kt
8.	Tolima	1.582,6 Kt
9.	Atlántico	1.055,2 Kt
10.	Cauca	933,0 Kt
11.	Córdoba	509,5 Kt
12.	N. de Santander	408,1 Kt
13.	Santander	371,8 Kt
14.	Risaralda	241,9 Kt
15.	Sucre	222,9 Kt
16.	Huila	121,6 Kt
17.	Meta	108,2 Kt
18.	Cesar	65,5 Kt
19.	Magdalena	64,6 Kt
20.	Guaviare	63,9 Kt
21.	Nariño	61,1 Kt
22.	Quindío	45,6 Kt
23.	Casanare	22,8 Kt
24.	Caquetá	18,9 Kt
25.	Putumayo	10,5 Kt
26.	Chocó	8,3 Kt
27.	Arauca	8,2 Kt
28.	La Guajira	7,6 Kt
29.	Vichada	3,2 Kt
30.	Guainía	2,3 Kt
31.	San Andrés	1,6 Kt
32.	Amazonas	1,6 Kt
33.	Vaupés	1,2 Kt

MINING AND ENERGY

1.	Santander	5.178,5 Kt
2.	Meta	4.202,1 Kt
3.	La Guajira	3.536,4 Kt
4.	Atlántico	3.451,6 Kt
5.	Casanare	3.274,4 Kt
6.	Boyacá	3.202,1 Kt
7.	Bolívar	2.984,2 Kt
8.	Cesar	2.915,6 Kt
9.	Córdoba	1.755,2 Kt
10.	Cundinamarca	1.367,0 Kt
11.	N. de Santander	1.271,3 Kt
12.	Arauca	476,0 Kt
13.	Huila	428,3 Kt
14.	Putumayo	363,2 Kt
15.	Antioquia	267,1 Kt
16.	Sucre	178,5 Kt
17.	Tolima	165,8 Kt
18.	San Andrés	144,3 Kt
19.	Valle del Cauca	72,5 Kt
20.	Nariño	55,3 Kt
21.	Amazonas	51,6 Kt
22.	Chocó	44,3 Kt
23.	Cauca	39,1 Kt
24.	Magdalena	34,1 Kt
25.	Guainía	32,6 Kt
26.	Vaupés	14,1 Kt
27.	Vichada	11,6 Kt
28.	Caldas	7,1 Kt
29.	Caquetá	3,4 Kt
30.	Bogotá	2,5 Kt
31.	Quindío	1,2 Kt
32.	Guaviare	0,9 Kt
33.	Risaralda	0,7 Kt

RESIDENTIAL AND TERTIARY

1.	Bogotá	981,8 Kt
2.	Antioquia	780,2 Kt
3.	Cundinamarca	502,3 Kt
4.	Valle del Cauca	460,9 Kt
5.	Santander	318,4 Kt
6.	Nariño	300,8 Kt
7.	Boyacá	255,9 Kt
8.	Atlántico	248,6 Kt
9.	Bolívar	240,1 Kt
10.	N. de Santander	202,6 Kt
11.	Córdoba	190,9 Kt
12.	Cesar	180,5 Kt
13.	Cauca	178,0 Kt
14.	Tolima	172,2 Kt
15.	Huila	140,9 Kt
16.	Risaralda	137,4 Kt
17.	La Guajira	136,3 Kt
18.	Magdalena	134,8 Kt
19.	Caldas	134,2 Kt
20.	Meta	130,5 Kt
21.	Sucre	102,5 Kt
22.	Quindío	66,7 Kt
23.	Chocó	62,4 Kt
24.	Casanare	58,3 Kt
25.	Caquetá	51,8 Kt
26.	Putumayo	37,5 Kt
27.	Guainía	33,5 Kt
28.	Arauca	25,9 Kt
29.	Guaviare	23,1 Kt
30.	Vichada	10,9 Kt
31.	Amazonas	9,8 Kt
32.	San Andrés	8,8 Kt
33.	Vaupés	3,6 Kt

TRANSPORTATION

1.	Bogotá	6.382,7 Kt
2.	Cundinamarca	5.333,6 Kt
3.	Antioquia	4.779,9 Kt
4.	Valle del Cauca	3.073,5 Kt
5.	Santander	2.140,7 Kt
6.	Atlántico	1.658,7 Kt
7.	Bolívar	1.094,9 Kt
8.	Boyacá	988,5 Kt
9.	Nariño	768,6 Kt
10.	Meta	758,5 Kt
11.	Tolima	672,8 Kt
12.	Magdalena	665,3 Kt
13.	Risaralda	645,7 Kt
14.	Huila	626,0 Kt
15.	Caldas	578,0 Kt
16.	N. de Santander	575,1 Kt
17.	Córdoba	542,8 Kt
18.	Cauca	446,6 Kt
19.	Quindío	382,7 Kt
20.	Cesar	352,0 Kt
21.	San Andrés	312,6 Kt
22.	Sucre	209,5 Kt
23.	Caquetá	168,5 Kt
24.	Casanare	159,7 Kt
25.	Putumayo	141,5 Kt
26.	Chocó	113,8 Kt
27.	La Guajira	107,9 Kt
28.	Arauca	89,3 Kt
29.	Amazonas	73,6 Kt
30.	Vaupés	64,3 Kt
31.	Vichada	43,2 Kt
32.	Guaviare	40,6 Kt
33.	Guainía	23,2 Kt

HOUSING AND SANITATION

1.	Bogotá	3.017,4 Kt
2.	Valle del Cauca	1.847,7 Kt
3.	Antioquia	1.790,3 Kt
4.	Atlántico	884,4 Kt
5.	Santander	779,2 Kt
6.	Cundinamarca	671,1 Kt
7.	Bolívar	627,8 Kt
8.	N. de Santander	557,1 Kt
9.	Tolima	474,1 Kt
10.	Magdalena	451,3 Kt
11.	Córdoba	434,8 Kt
12.	Caldas	399,7 Kt
13.	Nariño	395,0 Kt
14.	Boyacá	392,9 Kt
15.	Cesar	371,9 Kt
16.	Meta	366,8 Kt
17.	Cauca	345,2 Kt
18.	Risaralda	324,7 Kt
19.	Huila	259,8 Kt
20.	Sucre	259,6 Kt
21.	La Guajira	242,9 Kt
22.	Casanare	195,5 Kt
23.	Quindío	189,0 Kt
24.	Caquetá	104,6 Kt
25.	Arauca	96,6 Kt
26.	Putumayo	83,5 Kt
27.	Chocó	73,2 Kt
28.	San Andrés	31,7 Kt
29.	Vichada	23,2 Kt
30.	Guaviare	19,7 Kt
31.	Amazonas	15,8 Kt
32.	Guainía	9,9 Kt
33.	Vaupés	6,9 Kt

ABSORPTIONS

1.	Antioquia	-3.450 Kt
2.	Vichada	-2.919 Kt
3.	Meta	-2.773 Kt
4.	Valle del Cauca	-2.100 Kt
5.	Cauca	-1.445 Kt
6.	Córdoba	-1.067 Kt
7.	Santander	-1.016 Kt
8.	Huila	-870 Kt
9.	Caldas	-842 Kt
10.	Tolima	-788 Kt
11.	Cesar	-747 Kt
12.	Caquetá	-720 Kt
13.	Risaralda	-655 Kt
14.	Bolívar	-528 Kt
15.	Cundinamarca	-466 Kt
16.	N. de Santander	-453 Kt
17.	Magdalena	-402 Kt
18.	La Guajira	-357 Kt
19.	Casanare	-316 Kt
20.	Boyacá	-311 Kt
21.	Nariño	-260 Kt
22.	Quindío	-260 Kt
23.	Amazonas	-254 Kt
24.	Atlántico	-238 Kt
25.	Sucre	-199 Kt
26.	Guaviare	-124 Kt
27.	Vaupés	-76 Kt
28.	Putumayo	-66 Kt
29.	Arauca	-60 Kt
30.	Chocó	-56 Kt
31.	Guainía	-9 Kt
32.	Bogotá	-8 Kt
33.	San Andrés	0 Kt

Figure 16. Location of Major GHG Emission Sources at the Local Level in Colombia. Note: Adapted from the Departmental Greenhouse Gas Inventory, 2022.

5.3 Departmental-level emissions analysis

In Colombia, deforestation is a key activity impacting several sectors due to population growth and accelerated economic development. In 2018, deforestation significantly contributed to greenhouse gas emissions, generating approximately 94,446 Kt CO_2eq, according to the National GHG Inventory.

This impact is evident in departmental reports, where deforestation is identified as a major source of CO_2eq emissions, underscoring its importance in the national emissions analysis. The department of Caquetá stands out as the largest emitter of CO_2 among departments, reaching emissions of 28,172 Kt CO_2eq (figure 17).

The transportation sector emerges as one of the primary sources of CO_2 emissions in Colombia, particularly in Bogotá. The heavy reliance on private vehicles and public transportation, coupled with an aging and inefficient vehicle fleet, significantly contributes to pollutant emissions.

Additionally, public transportation infrastructure often fails to meet demand, leading to increased use of private vehicles. Urban and demographic growth further escalate transportation demand, driving emissions higher. Lastly, the effectiveness of environmental policies and regulations varies, impacting emissions management in this sector.

While the industrial sector is not the largest GHG emitter, it represents a significant potential source for CO_2 capture. According to the 2018 departmental inventory, this sector contributed approximately 28,029 Kt CO_2eq. Emissions are mainly associated with the burning of fossil fuels in industrial processes, vehicles, and machinery. The departments with the highest emissions in this sector are Valle del Cauca and Antioquia.

The department of Antioquia reported emissions of up to 27,475 Kt CO_2eq, primarily linked to food processing and industrial activities (Figure 15). The Valle del Cauca reported annual emissions of nearly 15,422 Kt CO_2eq, associated with industrial activities such as sugar mills, as well as manufacturing, textile, and food processing industries (Figure 15).

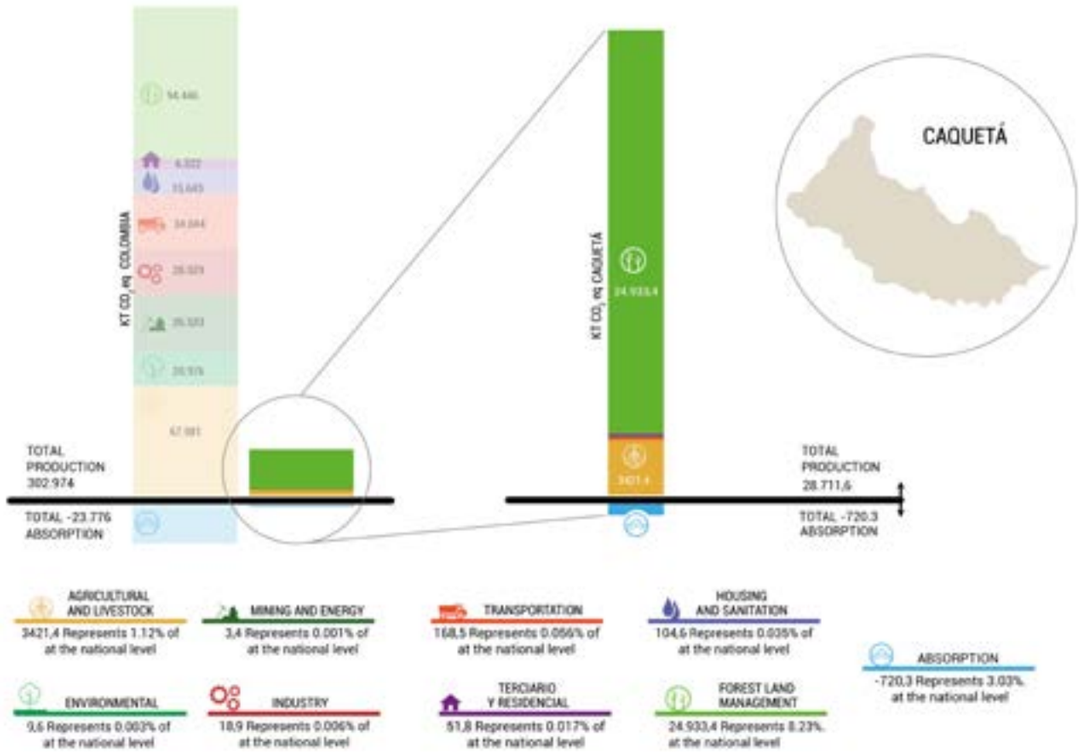

Figure 17. Evaluation of GHG Emissions for the Department of Caquetá.

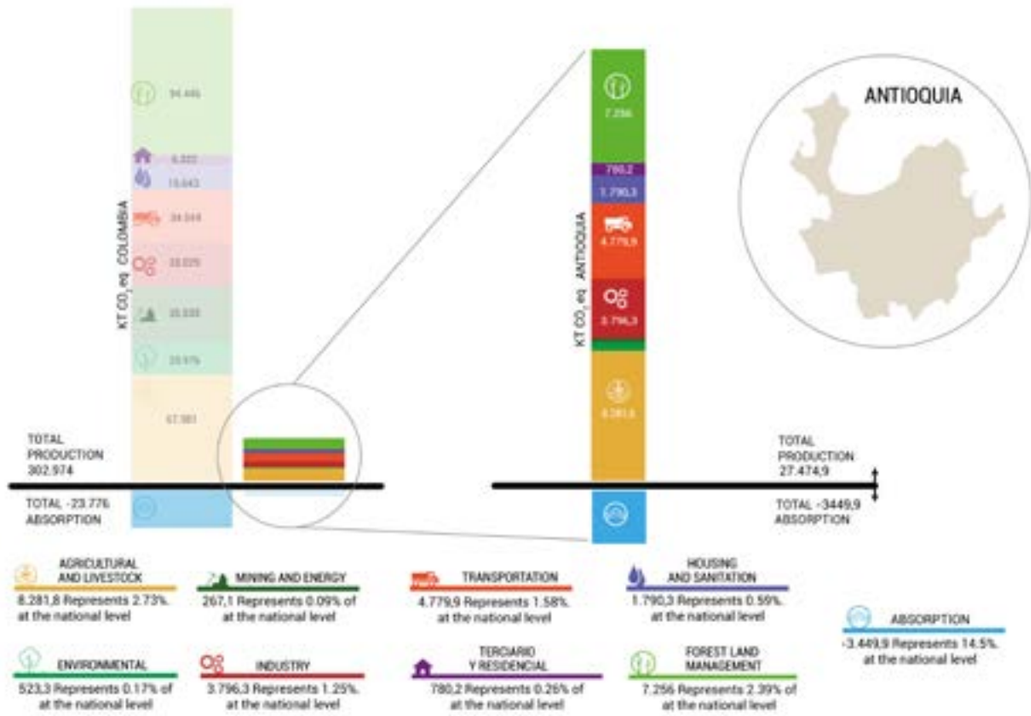

Figure 18. Evaluation of GHG Emissions for the Department of Antioquia.

5. GHG AND CO_2 IN COLOMBIA

In 2018, the mining and energy sector recorded emissions of approximately 35,533 Kt CO_2eq, making it the third-largest emitter in Colombia. These emissions are primarily associated with oil-related activities, with Santander and Meta as the leading departments in this sector. Additionally, La Guajira and Santander stand out for their use of fossil fuels in energy generation and coal production.

Regarding land management-related absorption, activities such as forest plantation implementation and timber product collection present a favorable net balance, with absorptions exceeding emissions. The departments with the highest absorptions from these activities are Vichada, Antioquia, Valle del Cauca, and Meta, collectively accounting for 64.7% of the national total for forestry management absorption.

At the local level, the three main GHG-emitting industries are refineries, thermoelectric plants, and cement factories. There are two main refining complexes: a primary one in Barrancabermeja and a secondary one in Cartagena (Figure 19).

Estimated GHG emissions for these complexes are 3.3 million tons and 0.8 million tons of CO_2 annually, respectively. Thermoelectric plants and cement factories have a broader national distribution (Figure 19). In total, there are 21 thermoelectric industrial complexes, generating 12.9 million tons of CO_2 annually.

Emission volumes vary significantly across industrial complexes. The largest source is the Termosierra complex in Medellín, emitting 1.8 million tons of CO_2 annually, while the smallest, Proeléctrica in Cartagena, emits 0.16 million tons of CO_2 annually. The median emission value per site is 0.5 million tons of CO_2 annually. Cement plants have a lower average emission potential compared to thermoelectric plants, averaging 0.35 million tons of CO_2 annually.

The variation in GHG emission volumes correlates with installed industrial capacity. Estimates range from 0.1 million tons of CO_2 annually at the Cementos Argos plant in San Gil to 0.75 million tons of CO_2 annually at the LafargeHolcim plant in Nobsa.

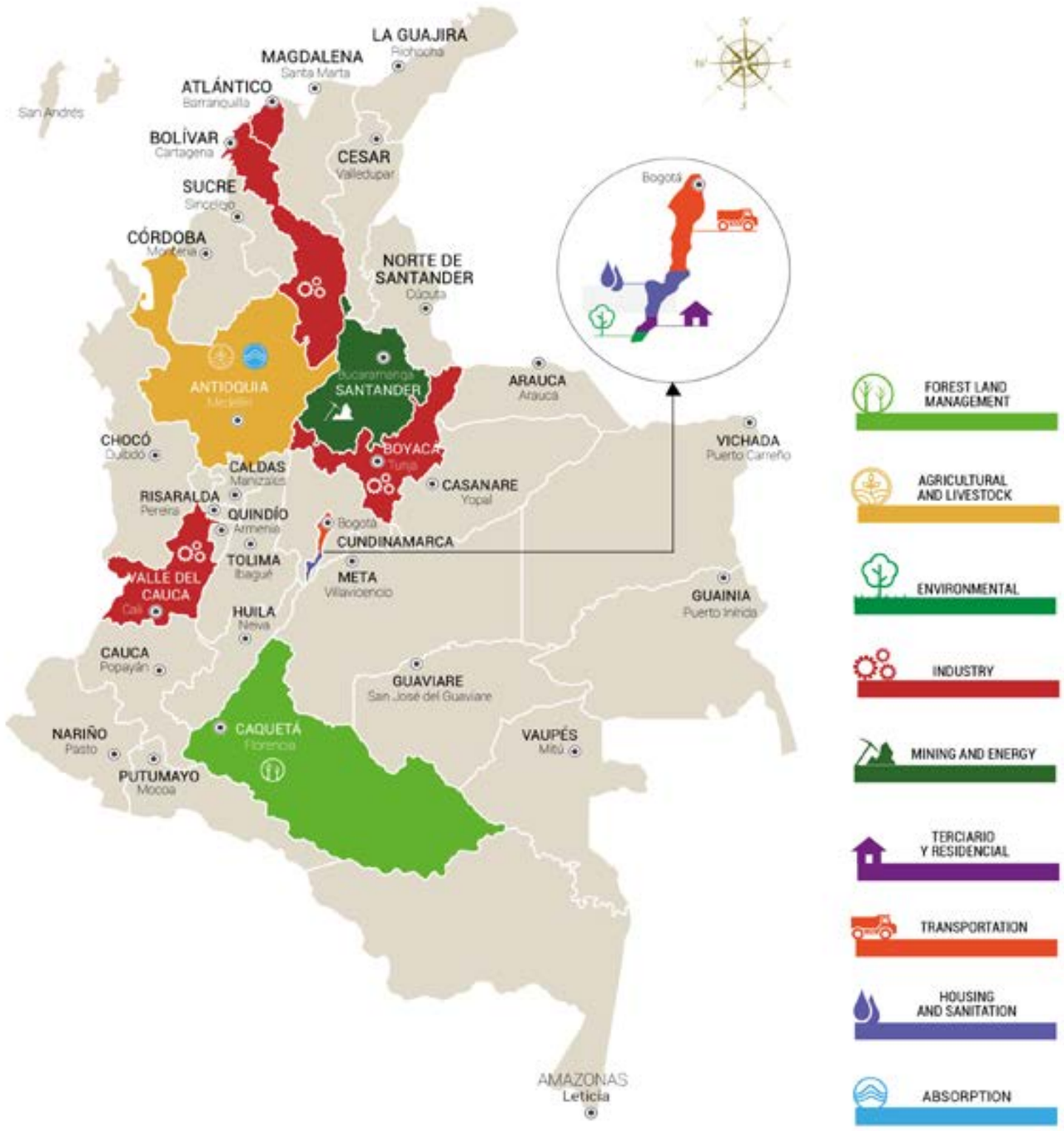

Figure 19. Infographic showing the location of the main sources of GHG emissions at the local level for Colombia. It can be observed the industrial grouping that adds the emissions of the different types of industry, as is the case of Barranquilla, Cartagena, Medellin, Cali and Tunja, especially due to their location near mature oil basins, represent outstanding targets for the development of CCUS activities. Adapted from the Departmental Greenhouse Gas Inventory, 2022.

5.4 Transportation

CO_2 can be transported in four states of matter: gaseous, liquid, solid, and supercritical. For commercial and global-scale transportation, the primary methods are tank trucks, pipelines, and ships, depending on whether the CO_2 is in its gaseous or liquid state.

The selection of suitable alternatives for CO_2 transportation at the national level requires a comprehensive analysis that considers various technical, economic, geographic, and environmental factors. The primary criteria in evaluating transportation potential are as follows:

1. Volume and Distance of Transportation: Taking into account Colombia's diverse geography, as well as the location of emission sources and potential storage sites.

2. Existing Infrastructure: Assessing the possibility of adapting or expanding current pipeline networks and port facilities to optimize transportation.

3. Investment and Operational Costs: Analyzing the long-term economic feasibility of each alternative, considering both initial investment and recurring costs.

4. Environmental Impact: Evaluating emissions associated with each transportation method and their ecological footprint, favoring alternatives that minimize adverse environmental effects.

5. Safety and Risks: Identifying and assessing potential risks to communities and natural environments along transportation routes.

6. Regulations and Permits: Considering the existing legal framework and potential regulatory barriers that may affect the implementation of transportation options.

7. Flexibility and Scalability: Determining the capacity for adaptation to changes in demand and future expansions.

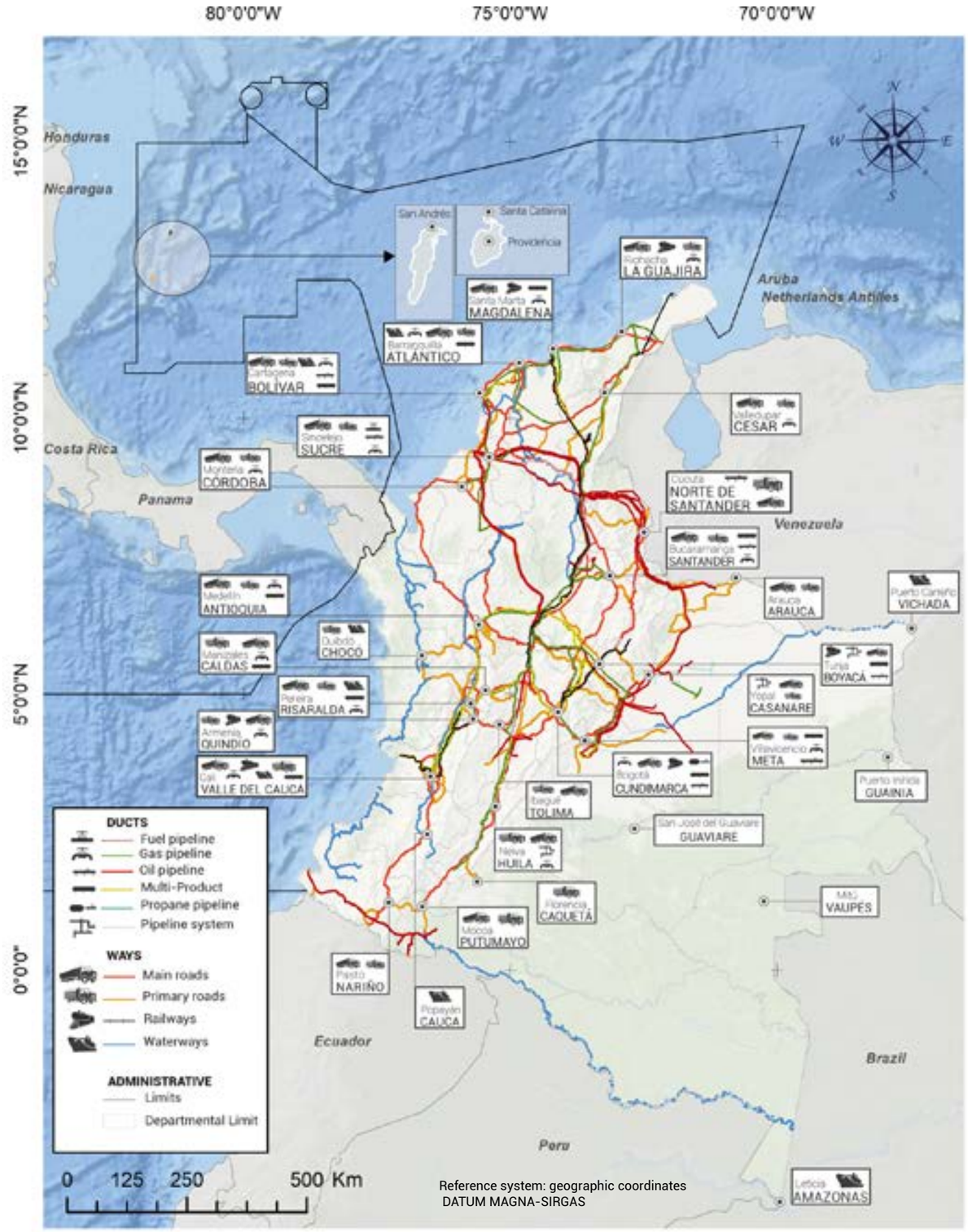

Figure 20. Map of Infrastructure and Main Roads Near GHG Emission Zones at the Local Level for Colombia.

5.4.1 National capacities for CO_2 transportation and required adaptations

The three main modes of CO_2 transportation considered are pipelines, river transport, and land transport. For each alternative, the geographic distribution and key technical characteristics are evaluated.Currently, Colombia lacks CO_2 pipelines (ceoductos). The available infrastructure has been developed primarily by the gas and oil industries and includes oil pipelines, gas pipelines, and multipurpose pipelines. This type of transport is prioritized in regions with high energy resources and relies on highly specialized infrastructure.

The thermodynamic characteristics of CO_2 differ significantly from those of natural gas. CO_2 is transported in a supercritical phase, and to avoid the formation of dual phases (liquid-vapor), operating pressure must exceed 80 bar, depending on the purity level of the CO_2. Additionally, the flow of CO_2 is considerably more aggressive than that of natural gas, especially when it contains certain impurities. Consequently, corrosion issues are far more critical in CO_2 transport compared to natural gas pipelines. One common impurity is water, which can lead to the formation of hydrates.

River transport presents an efficient and sustainable alternative in areas where roads are not viable or maritime transport lacks direct access. In Colombia, rivers play a crucial role in connecting inland regions and transporting goods over long distances. The Magdalena River is a key route for moving goods from the country's interior to the Caribbean coast.

Land and rail transport are essential for ensuring connectivity between cities and regions. They play a key role in transporting goods in areas without direct access to maritime, river, or pipeline networks. Roads are classified according to their capacity and importance within the transportation network (Figure 20; Table 1). These routes are further categorized based on specific functionalities, such as heavy freight routes designed to handle large volumes of goods and heavy vehicles, or passenger routes that prioritize comfort and road safety.

Railways in Colombia are underutilized compared to other countries, as the existing infrastructure focuses primarily on freight logistics. The system is fragmented and often outdated (Figure 20; Table 1). Where operational, the railway infrastructure serves critical functions, mainly for transporting bulk goods, such as coal from La Guajira.

Figure 21. Refinery Infrastructure (photo taken from Pixabay).

Figure 22. Ducts (photo taken from Pixabay).

Figure 23. Photograph of the Gualangay Tunnel. Note: Photograph taken by Jair Ramírez in the Gualanday district, on the Fraile hill, within the Girardot – Ibagué – Cajamarca road corridor, Colombia.

DUCT TYPE	EXTENSION (Km)
FUEL OIL PIPELINE	454,54
GAS PIPELINE	3871,3982
OIL PIPELINE	5981,669169
POLYPIPELINE	3154,67965
PROPANE PIPELINE	374,215
PIPELINE SYSTEMS (SD)	534,62617
RIVER TRANSPORTATION	5149,38
ROADS (INLAND) HIGHWAYS	19127,23
RAILROADS (LAND)	1856,00

Table 1. Extension of pipelines.

Regulations in this area require coordinated efforts between the government and sector stakeholders to establish an adequate legal framework for the efficient and safe transportation of CO_2 at an industrial scale. This process involves collaboration among public and private entities responsible for the task. Building new infrastructure entails fundamental requirements, including establishing clear public policy guidelines, developing strategic planning that considers technical, environmental, and economic aspects, ensuring significant investment, and setting realistic timelines for project execution and operation.

The integration of available information on CO_2 transportation alternatives in Colombia highlights areas with greater connectivity, such as industrial urban zones, oil basins, and regions with lower potential (e.g., the Sierras and the Amazon region).

6. SITES WITH POTENTIAL FOR GEOLOGICAL CO_2 STORAGE

6.1 Calculation of capacity in sedimentary basins

Conditional Factors for Capacity Calculation

- **Reservoir presence**

Minimum Geometry: 800 m >100 bar
Maximum Geometry: Up to the average structural closure production level

- **Reservoir quality**

Porosity (POR)Permeability (PERM)Aquifer Salinity

Net/Gross Ratio is calculated based on values from producing fields located within the same reservoirs analyzed in each study.

- **Storage volumes**

Saline Aquifers, depleted gas or oil fields.
Unconventional Reservoirs: Igneous Rocks (Basalts), (Unmineable Coal Seams), (Organic Shales)

Where:

Mco2: Mass of CO_2
Vb: Bulk volume
Φ : Poricity
n/g: net-to-gross ratio
ρco2: Density of CO_2 under reservior conditions
Self: Storage efficiency factor

$$M_{CO2} = Vb * \phi * \frac{n}{g} * \rho_{CO2} * S_{elf}$$

In the context of geological CO_2 storage, the most relevant properties are the reduction in its volume and the increase in its density, which are key factors for maximizing storage efficiency in geological formations.

At a depth of 800 meters, 1,000 m³ of CO_2 compresses to occupy approximately 3.8 m³ reaching a density of nearly 700 kg/m³.

Methodology

1. Structural surfaces of reservoir and seal units (if present) are reconstructed.

2. Net and Gross parameters are defined for each reservoir level.

3. Average porosity is determined based on reports from the National Hydrocarbons Agency (ANH), referencing operator-submitted data.

4. The total rock volume is calculated using the structural surface geometry, bounded by upper and lower stratigraphic limits.

5. Storage capacity is estimated for the rock fraction between 2,400 feet (approximately 800 m) and the average structural closure level, as defined by each surface's geometry.

6. A storage efficiency factor of 0.5 is applied.

7. A structural section is presented, highlighting the geometric relationships between structural surfaces and emphasizing thickness distribution.

Summary

BASIN	UNIT	ROCK VOLUME (m3)	CAPACITY (kg)	GTONNAGE CAPACITY	GT IN STRUCTURAL CLOSURES
MMV	COLORADO	4384203584538	21175703313318	21.2	5.0
MMV	MUGROSA	2500033559183	8478863815969	8.5	0.7
LMV	PORQUERO	83951796429845	117532515001783	117.5	42.3
LMV	CDO	44649855557344	156274494450704	156.3	64.1
SSJ	CHENGUE	57856834498963	60749676223911	60.7	7.2
CATATUMBO	BARCO	10784032866174	157267145965037	157.3	22
CATATUMBO	LUNA	5409738259853	26507717473278	26.5	15
LLANOS	MIRADOR	117479396852160	2878245222877920	2878.2	
GUAJIRA	SIAMANA	19142970647424	223334657553280	223.3	50
TOTAL				3650	50

Table 2. Calculation of capacity in sedimentary basins.

6.2 Basin

6.2.1 Middle Magdalena Valley (MMV)

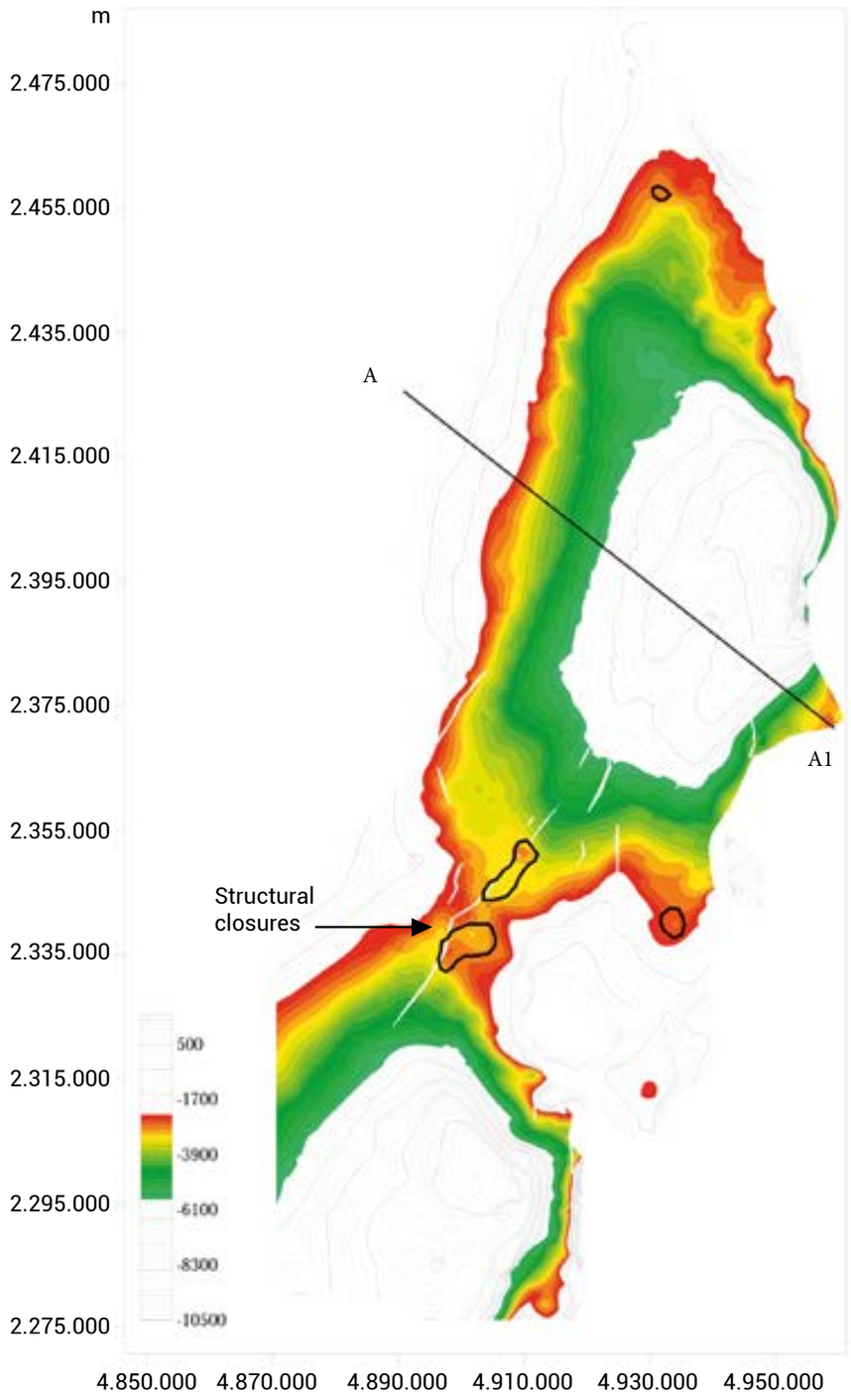

Figure 24. Structural Surface for the COLORADO Formation, Indicating the Location of the Reservoir Portion Available for CO_2 Injection.

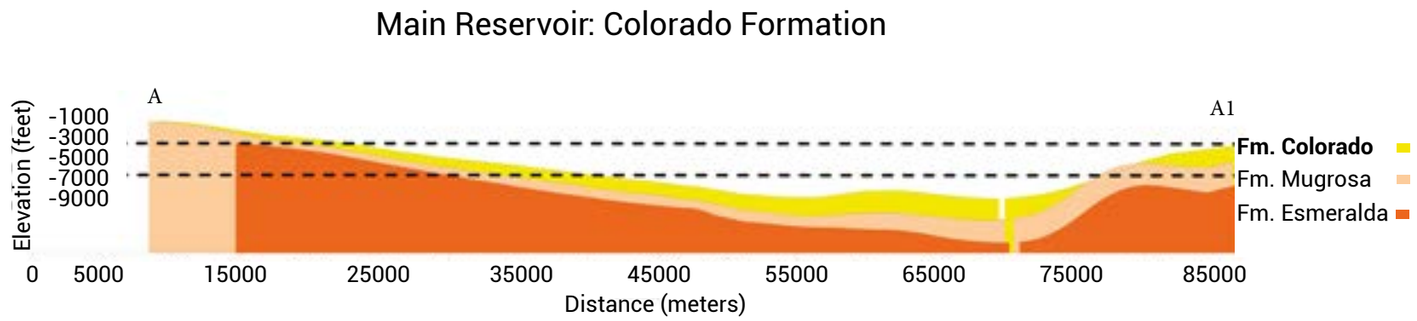

Figure 25. Stratigraphic Section A-A1 of the Colorado Reservoir Formation.

Reservoir type:

The Colorado Formation corresponds to a stratigraphic succession of thick conglomeratic sandstone layers interbedded with varicolored mudstones and claystones. These were deposited in environments associated with braided and meandering river channels and piedmont alluvial fans.

Age: Late Oligocene to Miocene

Net/Gross Ratio: 60/1000

Average Porosity (%): 23

Basin Geometry:

Asymmetric synclinal distribution. On the gently sloping eastern flank, this formation pinches out over the underlying Mugrosa Formation. On the western flank, its thickness increases but is truncated by faulted and folded structures of the eastern Cordillera's foothills.

Closure Types:

Anticline closures occur in four directions, with depths ranging from 2,500 to 3,200 feet.

BASIN	UNIT	ROCK VOLUME (m3)	CAPACITY (kg)	GTONNAGE CAPACITY	GT IN STRUCTURAL CLOSURES
MMV	COLORADO	4384203584538	21175703313318	21.2	5.0

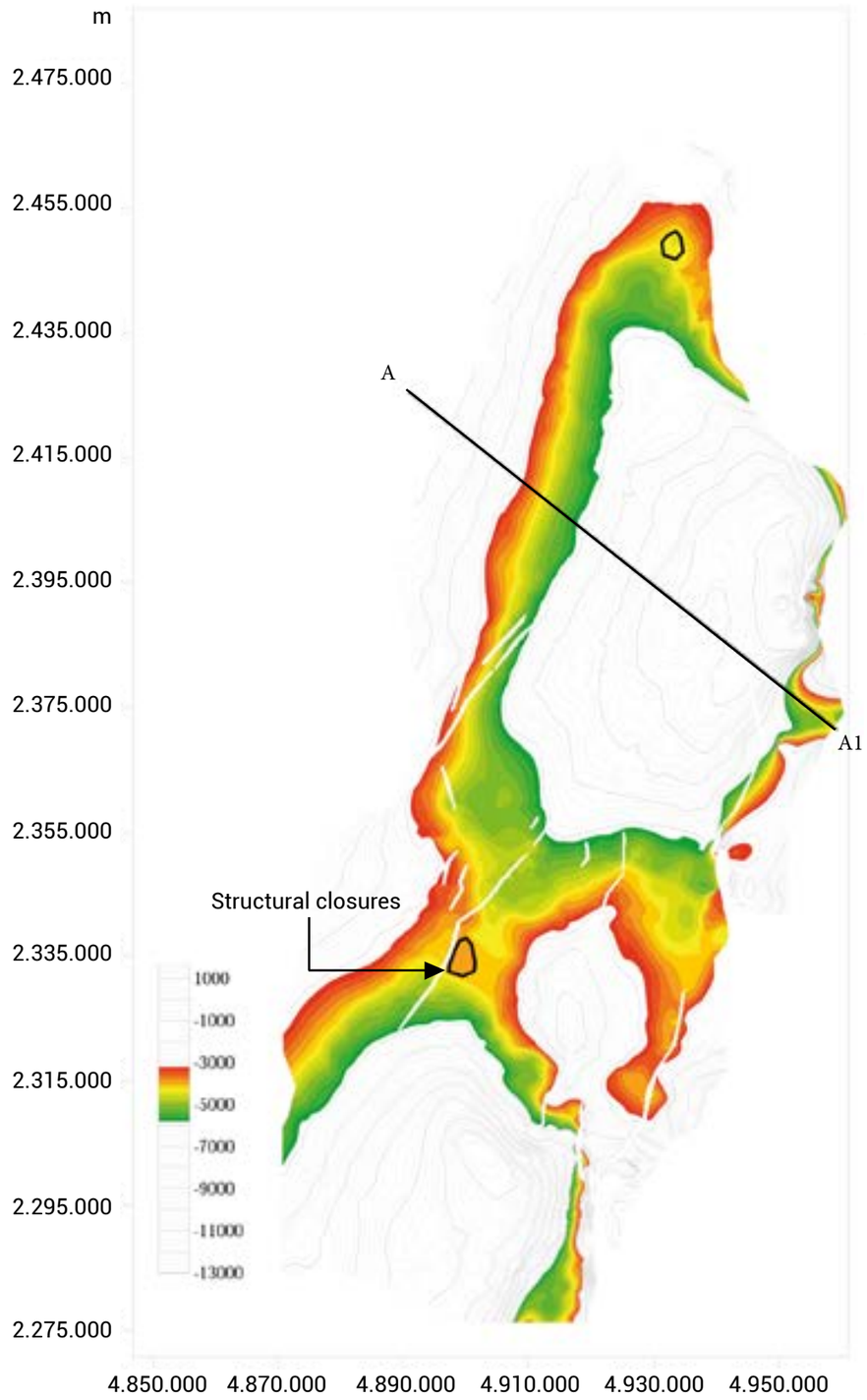

Figure 26. Structural Surface for the MUGROSA Formation, Indicating the Location of the Reservoir Portion Available for CO_2 Injection.

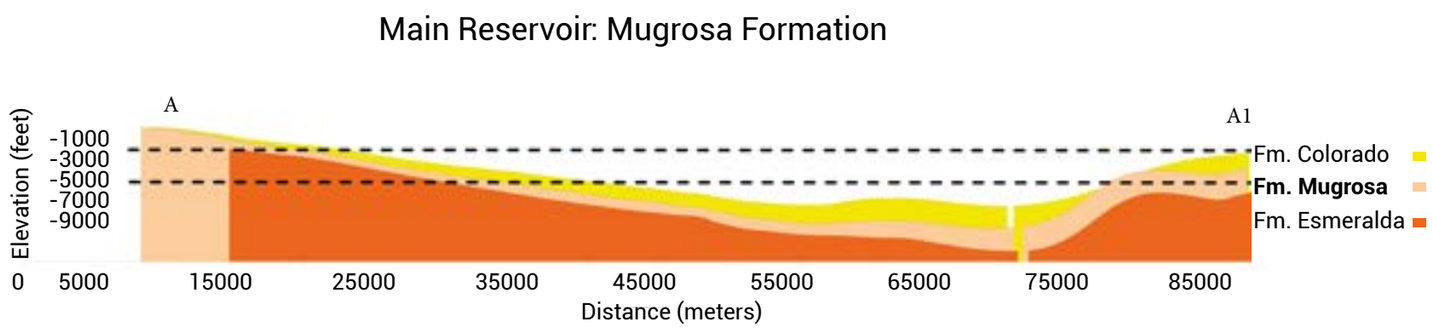

Figure 27. Stratigraphic Section A-A1 of the Mugrosa Reservoir Formation.

Reservoir Type:

This formation comprises thick, coarse-grained conglomeratic sandstone layers interbedded with varicolored mudstones and claystones. The depositional environment is associated with meandering river systems and over-bank lobes, with sediment contributions from piedmont fans.

Age: Middle Oligocene to Lower Miocene

Net/Gross Ratio: 51/1000

Average Porosity (%): 19

Basin Geometry:

Asymmetric synclinal distribution. The formation pinches out over the underlying unit on the eastern flank. On the western flank, thickness increases but terminates against faulted and folded structures of the foothills.

Closure Types:

Anticline closures in four directions, with depths ranging from 2,500 to 3,200 feet.

BASIN	UNIT	ROCK VOLUME (m^3)	CAPACITY (kg)	GTONNAGE CAPACITY	GT IN STRUCTURAL CLOSURES
MMV	MUGROSA	2500033559183	8478863815969	8.5	0.7

6.2 Basin

6.2.2 Lower Magdalena Valley (LMV) - Sinú San Jacinto Basin (SSJ)

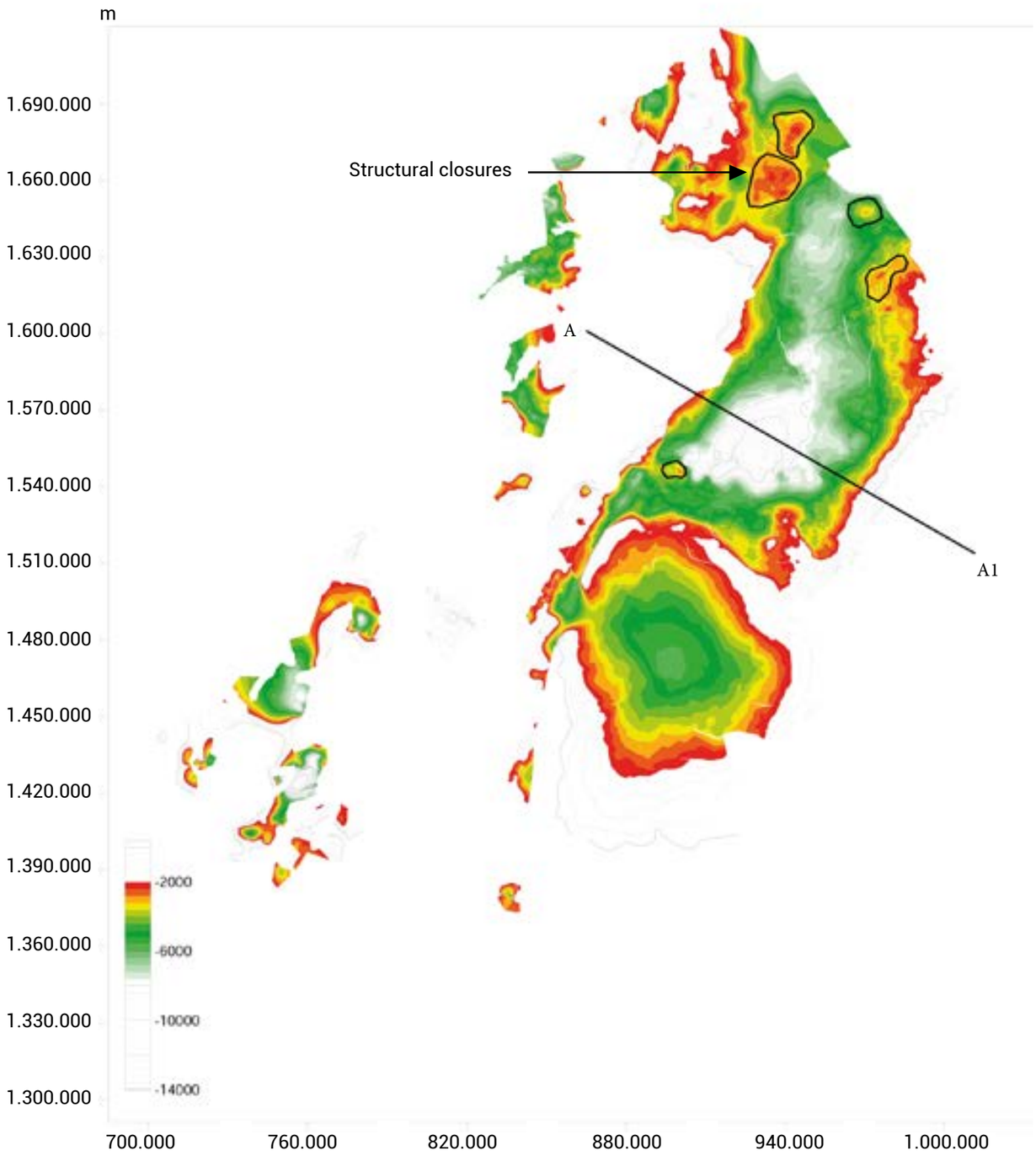

Figure 28. Structural Surface for the PORQUERO Formation, Indicating the Location of the Reservoir Portion Available for CO_2 Injection.

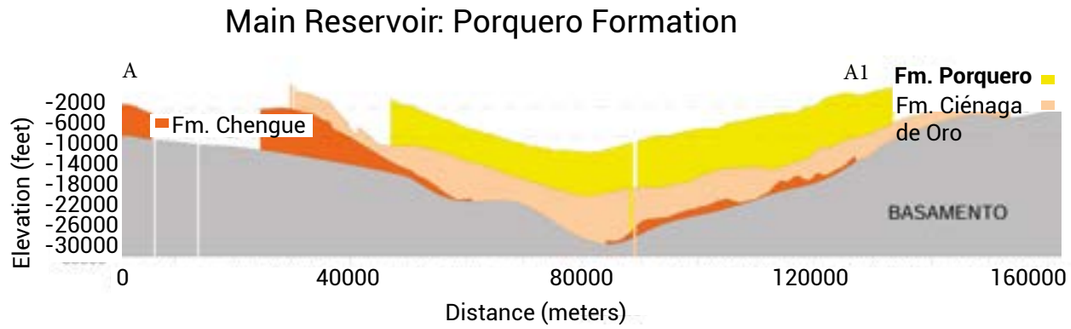

Figure 29. Stratigraphic Section A-A1 of the Porquero Reservoir Formation.

Reservoir Type:

A thick sequence of olive-colored friable arkosic sandstones, alternating with thin layers of light greenish-gray mudstones. These were deposited in deltaic fan environments.

Age: Lower to Middle Miocene

Net/Gross Ratio: 100/3000

Average Porosity (%): 12

Basin Geometry:

Asymmetric synclinal distribution with symmetric flanks. The eastern flank shows growth sequences linked to the San Jacinto province, while the western side pinches out over basement highs.

Closure Types:

Anticline closures in four directions, with depths ranging from 2,500 to 4,000 feet.

BASIN	UNIT	ROCK VOLUME (m^3)	CAPACITY (kg)	GTONNAGE CAPACITY	GT IN STRUCTURAL CLOSURES
LMV	PORQUERO	83951796429845	117532515001783	117.5	42.3

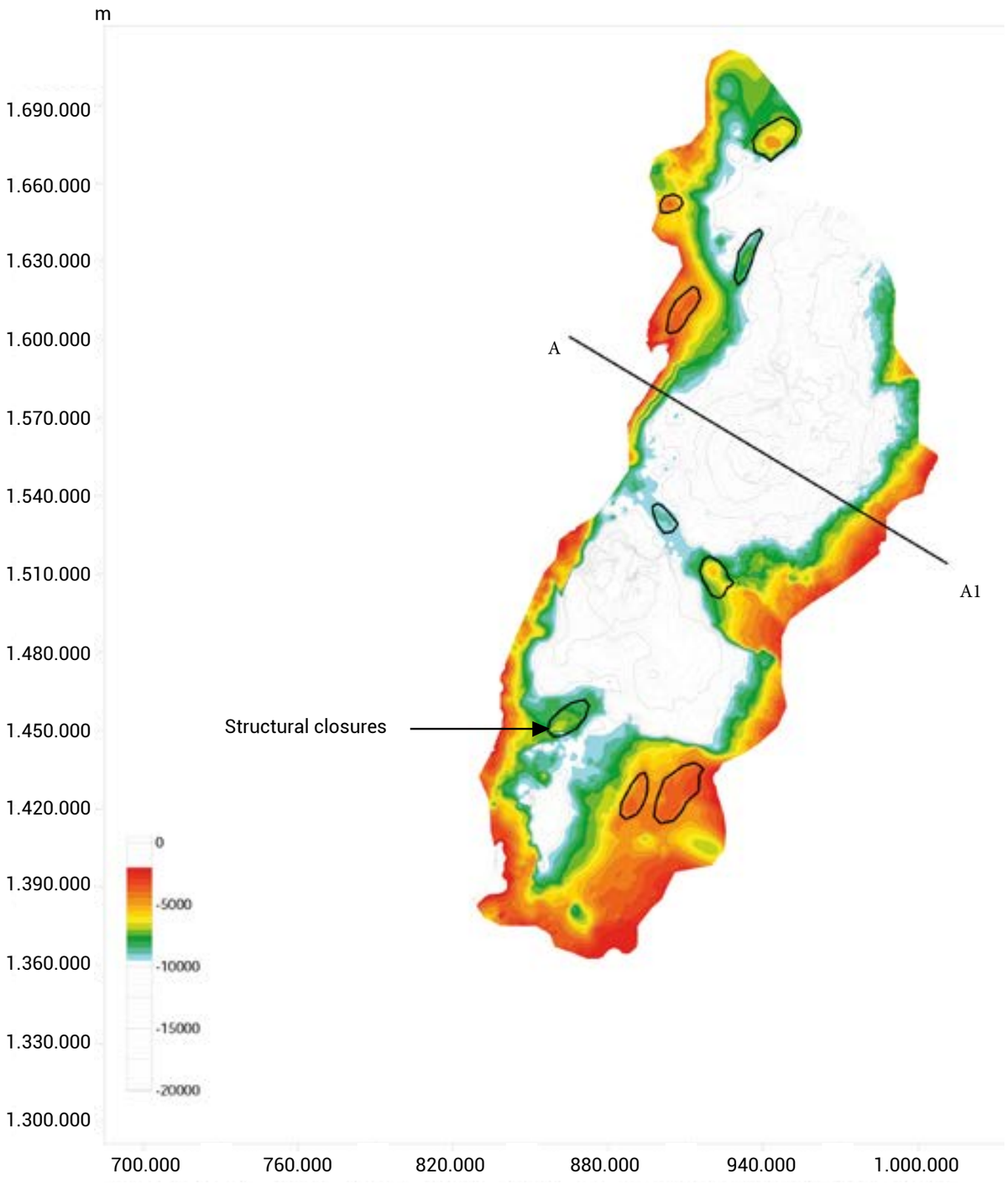

Figure 30. Structural Surface for the Cienaga de Oro Formation, Indicating the Location of the Reservoir Portion Available for CO_2 Injection.

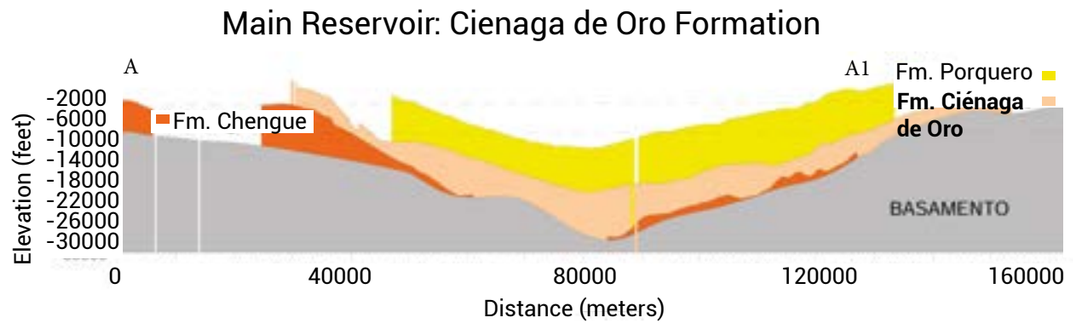

Figure 31. Stratigraphic Section A-A1 of the Ciénaga de Oro Reservoir Formation.

Reservoir Type:

Comprises thick to very thick layers of coarse quartzarenites with calcareous content, formed in an internal marginal basin environment.

Age: Late Oligocene

Net/Gross Ratio: 100/2000

Average Porosity (%): 20

Basin Geometry:

It is asymmetrically distributed in the shape of a syncline with symmetrical flanks. On the eastern flank, this formation (FM) is defined as a growth sequence of the mountain ranges in the San Jacinto province. To the west, it is pinched over basement highs.

Closure Types:

Anticline closures in four directions, with depths ranging from 2,500 to 7,000 feet

BASIN	UNIT	ROCK VOLUME (m^3)	CAPACITY (kg)	GTONNAGE CAPACITY	GT IN STRUCTURAL CLOSURES
LMV	CDO	44649855557344	156274494450704	156.3	64.1

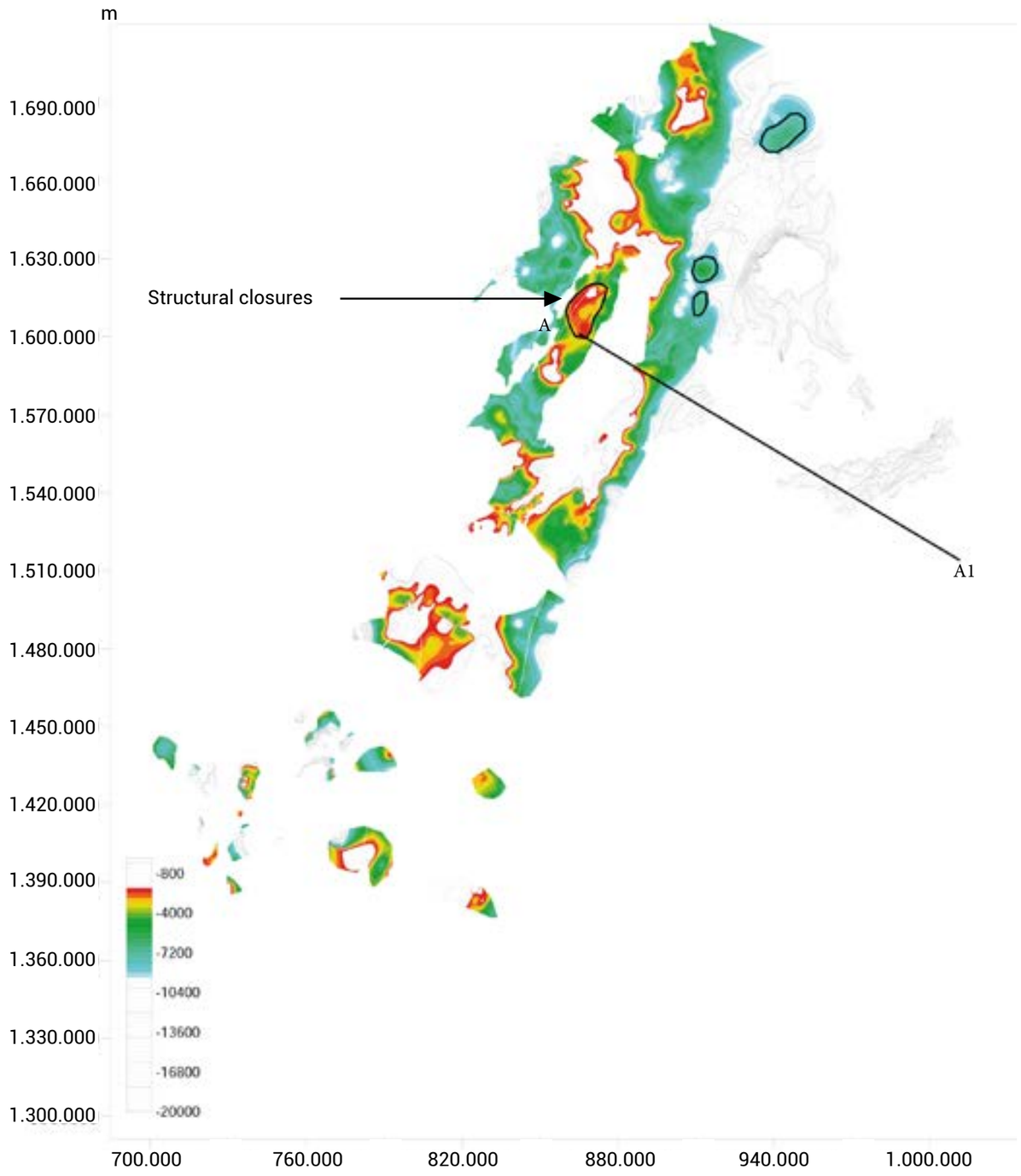

Figure 32. Structural Surface for the CHENGUE Formation, Indicating the Location of the Reservoir Portion Available for CO_2 Injection.

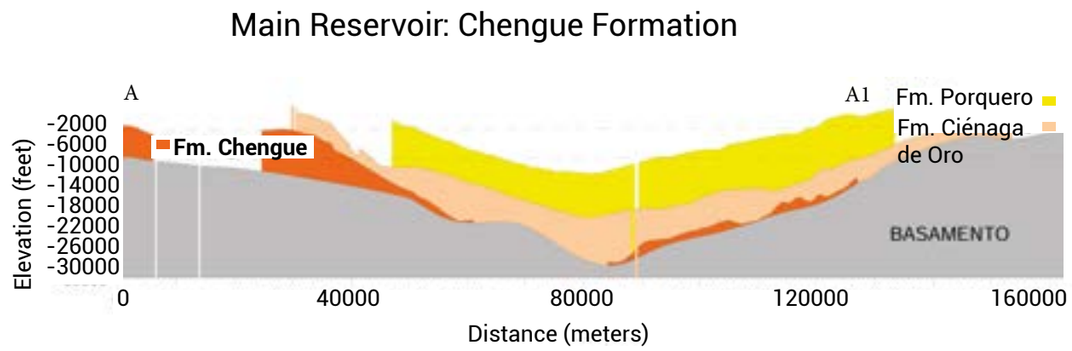

Figure 33. Stratigraphic Section A-A1 of the Chengue Reservoir Formation.

Reservoir Type:

The Chengue Formation consists of thick to very thick quartzarenite layers, with calcareous cementation, ranging from coarse to pebbly grains. Depositional environments correspond to an internal marginal basin setting.

Age: Late Oligocene

Net/Gross Ratio: 50/2000

Average Porosity (%): 12

Basin Geometry:

Distributed along the San Jacinto fold belt, showing progressively increasing thickness toward the western sector.

Closure Types:

Anticline closures in four directions, with depths ranging from 2,500 to 8,000 feet.

BASIN	UNIT	ROCK VOLUME (m^3)	CAPACITY (kg)	GTONNAGE CAPACITY	GT IN STRUCTURAL CLOSURES
SSJ	CHENGUE	57856834498963	60749676223911	60.7	7.2

6.2.3 Catatumbo

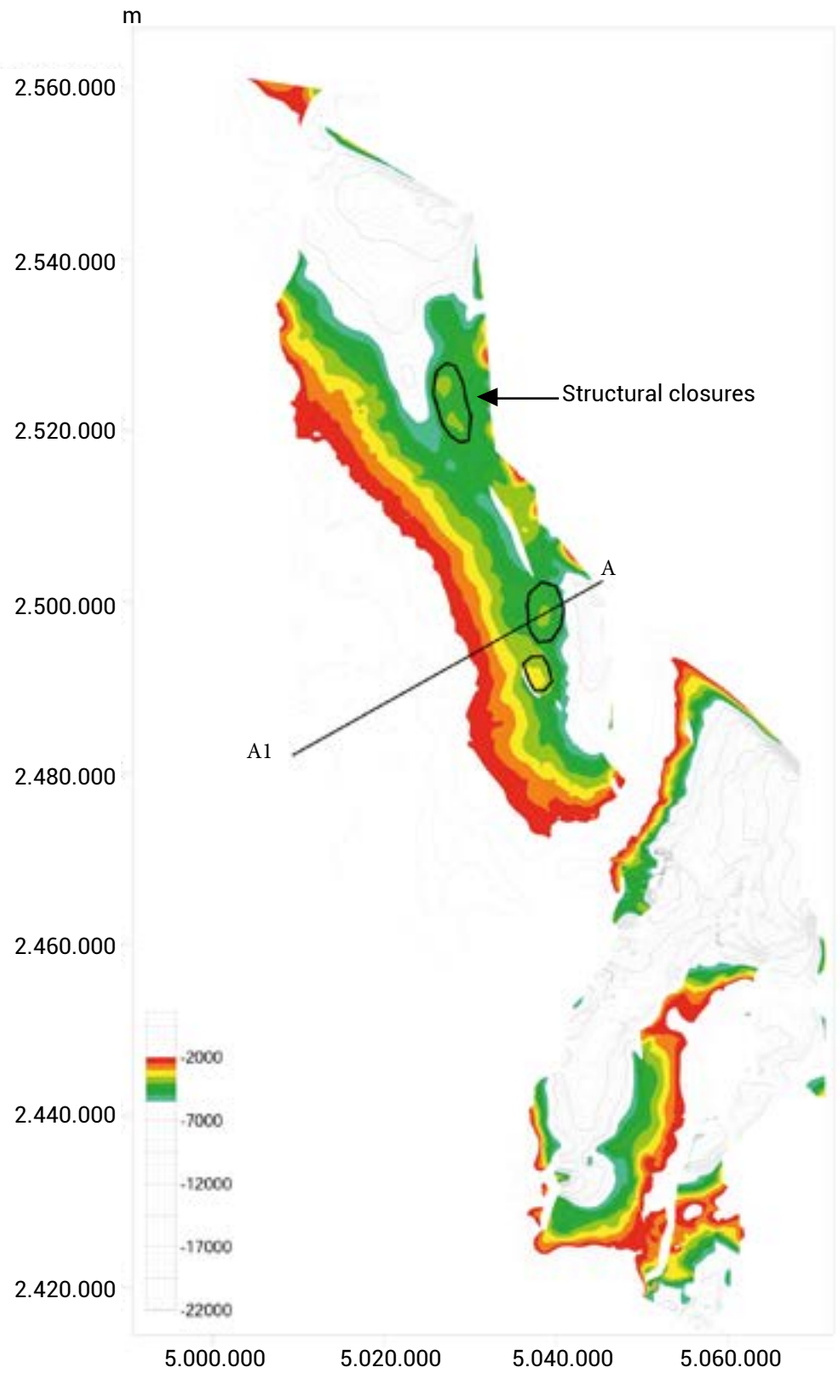

Figure 34. Structural Surface for the BARCO Formation, Indicating the Location of the Reservoir Portion Available for CO_2 Injection.

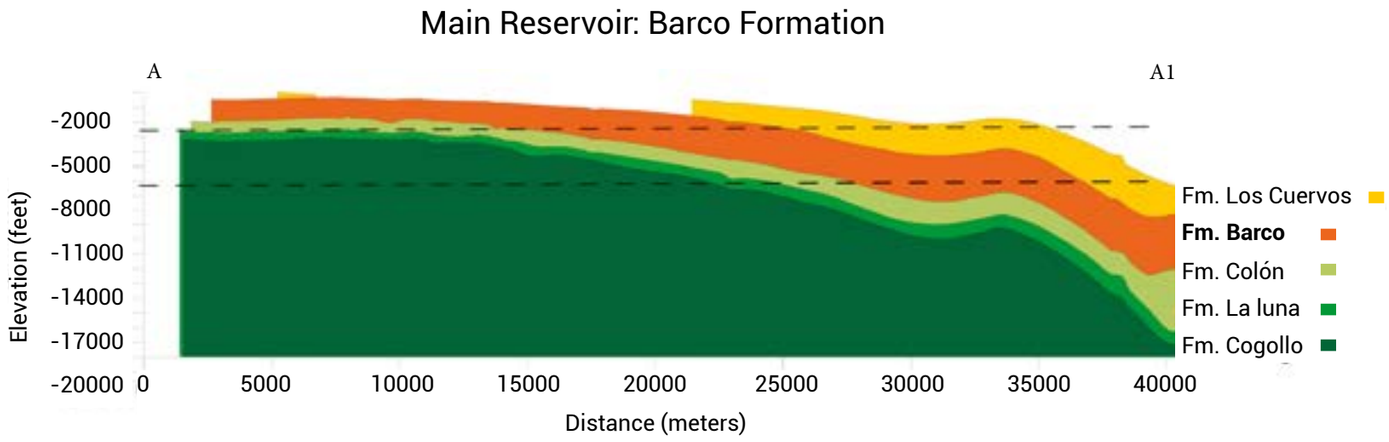

Figure 35. Stratigraphic Section A-A1 of the Barco Reservoir Formation.

Reservoir Type:

This reservoir consists of upward-coarsening sequences composed of friable medium-to-coarse-grained sandstones, with sporadic intercalations of thin limestone layers, coal seams, and shales. Depositional environments are associated with the progradation of deltaic lobes into tidal plains.

Age: Paleocene to Early Eocene

Net/Gross Ratio: 125/300

Average Porosity (%): 10

Basin Geometry:

Distributed along a monocline faulted and folded due to transpressive deformation.

Closure Types:

Anticline closures in four directions, with depths ranging from 3,500 to 5,000 feet.

BASIN	UNIT	ROCK VOLUME (m^3)	CAPACITY (kg)	GTONNAGE CAPACITY	GT IN STRUCTURAL CLOSURES
CATATUMBO	BARCO	10784032866174	157267145965037	157.3	22

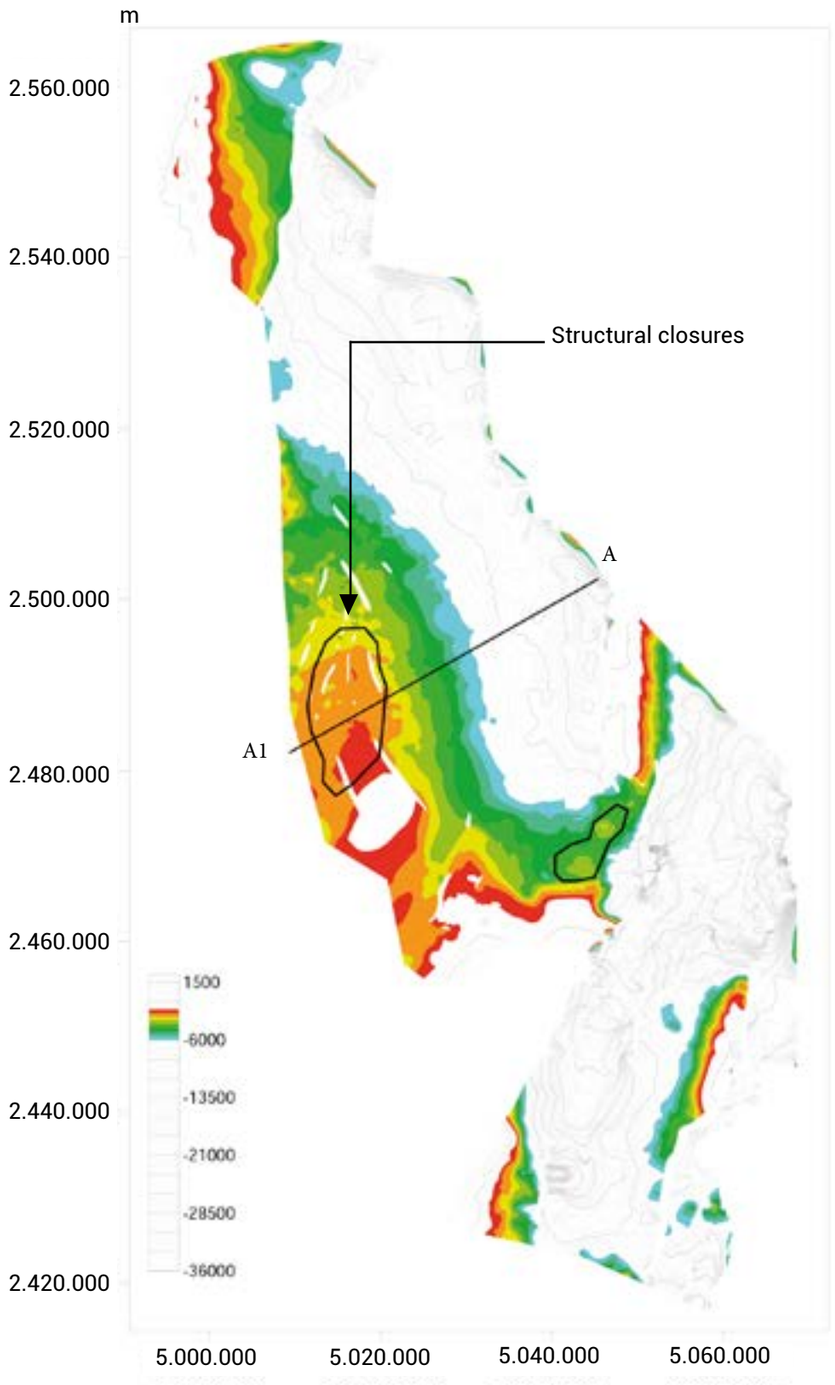

Figure 36. Structural Surface for the LA LUNA Formation, Indicating the Location of the Reservoir Portion Available for CO_2 Injection.

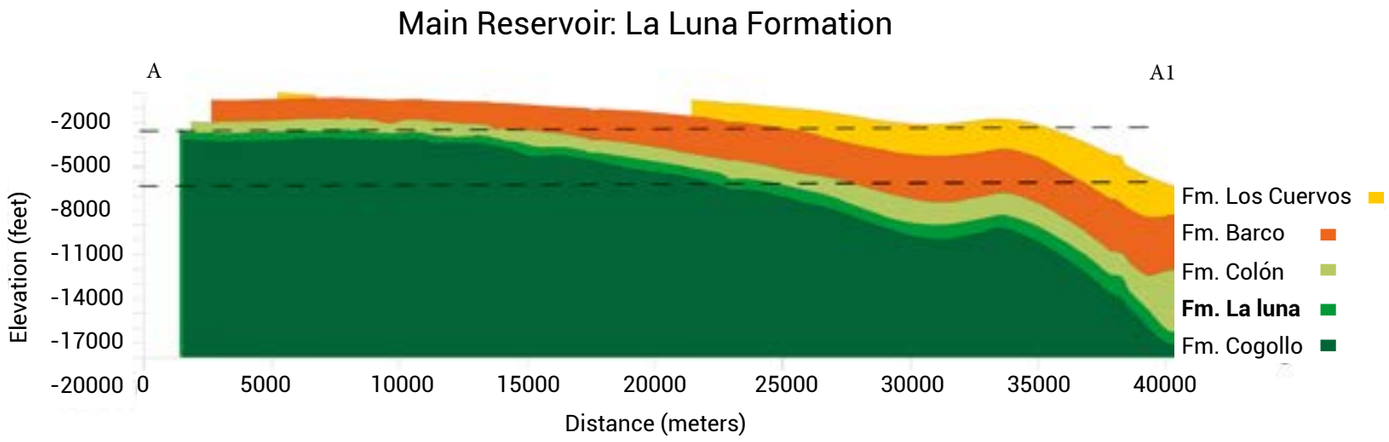

Figure 37. Stratigraphic Section A-A1 of the La Luna Reservoir Formation.

Reservoir Type:

Primarily composed of alternating shales, marls, and limestones with gradual variations across the sequence. Grouped into Salada, Pujamana, and Galembo members, the depositional environment is an internal carbonate platform with shallow, open conditions, varying between high-energy zones and partially restricted areas.

Age: Turonian to Santonian

Net/Gross Ratio: 35/200

Average Porosity(%): 8

Geometry in the basin:

It is distributed along a monocline to the east, faulted and folded by faults with transpressive deformation.

Closure Types:

Anticline closures in four directions, with depths ranging from 2,400 to 4,000 feet.

BASIN	UNIT	ROCK VOLUME (m^3)	CAPACITY (kg)	GTONNAGE CAPACITY	GT IN STRUCTURAL CLOSURES
CATATUMBO	LUNA	5409738259853	26507717473278	26.5	15

6.2.4 Eastern Llanos

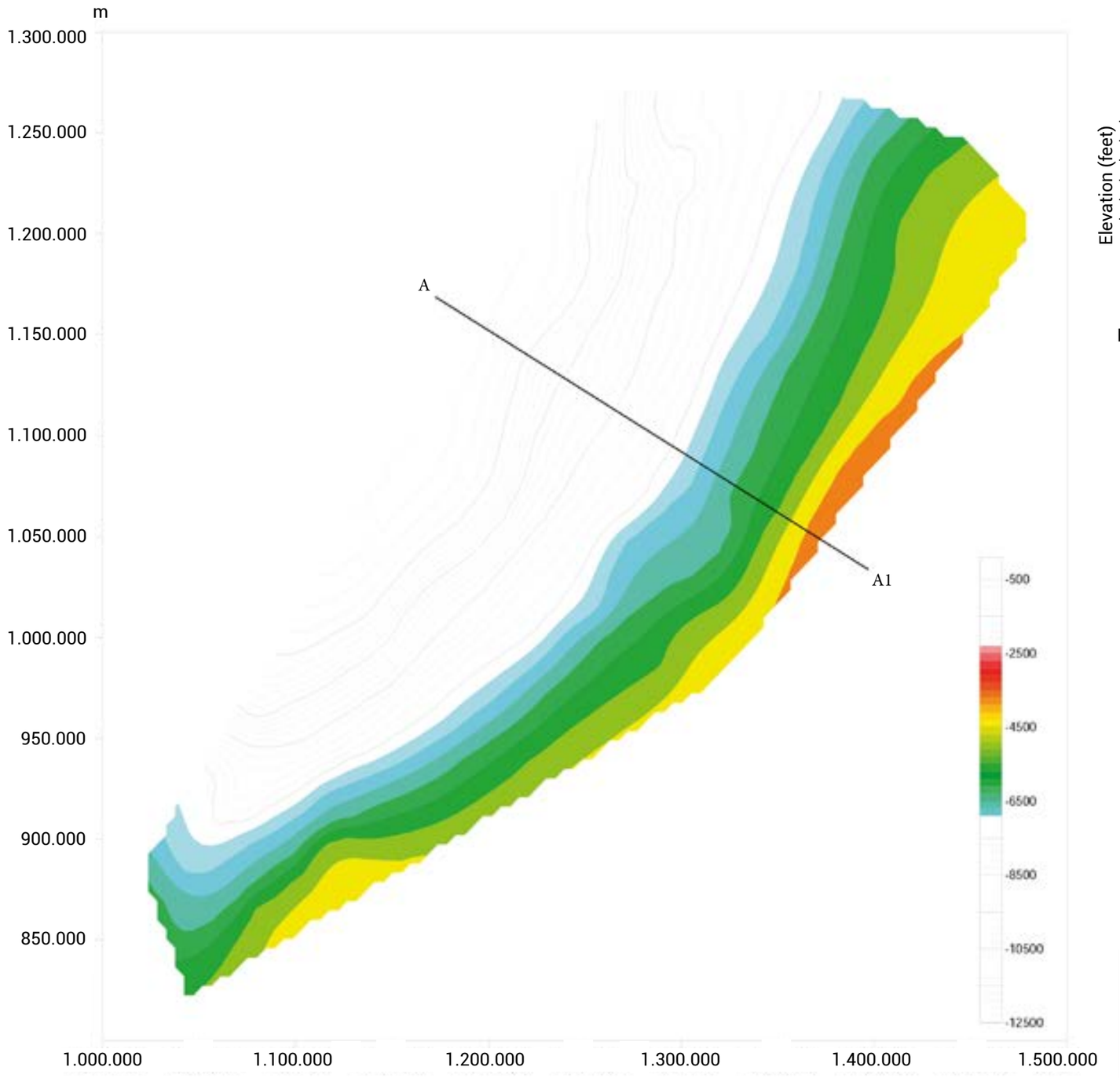

Figure 38. Structural Surface for the MIRADOR Formation, Indicating the Location of the Reservoir Portion Available for CO_2 Injection.

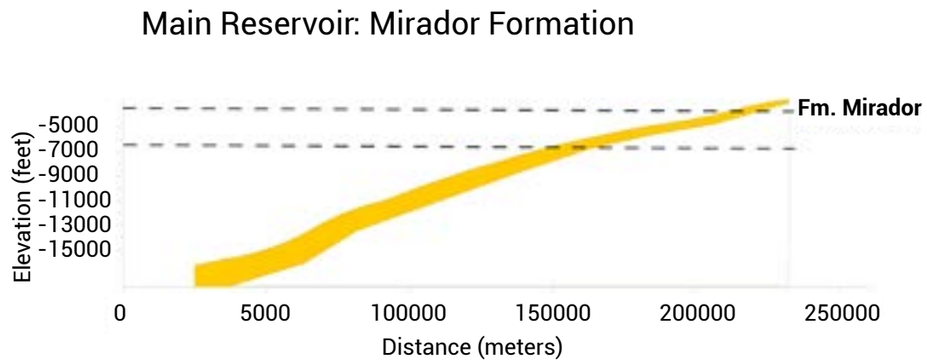

Figure 39. Stratigraphic Section A-A1 of the Mirador Reservoir Formation.

Reservoir type:

This formation comprises mainly white, clean, massive sandstones, ranging from friable to well-cemented, with fine to coarse grains, and some conglomeratic layers. Thin layers of micaceous gray shale and sandy mudstones are also present. Depositional environments correspond to fluvial systems within delta plains and brackish swamps.

Age: Late Eocene

Net/Gross Ratio: 35/100

Average Porosity(%): 20

Basin Geometry:

Distributed along a monocline dipping westward and pinched and truncated by Neogene progressive unconformities.

Closure Types:

It is defined as stratigraphic closures across the monocline's extent.

BASIN	UNIT	ROCK VOLUME (m^3)	CAPACITY (kg)	GTONNAGE CAPACITY	GT IN STRUCTURAL CLOSURES
LLANOS	MIRADOR	117479396852160	2878245222877920	2878.2	

6.2.5 Guajira

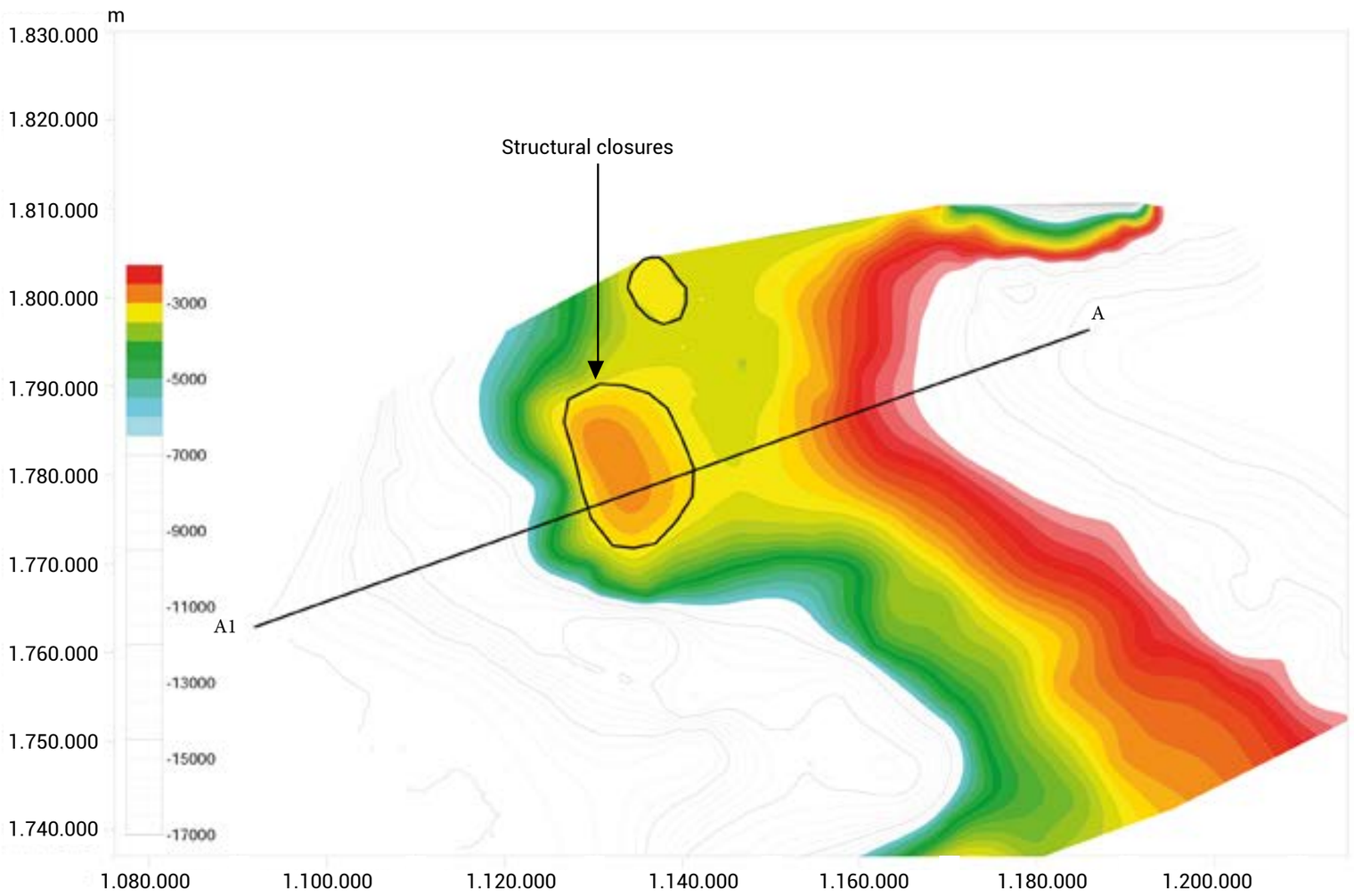

Figure 40. Structural Surface for the Siamana Formation, Indicating the Location of the Reservoir Portion Available for CO_2 Injection.

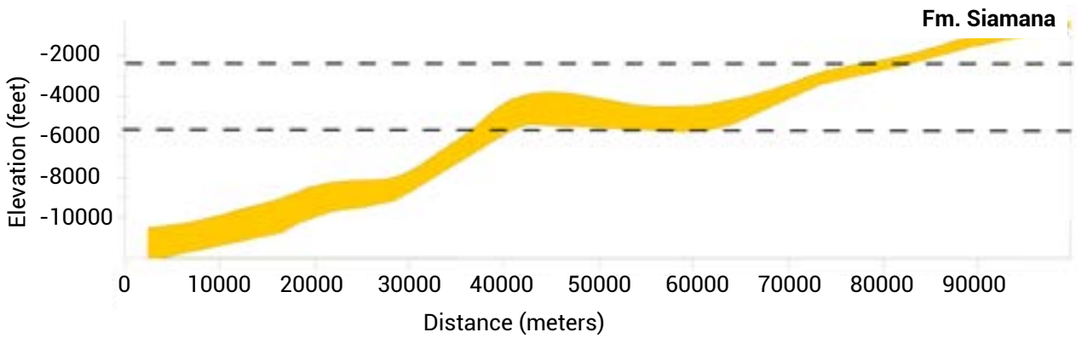

Figure 41. Structural Surface for the Siamana Formation.the Location of the Reservoir Portion Available for CO_2 Injection.

Main Reservoir: Siamana Formation

Reservoir Type:

Composed of fine-grained sandstones interbedded with calcareous fossiliferous sandstones and locally clayey sandstones. Alternations with fossiliferous sandy or clayey limestones are also observed. This unit was deposited in a shallow marine platform environment.

Age: Late Oligocene to Early Miocene

Net/Gross Ratio: 100/300

Average Porosity (%): 10

Basin Geometry:

Distributed along a monocline dipping westward, pinched and truncated against the basement to the east. Additionally, it forms calcareous banks in the low basement blocks of antithetic normal faults.

Closure Types:

Defined in calcareous growths

BASIN	UNIT	ROCK VOLUME (m^3)	CAPACITY (kg)	GTONNAGE CAPACITY	GT IN STRUCTURAL CLOSURES
GUAJIRA	SIAMANA	19142970647424	223334657553280	223.3	50

6.3 Coals and basalts

6.3.1 Coal zones in Colombia and their potential for CO_2 storage

Colombia's coal zones represent a strategically significant natural resource. Traditionally exploited for their mineral wealth, these areas are emerging as key points of interest in the context of climate change mitigation. Coal seams, known for their capacity to adsorb and retain gases, offer a viable option for geological CO_2 storage—an essential strategy in the fight against global warming.

This analysis aims to explore the geological and structural characteristics of the country's main coal basins, evaluating variables such as the thickness, depth, ash content, and permeability of the coal seams. These factors are critical for estimating the feasibility of coal zones as CO_2 reservoirs.

6.3.2 Areas with potential for CO_2 storage in coal

In Colombia, twelve coal zones have been identified based on the presence of coal-bearing geological formations, their geographic distribution, and associated parameters such as coal quality and type. The country's geological conditions favor the presence of this mineral throughout the national territory, with the northern coal zones, such as La Guajira and Cesar, standing out for holding the largest reserves.

Through an evaluation of geological factors—such as the complexity and depth of structures, the quantity and thickness of coal seams, the material's porosity, and previous estimates of gas content associated with the coal—two areas have been identified with significant potential for CO_2 storage within the country's twelve coal zones:

1. Guajira South Area: located within the coal zone of La Guajira, in the northern region of the country.

2. Checua-Lenguazaque Area: situated in the coal zones of Cundinamarca and Boyacá, in the central region of the country.

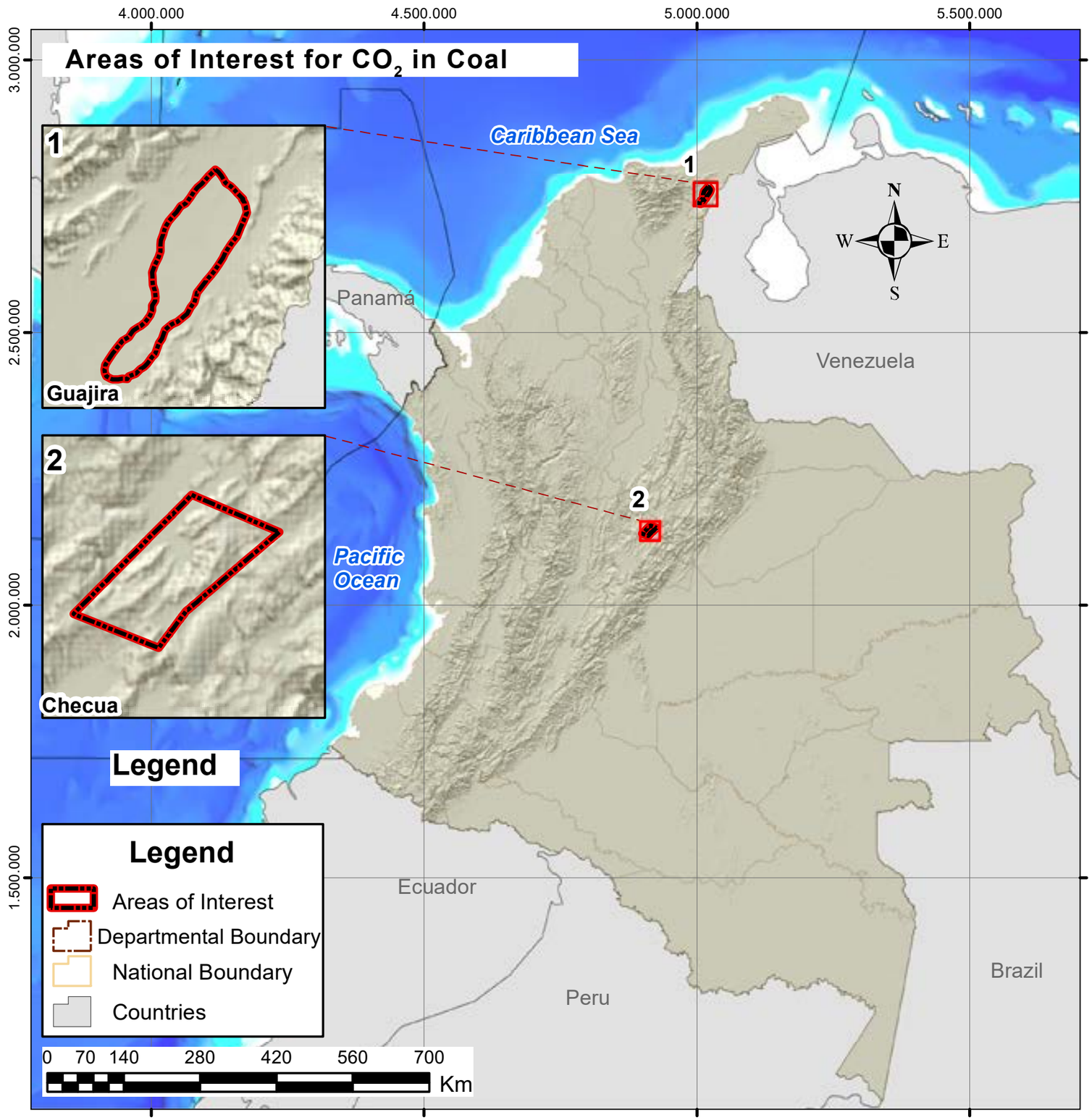

Figure 42. Map of Areas with CO_2 Storage Potential.

6.3.2.1 Checua-Lenguazaque area: characterization and potential for CO_2 storage

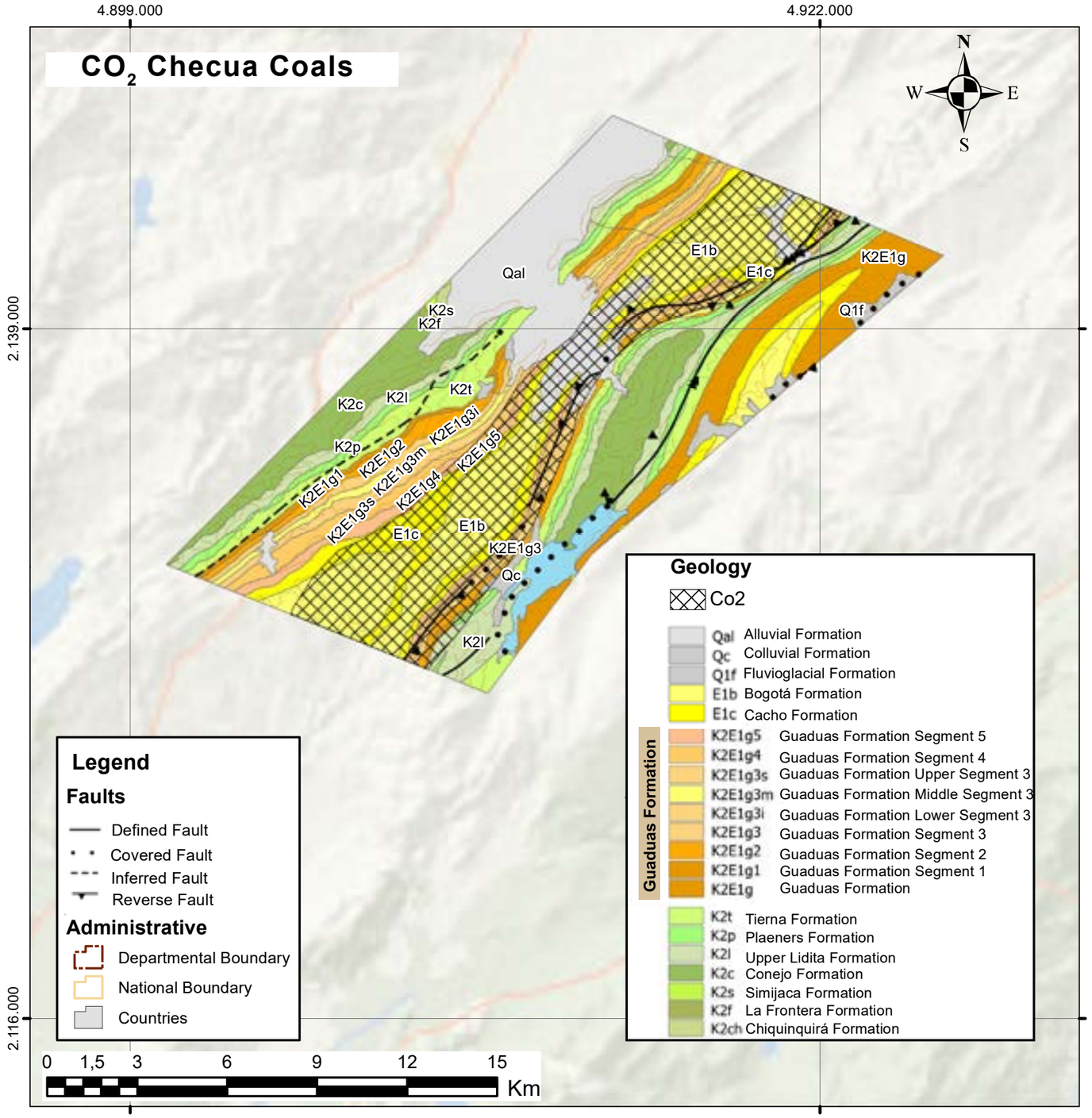

Figure 43. Map of Identification of Areas with CO_2 Storage Potential in Coal Beds.

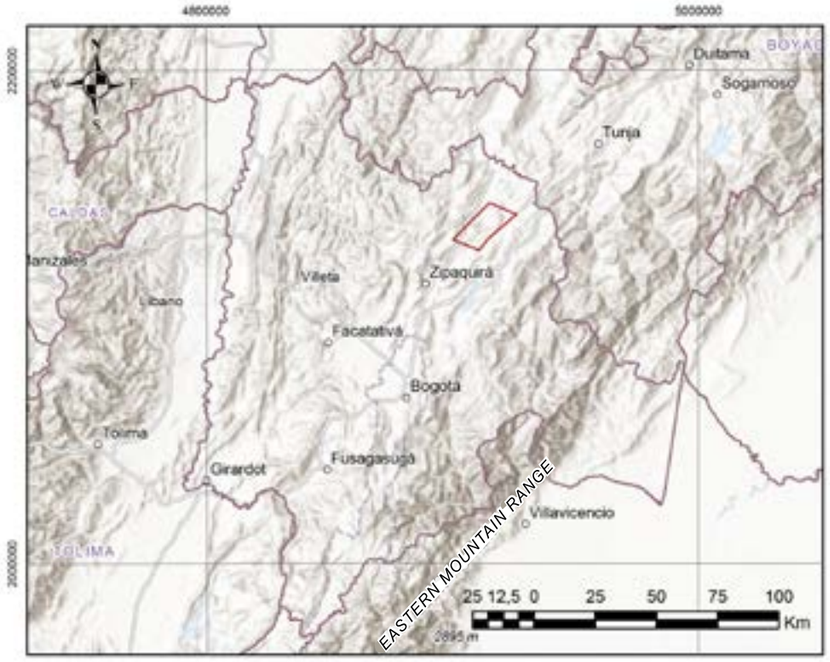

Figure 44. Map of the Location of the CO_2 Storage Potential Area in Coal Beds in the Boyacá Coal Region.

The Checua-Lenguazaque area, located in the central region of Colombia, spans the northeastern edge of the Cundinamarca coal zone and the southwestern edge of the Boyacá coal zone. This elongated strip, covering approximately 182 km², extends from the municipality of Samacá in Boyacá to the municipality of Nemocón in Cundinamarca.

The area lies within the Checua-Lenguazaque syncline, whose structure is controlled by thrust fault systems, including the following main faults:

- **Cambrás Fault:** Oriented south-north to north-northeast, with a northwest (NW) vergence. It thrusts Upper Cretaceous and Paleogene rocks over Neogene rocks.
- **Bituima-La Salina Fault:** Oriented south-southwest to north-northeast, also with a NW vergence.
- **Servitá Fault:** With a northeast (NE) vergence, it thrusts Paleozoic rocks over Cretaceous and Cenozoic rocks.

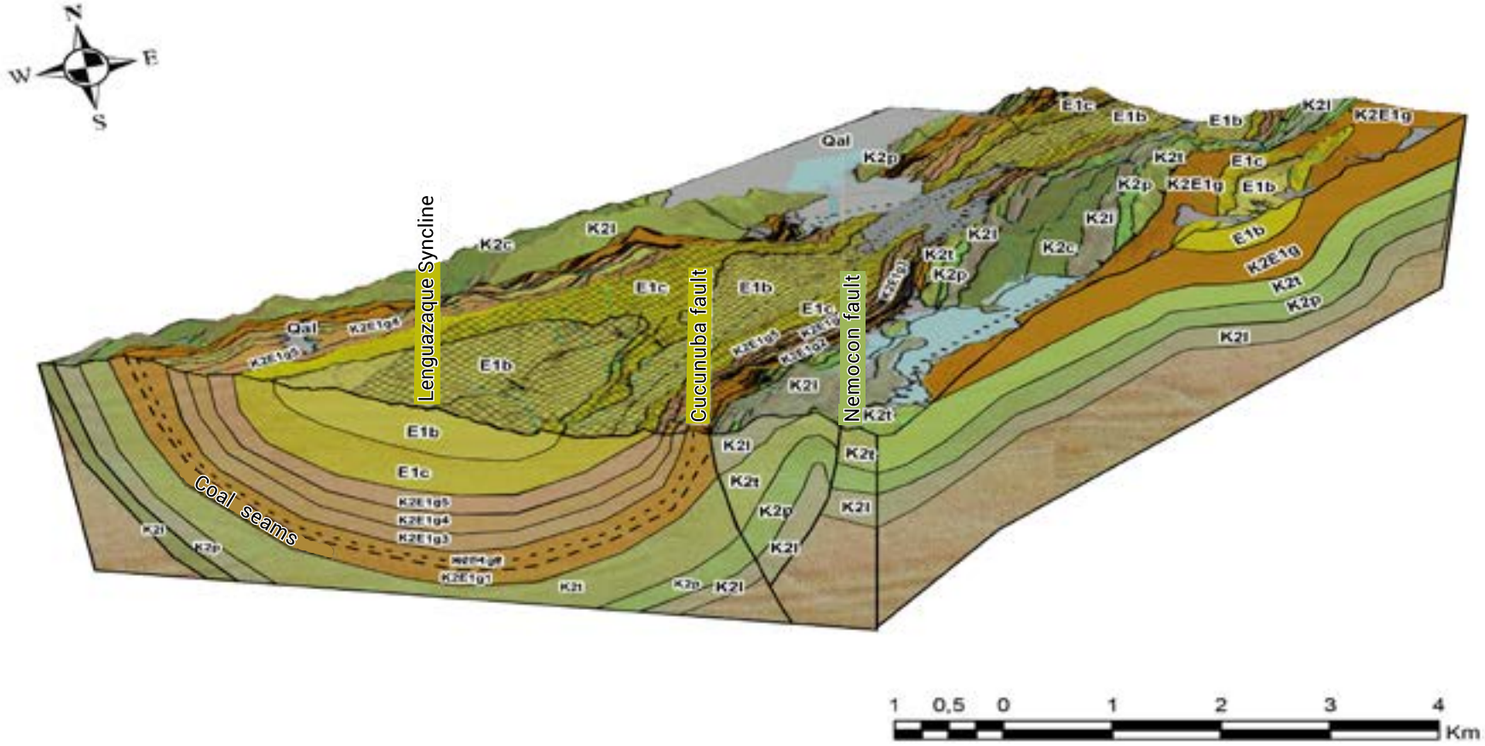

Figure 45. Block Diagram of the Checua - Lenguazaque Area and Projection of the Zone with CO_2 Storage Potential in Coal Seams.

While there are other minor faults in the area, these three are the main ones controlling the structural configuration.

From a geological perspective, the coal seams in this area primarily belong to the Guaduas Formation, known for its variability in coal quality, ranging from thermal coals to those suitable for metallurgical use. The formation consists of interbedded shales, sandstones, and bituminous coal seams.

The Checua-Lenguazaque Area spans an extension of 182 km², equivalent to 182,000,000 m². The Cisquera and Siete Bancos seams, the main coal formations in this region, have a cumulative thickness of 6 meters.

An analysis of the coals in this syncline reveals moderate ash content and a high proportion of fixed carbon, indicating a suitable matrix for gas adsorption. In this context, a reasonable theoretical value for Cs,max is 18 m³/ton. For this calculation, the standard density of CO_2 is set at 1.977 kg/m³, and the Ecoal, or CO_2 storage efficiency factor, is established at 0.7.

Geologically, the area is dominated by the Guaduas Formation, which outcrops along the axis of the Checua-Lenguazaque syncline. Overlying this formation are the Cacho and Bogotá formations, with thicknesses reaching up to 300 meters in the core of the syncline. The Cisquera and Siete Bancos seams, each with a thickness of 3 meters, represent the main potential for CO_2 storage. Only sections of these seams located at depths exceeding -800 meters from the surface are considered.

Additionally, the interbedded lithological layers of silty mudstones and claystones, characterized by low permeability and high retention capacity, serve as essential natural seals to prevent leakage.

CO_2 Storage Capacity

The storage capacity in this area is calculated using the following equation:

$GCO_2 = A\ hg\ Cs,max\ \rho CO_2 std\ Ecoal$

Where:

- A: Geographical area delimiting the basin or coal region for the CO_2 storage calculation.
- hg: Gross thickness of the coal seams evaluated for CO_2 storage within the determined basin or region.
- Cs,max: Maximum standard volume of CO_2 adsorbed per unit mass of in situ coal, assuming complete CO_2 saturation and dry, ash-free coal conditions (requires prior conversion).
- $\rho CO_2 std$: standard density of CO_2.
- Ecoal: factor de eficiencia de almacenamiento de CO_2 que refleja la fracción del volumen total de carbón a granel en contacto con el CO_2.

$GCO_2 = 182.000.000 m^2 * 6m * 18\ m^3/ton * 1,977 kg/m^3 * 0,7$
$GCO_2 = 27,21$ million tonnes
Equivalent to 24,91 kg de CO_2 per m^3 of coal.

6.3.2.2 Guajira south area: characterization and potential for CO_2 storage

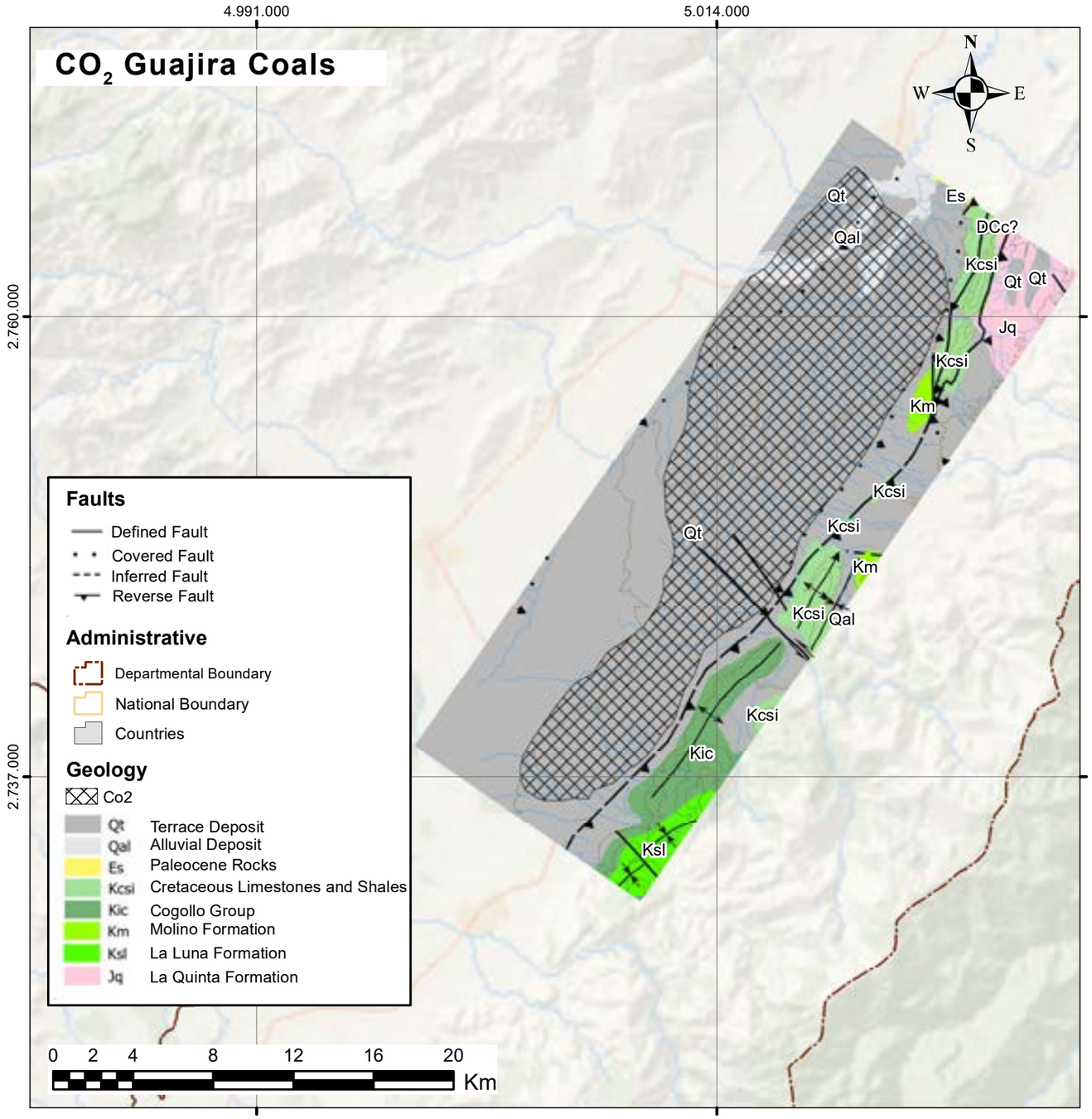

Figure 46. Geological Map of the Guajira South Area and Projection of the Zone with Potential for CO_2 Storage in Coal Seams.

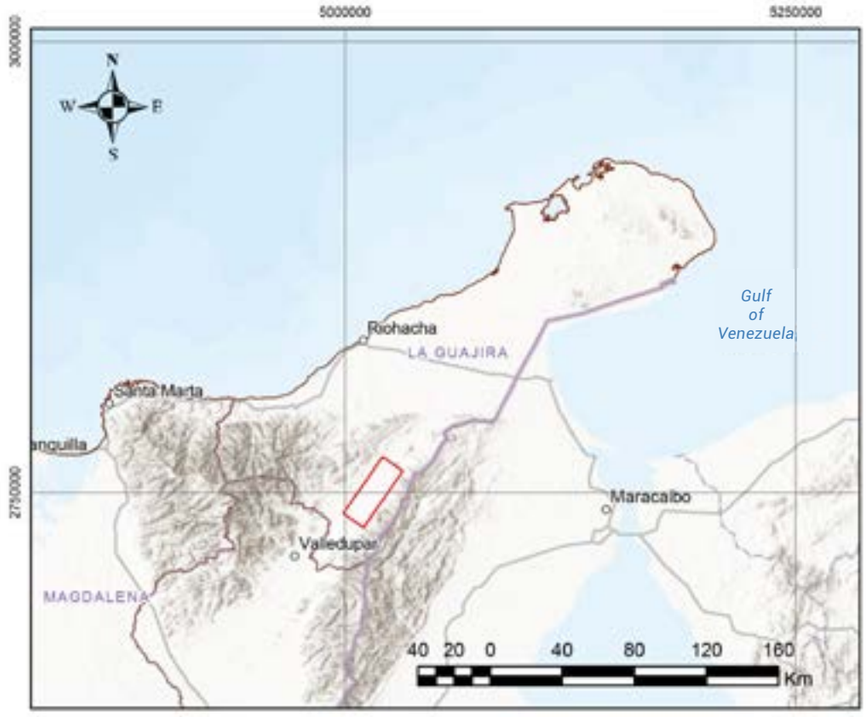

Figure 47. Location Map of the Area with Potential for CO_2 Storage in Coal Seams, Guajira South Area.

The Guajira Sur area is located in northern Colombia, within the department of La Guajira, specifically in the southern portion of the La Guajira coal zone. It covers an approximate area of 228 km², encompassing the municipalities of Fonseca, San Juan del Cesar, and El Molino.

In this region, the main host unit is the Cerrejón Formation, dating to the Paleocene, with a variable thickness ranging between 600 and 1,400 meters. This formation consists of an interbedded sequence of gray and black clayey-silty shales rich in organic matter, fine-textured and well-laminated, feldspathic sandstones, and coal seams.

The observed lithological alternation reflects homogeneous sedimentary cycles in low-energy environments, such as lacustrine settings, explaining the fine lamination of the shales.

It also includes anoxic environments, such as swamps or floodplains, capable of preserving organic matter, which led to the formation of bituminous coal seams and carbonaceous shales.

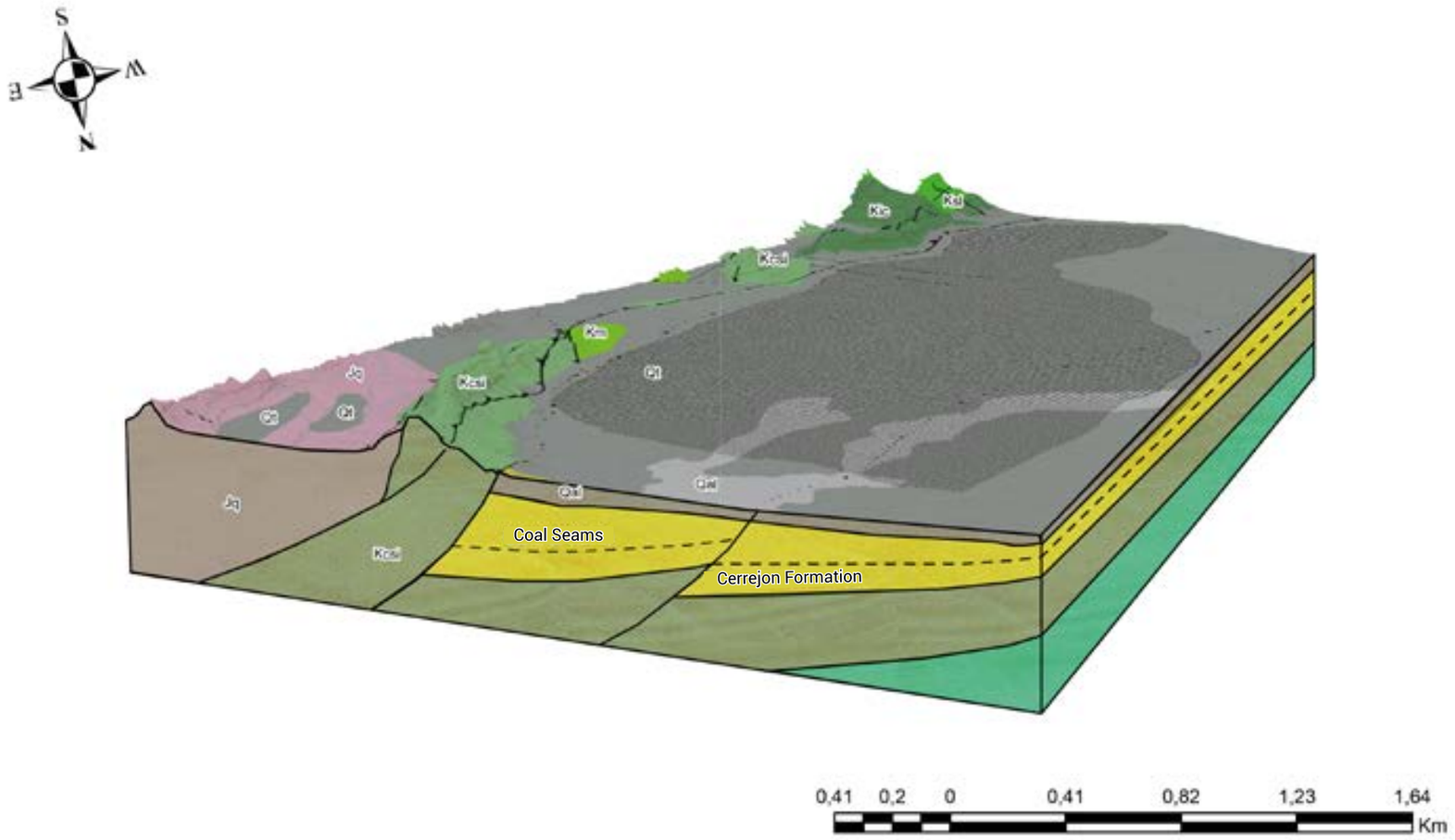

Figure 48. Block Diagram of the Guajira South Area and Projection of the Zone with Potential for CO_2 Storage in Coal Seams.

From a structural perspective, the La Guajira coal zone is dominated by the Oca fault system, which delimits the northern boundary of the basin and interrupts thrust trains trending northeast. These structures resulted from tectonics associated with the Cerrejón Formation. Additionally, in the eastern part of the basin, a shallow-dipping monocline is locally affected by reverse faults that form the mentioned thrust trains (Figure 46). The depth of the Paleogene sequence, where the Cerrejón Formation is located, enhances the conditions for CO_2 storage.

The Guajira Sur area spans approximately 228 km² (equivalent to 228,000,000 m²). The estimated thickness of coal seam 045 is 6 meters. The coal characteristics in this region, such as high fixed carbon content, moisture, volatile matter, and low ash content, indicate a suitable matrix for gas adsorption. For this reason, a theoretical value of Cs,max of 18 m³/ton is considered reasonable.

The standard density of CO_2 used in this calculation is 1.977 kg/m³, and the Ecoal or CO_2 storage efficiency factor is set at 0.7.

In this area, the coal-bearing Cerrejón Formation is homogeneously distributed. Based on the interpretation of various seismic programs conducted in the Ranchería River basin and exploratory drilling such as El Molino-1 and El Molino-1X wells, the Cerrejón Formation is estimated to lie beneath recent deposits with an average thickness of 450 meters. These deposits, known as the conglomeratic suite, form a surface cover in the area.

Storage Capacity

$GCO_2 = A\ hg\ Cs,max\ \rho CO_2 std\ Ecoal$

Where:

- A: Geographical area delimiting the coal basin or region for CO_2 storage calculation.
- hg: Gross thickness of the coal seams for which CO_2 storage is evaluated within the basin or region defined by A.
- Cs,max: Maximum standard volume of CO_2 adsorbed per unit volume of in-situ coal; assumes 100% CO_2 saturation conditions. If the coal is free of dry ash, conversion is required.
- $\rho CO_2 std$: Standard density of CO_2.
- Ecoal: CO_2 storage efficiency factor reflecting the fraction of the total bulk coal volume that comes into contact with CO_2.

6.3.3 CO_2 Storage in basalts

The search for basalts in Colombia is based on the work and research carried out in Iceland, specifically the CarbFix project. This project, whose pilot phase lasted nearly a decade, laid the foundation for CO_c fixation in the subsurface through in-situ carbonation in basalts. During 2012 and 2013, approximately 200 tons of CO_2 were injected and mineralized, achieving a 90% efficiency in this process.

The geochemistry of the formations in Iceland is homogeneous, characterized by tholeiitic basalts generated from a decompression melting of an impoverished mantle. For this reason, the exploration of basaltic bodies in Colombia focused on identifying basalts of similar tectonic origin (MORB-type basalts) and comparable geochemical composition (tholeiitic basalts). MORB-type basalts are silica-rich and contain a mineralogical composition including plagioclase, pyroxene, and olivine, sharing similarities with other types of basalts.

In Colombia, it is considered that these basalts are associated with complex tectonic processes, such as subduction and volcanic activity related to the formation of oceanic basins. Tholeiitic basalts are primarily found in the Andes region, where volcanic activity has been prominent. Notable areas include the Colombian massif and the volcanic system of the central Andes. These basalts are part of volcanic sequences that have shaped the topography and landscape of the country.

The geological evaluation of areas with basalt presence in Colombia is carried out considering the chronostratigraphic units defined by the Colombian Geological Survey (SGC) in the 1:1,000,000 scale geological map of Colombia, published in 2023. Three main areas were identified where basalts are predominant rocks and exhibit significant lateral continuity, extending over tens of kilometers (Figura 49).

- **Porosity:** A crucial factor in determining its CO_2 storage capacity. Tholeiitic basalts in Colombia may show variations in porosity due to factors such as geological history and volcanic activity. It is essential to evaluate porosity to estimate the amount of CO_2 that can be stored.

- **Permeability:** The ability of a rock to allow the passage of fluids. Basalts tend to have variable permeability, influenced by rock fracturing and alteration. For CO_2 to be effectively injected, the formations must have sufficient permeability to allow the migration of the gas.

The CO_2 storage capacity in basalts is primarily evaluated through a process known as CO_2 mineralization. This process involves a chemical reaction between CO_2 and the silicate-rich minerals present in basaltic rocks, such as olivine and clinopyroxene, resulting in the formation of stable carbonates, such as calcite or magnesite.

This capacity serves as a fundamental benchmark for selecting geological CO_2 storage sites. Based on the CO_2 capture mechanism, the mineral storage capacity in basalts can be calculated using documented methodologies, such as those proposed by Zhang et al. (2023).

Equation:

$$m_{CO2}=\sum \rho_r \cdot f_i/n_i \cdot n_{CO2},\ i = CaO,\ MgO,\ FeO$$

$$M_{CO2} = m_{CO2} \cdot A \cdot H \cdot (1-\varphi)$$

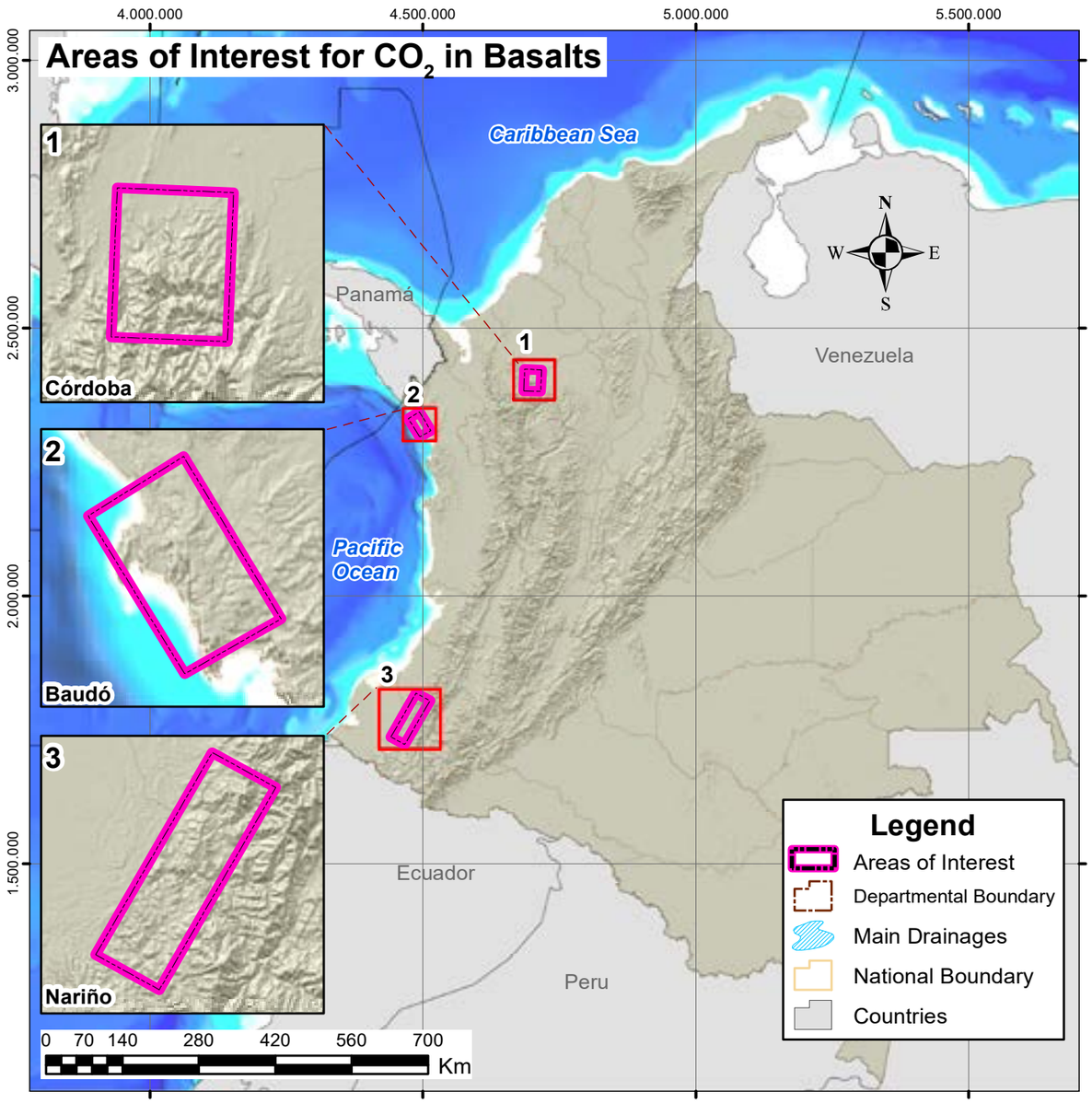

Figure 49. Zones with Morb-Type Basalts in Colombia and Location of the Study Areas for this Project.

Where:

mCO_2= Theoretical storage capacity per unit volume of basalt (t/m3)
ρr: Density of basalt (t/m3)
fi= Mass fraction of CaO, MgO, and FeO in basalts.
ni: Molecular weight of CaO, MgO, and FeO (g/mol).
nCO_2: Molecular weight of CO_2 (g/mol).MCO_2 = is the theoretical mineral storage capacity
mCO_2: Theoretical mineral CO_2 storage capacity in basalts (106t)..

6.3.4 Zone 1 Baudó: characterization and potential for CO_2 storage

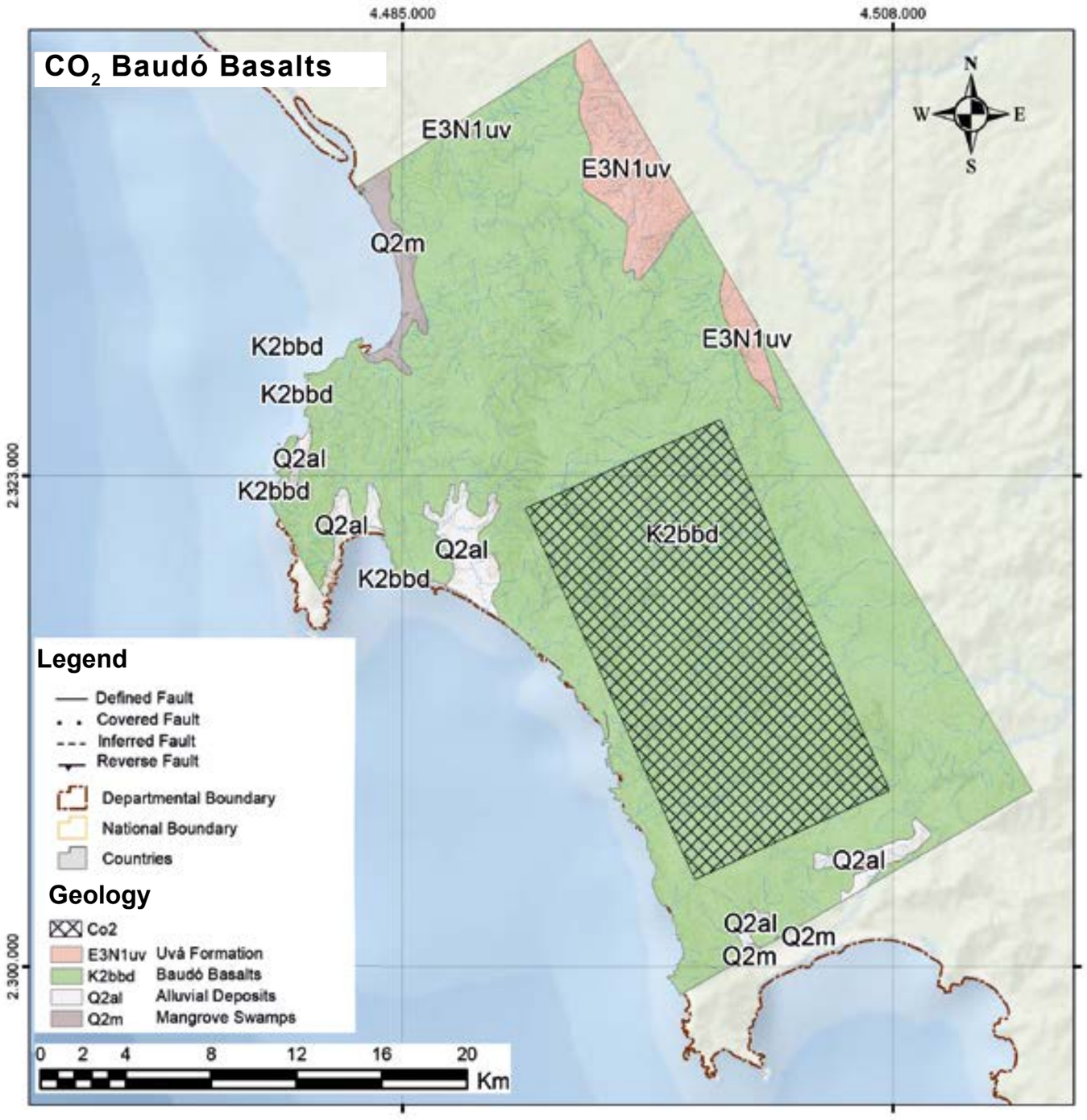

Figure 50. Location Map and Block Diagram of the Baudó Zone.

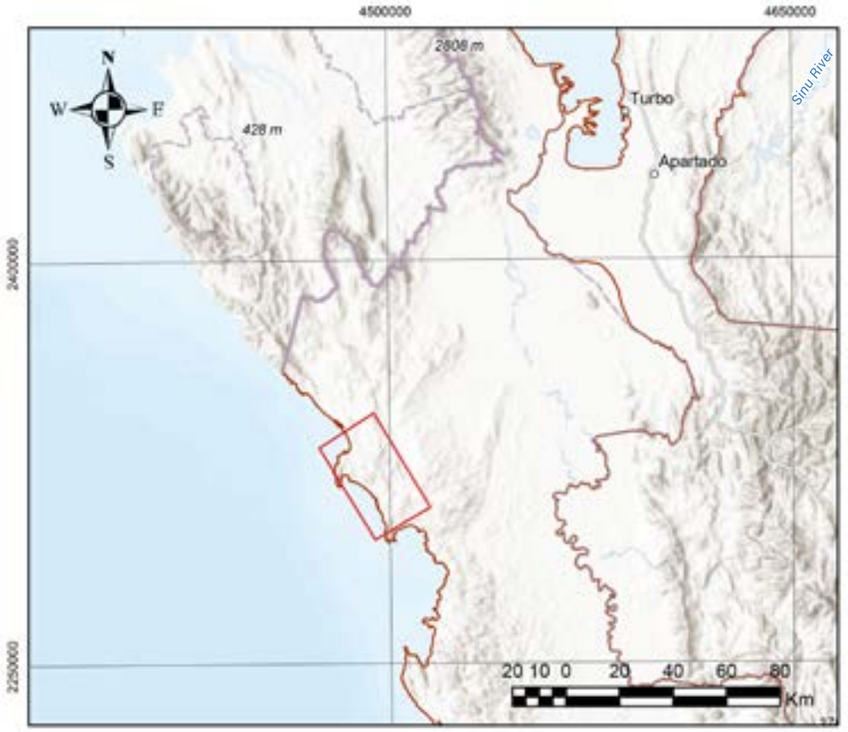

Figure 51. Location Map of the Area with Potential for CO_2 Storage in Basalts in the Baudó Area.

The basalts of the Baudó Mountain Range are located in the department of Chocó, in the northern sector of the Colombian Pacific coast, near the border with the Republic of Panama, and to the south, bordered by the coastline with the Pacific Ocean. The Baudó Mountain Range, also known as the Serranía de Los Saltos, consists of basalts and diabases with minor intercalations of chert, tuff, and tuffites. This unit is known as the Baudó Basalts, with a late Cretaceous age (72 to 76 million years). In fresh outcrops, the rocks are massive, hard, aphanitic, and have a greenish-gray to bluish-gray color; it is common to find veins filled with chalcedony and calcite (Cossio, 2002).

The basic rocks are covered by a sequence of sedimentary rocks of marine transitional origin, ranging in age from the Oligocene to the middle Miocene. These lithologically correlate with the Uva, Napipí, and Sierra formations (Ingeominas, 2002). The unit presents excellent, almost continuous outcrops along the cliffs over nearly 200 km of coast from Cabo Corrientes to Panama, as well as in the rivers and streams that drain the western slope of the Baudó Mountain Range (Cossio, 2002).

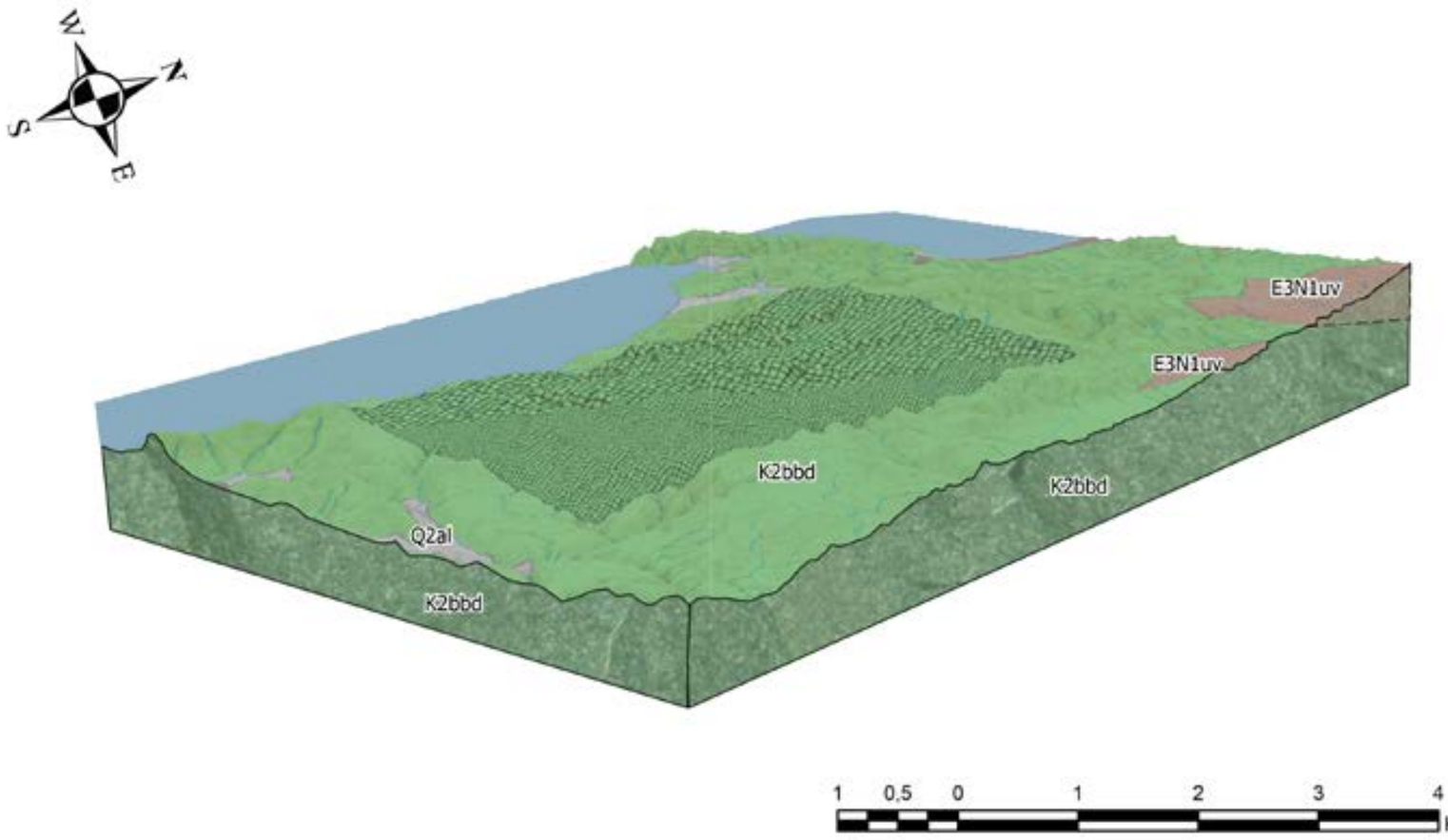

Figure 52. Block Diagram of the Baudó Area and Projection of the Zone with Potential for CO_2 Storage in Basalts.

Various geological mapping works have estimated that the thickness of the Baudó Basalts can reach up to 1000 meters. These rocks may constitute the basement of the basin, so it is assumed that their depth in the subsurface could extend to kilometer levels.

Microscopically, the basalts are composed of plagioclase, pyroxene, glass, opaque minerals, and, in smaller proportions, ilmenite as primary minerals; while the alteration minerals include calcite, epidote, saussurite, sericite, and chlorite. Ingeominas (2002) concludes that the close relationship between basalts, diabases, and the minor intercalations of chert, sandstones, basic tuffs, and calcareous rocks suggests an origin from an oceanic ridge.

The association with jasperoid indicates a reducing exhalative environment with conditions favorable for the precipitation of iron and manganese, linked to basic volcanism processes in oceanic ridge environments (MORB). The basalts of the Baudó Mountain Range, due to their geochemical and mineralogical composition, may have great potential for CO_2 storage, as their magnesium- and calcium-rich components (pyroxene and plagioclase) react with CO_2 dissolved in water, generating immediate solubility trapping. Most of the carbon would be trapped in the minerals through mineral carbonation.

For the Baudó area, assuming an area of 191.7 km² (Figure 51) and a height of 2 km (maximum altitude at Alto del Buey), the volume of the rock body can be calculated using the equation:

Rock volume = area x thickness.

This results in a volume of 383.4 km³.

With the geochemical data, area, and thickness of the rock body, the theoretical storage capacity was calculated using equation 1 and theoretical values of porosity in basalts, molecular weight of CaO, MgO, FeO, and CO_2 density.

Parameters

Baudó

mCO_2: Theoretical storage capacity per unit volume of basalt (t/m³) = 5.323 x 10-⁴

mCO_2: Theoretical mineral CO_2 storage capacity in basalts (Gt) = 297.34

Mass fraction of CaO on average (mol)	0.13
Mass fraction of MgO on average	0.22
Mass fraction of FeO on average	0.076
Porosity (theoretical in fraction	0.05
Density of Basalt (theoretical t/m³)	2.8
Molecular weight of CO_2 (g/mol)	44
Molecular weight of CaO (g/mol)	56
Molecular weight of MgO (g/mol)	40
Molecular weight of FeO (g/mol)	71.8
Area (km2)	191.7
Thickness (m)	2000

6.3.5 Zone 2: Nariño – characterization and potential for CO_2 storage

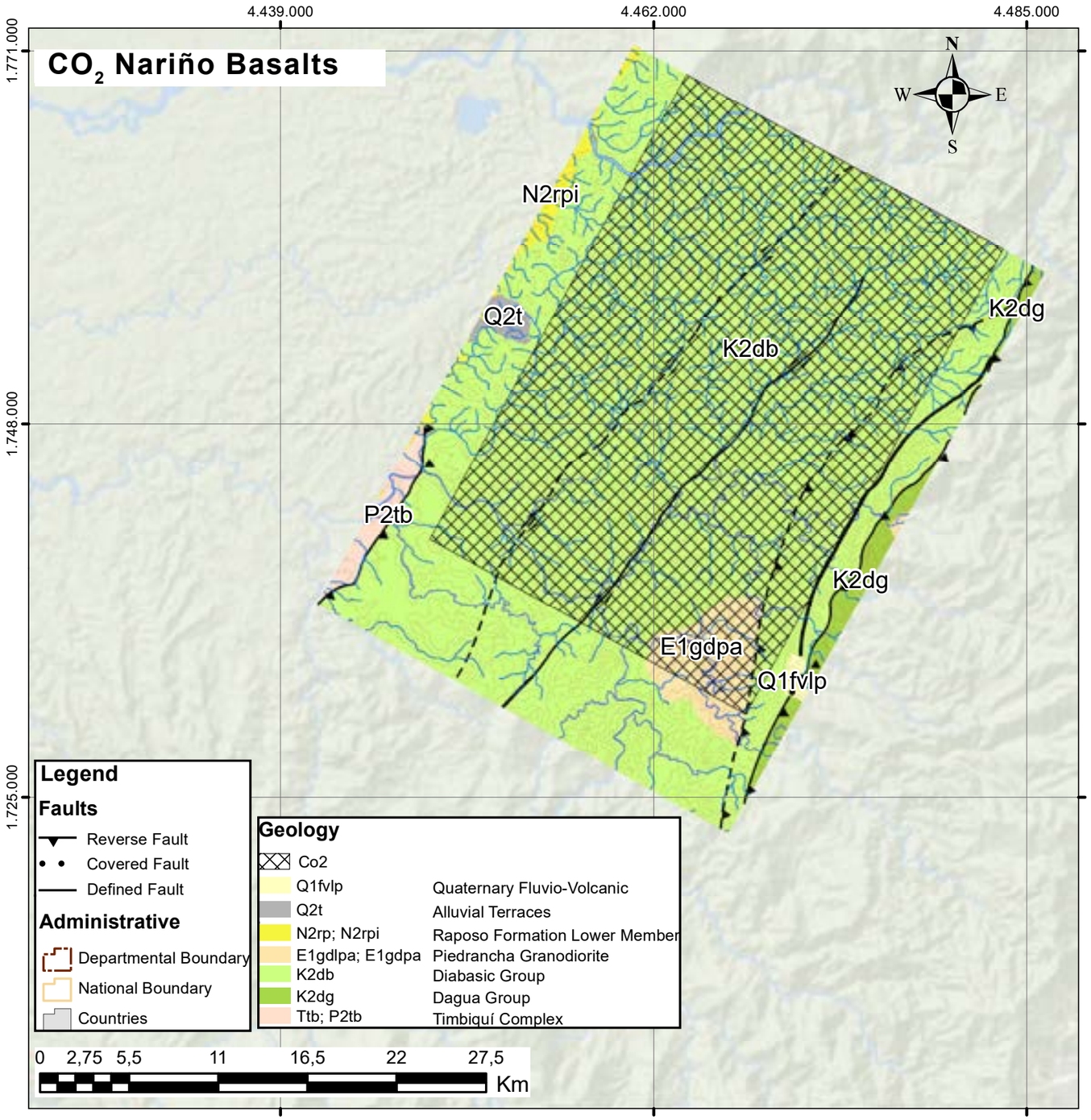

Figure 53. Location Map of the Area with Potential for CO_2 Storage in Basalts in Nariño.

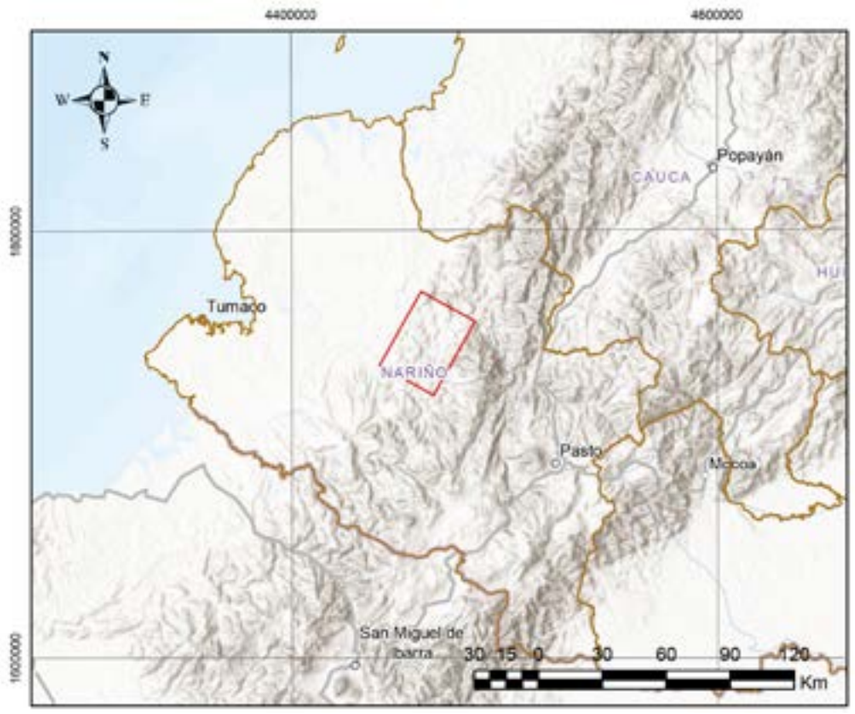

Figure 54. Location Map of the Area With Potential for CO_2 Storage in Basalt Layers in Nariño.

In the department of Nariño and the southern part of the department of Cauca (Mercaderes municipality), basalt units with a tholeiitic affinity of Cretaceous age are reported. These units correspond to what some authors call the Diabase Group, composed of green basalts and gray to gray-green basalt agglomerates. Although the unit is predominantly of volcanic origin, it also contains marine-origin lodolites.

Rocks from the Diabase Group show enrichment in light rare earth elements up to 15.15 times the normal chondrite value, while heavy rare earth elements have an average enrichment of 8 times. The La/Yb(N) ratio ranges between 1.07 and 1.56, and the La/Sm(N) ratio ranges from 0.87 to 1.32, indicating no significant contrast in the enrichment of light versus heavy rare earth elements. For this reason, these rocks are associated with a MORB-type source (ANH, 2012).

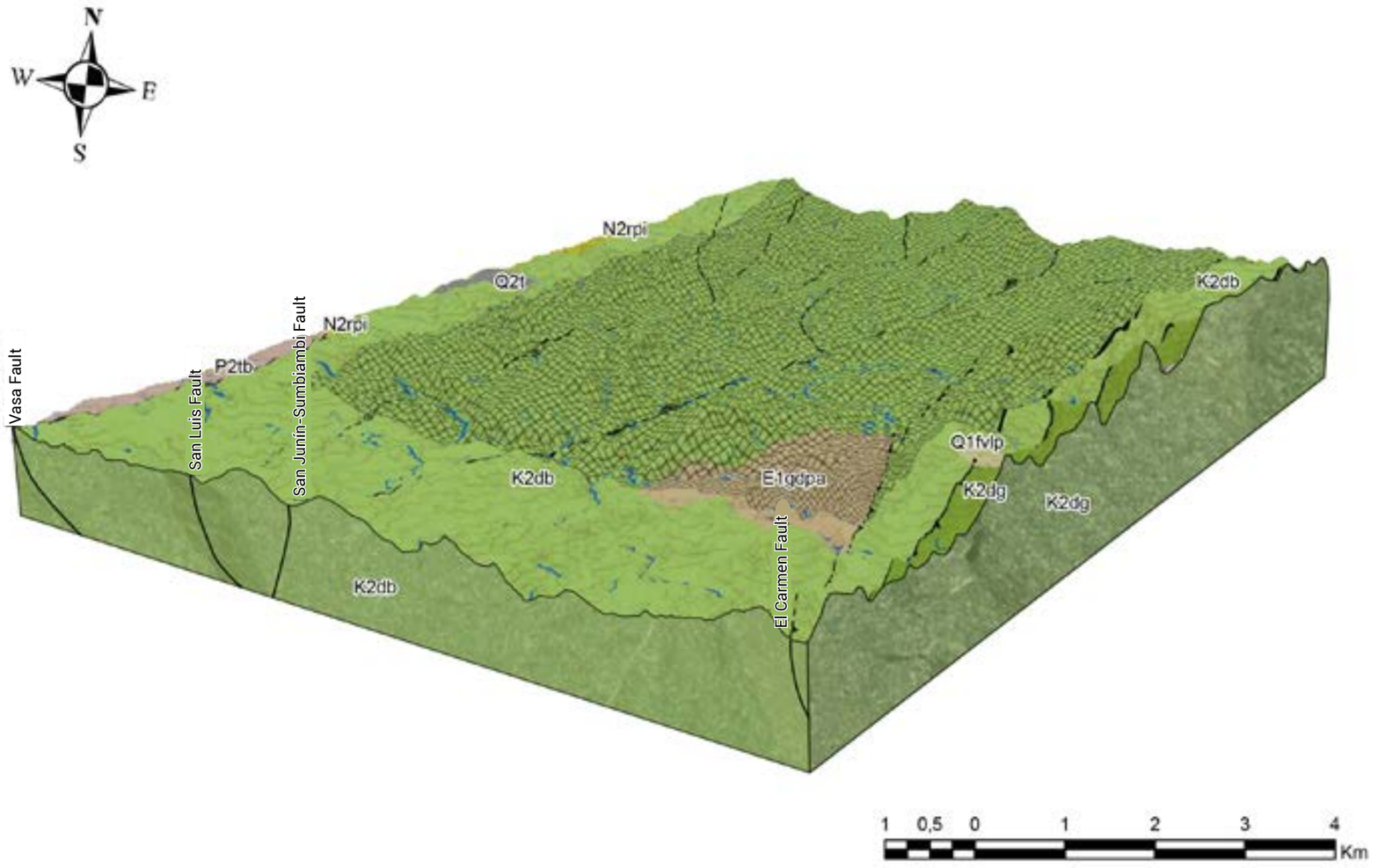

Figure 55. Block Diagram of the Nariño Area For CO_2 Storage in Basalt Seams.

In the Nariño area, a polygon was selected where the Diabase Group outcrops entirely (Figure 54) with an area of 599 km² and an elevation of 1.6 km, allowing the calculation of a rock volume = 958.4 km³. For the theoretical storage capacity calculation, Equation 1 is used along with the theoretical values for porosity in basalts, molecular weight of CaO, MgO, FeO, and CO_2 density:

Parameters

Nariño

Average mass fraction of CaO (mol)	0.13
Average mass fraction of MgO	0.14
Average mass fraction of FeO	0.12
Porosity (theoretical in fraction)	0.05
Basalt density (theoretical t/m³)	2.8
Molecular weight of CO_2 (g/mol)	44
Molecular weight of CaO (g/mol)	56
Molecular weight of MgO (g/mol)	40
Molecular weight of FeO (g/mol)	71.8
Area (km2)	599
Thickness (m)	1600

mCO_2= Theoretical storage capacity per unit volume of basalt (t/m³) = 4.753 x 10-⁴

mCO_2 =Theoretical mineral storage capacity of CO_2 in basalts (Gt) = 428.80

In the Mercaderes region, the Diabase Group appears as a mountainous area with steep cliffs and deep “V"-shaped canyons, reflecting a youthful state of geomorphological development. The structural style is mainly compressional, generating thrusts with fault planes towards the west and a northeast (NE) – southwest (SW) direction, accompanied by a NW – southeast (SE) extensional transversal system, which creates tectonic blocks (Ingeominas, 2002).

6.3.6 Zone 3: Antioquia - characterization and potential for CO_2 storage

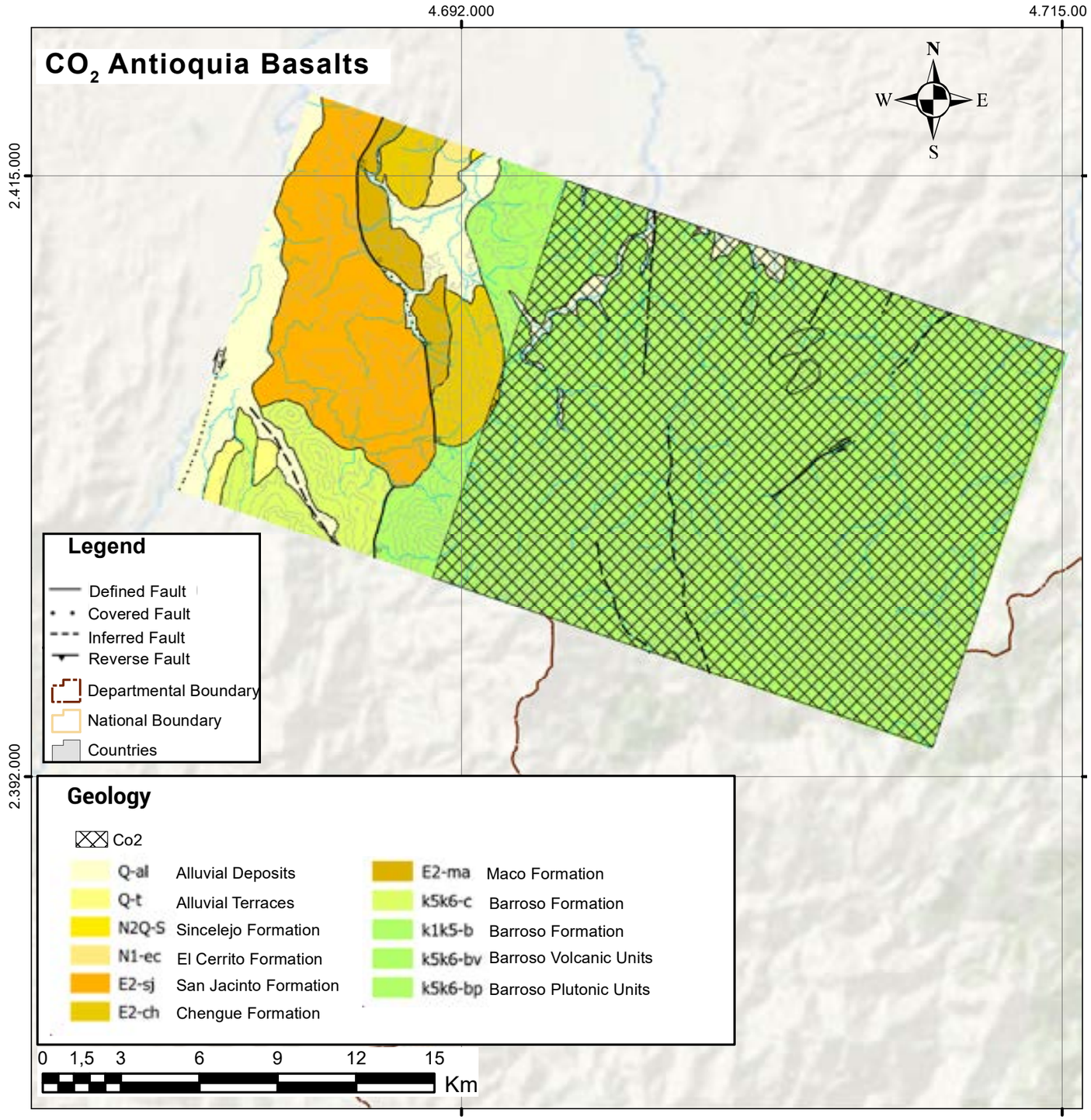

Figure 56. Location Map and Block Diagram for the Antioquia Zone.

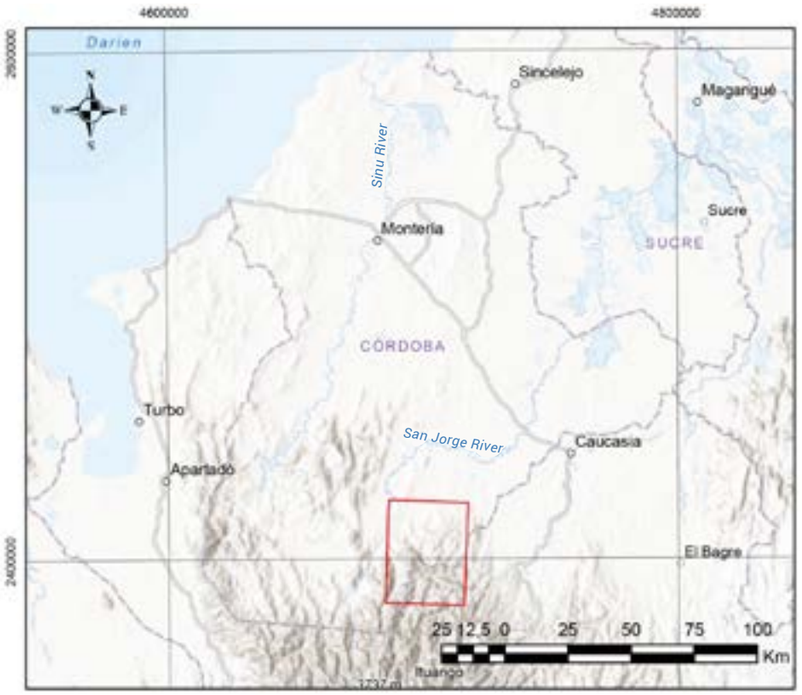

Figure 57. Location Map of Antioquia.

This region includes outcropping units located on the eastern flank of the Western Cordillera (left bank of the Cauca River) and spans parts of the departments of Risaralda, Caldas, and Antioquia. The basalts reported in this area belong to the Barroso Formation.

In the department of Antioquia, the Barroso Formation outcrops on the eastern edge of the northern segment of the Western Cordillera. This formation corresponds to a volcanosedimentary unit composed of basalts and andesites with porphyritic and amygdaloidal textures, alongside agglomerates, tuffs, and marine sedimentary packages (Rodríguez et al., 2013).

In the field, the basalts display ophitic, subophitic, microcrystalline, and amygdaloidal textures. In some cases, the preservation of layering in pillow lava flows is observed. These basalts have a microlitic matrix composed of albite-plagioclase and augite, with amygdales filled with zeolites, quartz, and calcite (Zapata et al., 2017).

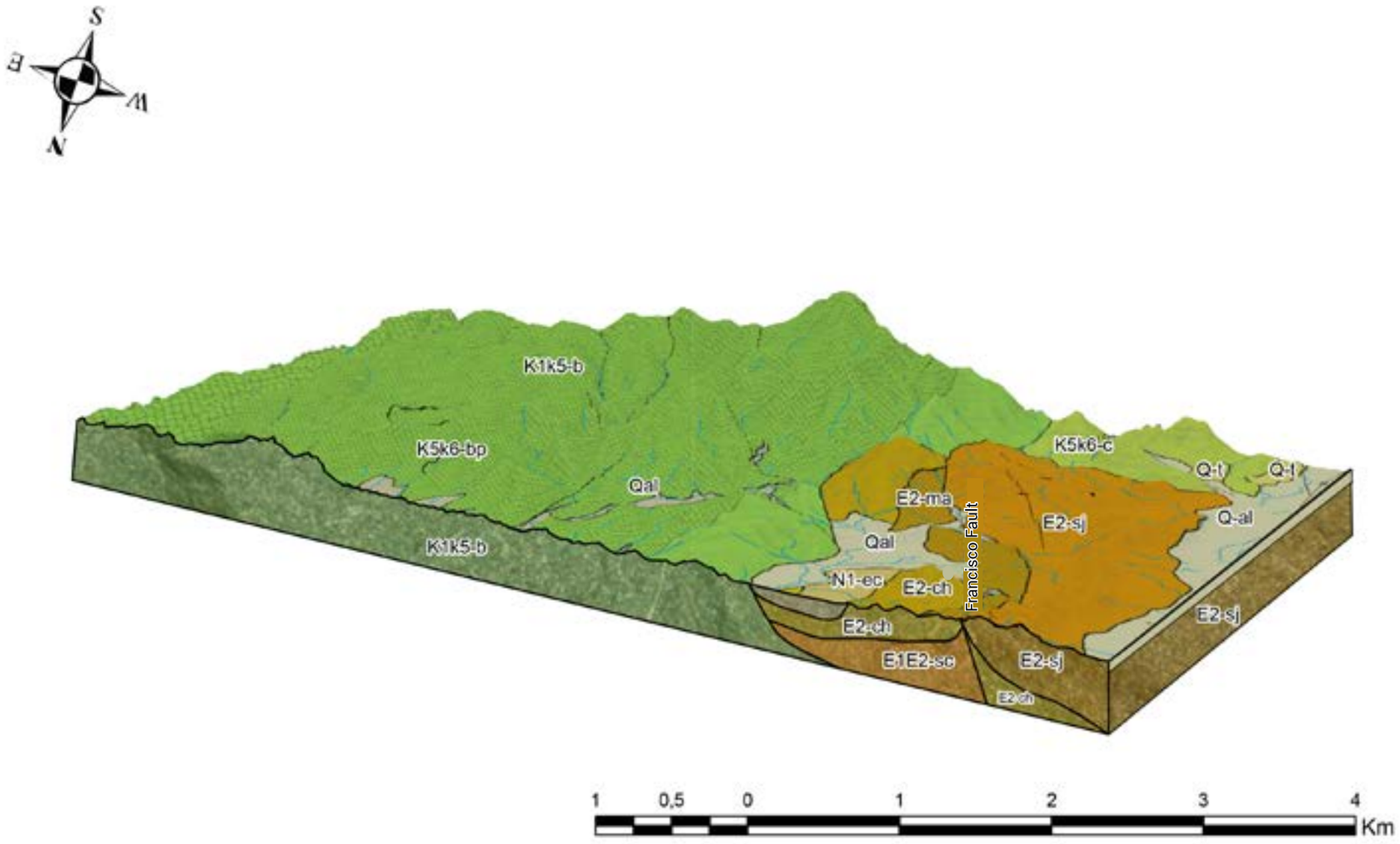

Figure 58. Block Diagram of the Antioquia Area for CO_2 Storage in Basalt Seams.

The geochemical analyses performed by Zapata et al. (2017) for the Barroso Formation reveal considerable values of iron, magnesium, and calcium oxides in basaltic rocks. The Nb/Yb vs Th/Yb ratios show that the basalts have typical E-MORB characteristics and overlap in the Plateau Colombia-Caribbean field. This E-MORB geochemical affinity is comparable to other rocks that make up the Colombian and Equatorial Western Cordillera, as well as the Circum-Caribbean, which are associated with an oceanic plateau environment.

For the Antioquia zone, an area where the entire Barroso Formation outcrops was selected (Figure 57), with an approximate extension of 466 km² and a maximum elevation of 2.2 km, allowing an estimated rock volume of 1025.2 km³.

As with the previous blocks, using geochemical data, area, and thickness of the rock body, the theoretical storage capacity was calculated using Equation 1. For this calculation, theoretical values of porosity in basalts, the molecular weight of CaO, MgO, FeO, and the density of CO_2 were considered.

Parameters

Antioquia

Average mass fraction of CaO (mol)	0.205
Average mass fraction of MgO	0.20
Average mass fraction of FeO	0.129
Porosity (theoretical in fraction)	0.05
Basalt density (theoretical t/m³)	2.8
Molecular weight of CO_2 (g/mol)	44
Molecular weight of CaO (g/mol)	56
Molecular weight of MgO (g/mol)	40
Molecular weight of FeO (g/mol)	71.8
Area (km2)	466
Thickness (m)	2208

mCO_2= Theoretical storage capacity per unit volume of basalt (t/m³)= 6.64x10-4

mCO2= Theoretical mineral storage capacity of CO_2 in basalts (Gt) = 649.37

6.4 Serpentinites and geothermal energy

6.4.1 CO_2 storage in serpentinites

The search for serpentinites in Colombia is based on studies and research conducted in Italy (Boschi et al., 2009) and Spain (Barrero, 2012), where the main focus of research is the geochemistry and mineralogy of ultramafic rocks from ophiolitic complexes and serpentinites resulting from their weathering. In Colombia, these complexes were mainly formed during the Mesozoic, a period marked by significant tectonic events in the region.

The geological assessment of areas with serpentinites associated with ophiolites and ultramafic rocks in Colombia was carried out based on the chronostratigraphic units defined by the SGC in the geological map of Colombia at a scale of 1:1,000,000, published in 2023. Two zones with serpentinized ultramafic rocks were identified as candidates for CO_2 storage: Cauca and Antioquia. These zones cover a large surface area and have easy access routes.

6.4.2. Viability of the serpentinite zones

The capacity for CO_2 storage in serpentinites depends on various geological and chemical factors, including:

- **Reactive minerals:** primarily olivine and serpentine.
- **Porosity and permeability of the rocks:** serpentinites typically have low to moderate permeability. However, natural fractures in the rock and techniques such as hydraulic fracturing could improve permeability.
- **Environmental conditions:** pressure, temperature, and availability of water.

The estimation of CO_2 storage capacity in these rocks is based on several key factors, such as the amount of reactive mineral (mainly olivine and serpentine), rock density, porosity, efficiency of the carbonation process, and the extent of the formation. According to Kelemen et al. (2008), these factors allow for the application of a formula to calculate the theoretical storage capacity in serpentinites.

Although there is no single standard formula due to the complexity of the factors involved, an approximate estimation of the storage capacity can be calculated.

$$Q = V \times \phi \times \rho_m \times \left(\frac{MCO_2}{M_m}\right) \times \eta$$

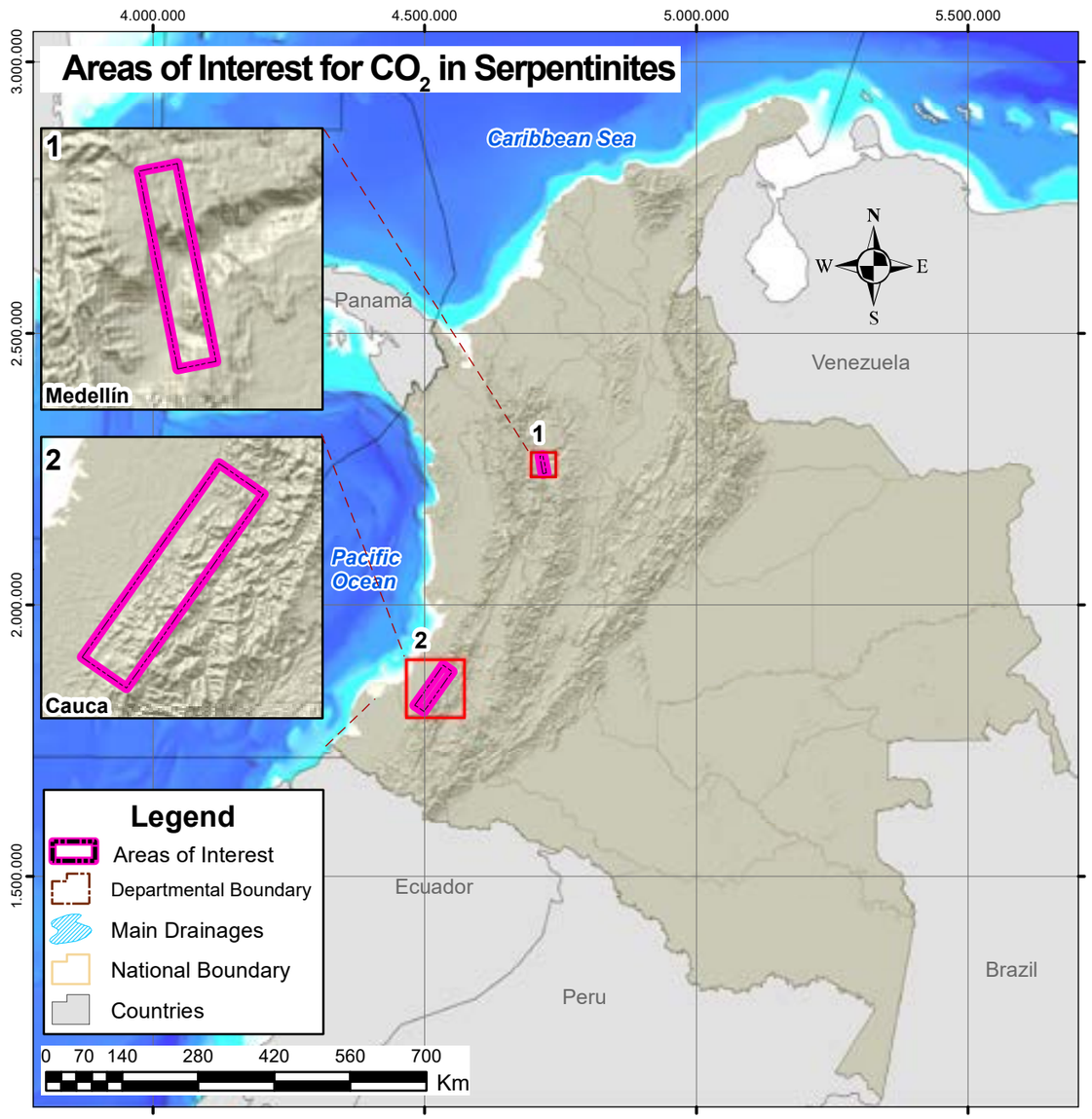

Figure 59. Location Map of the Area with Potential for CO_2 Storage in Serpentinite in Colombia.

Where:

Q = CO_2 storage capacity (in tons).
V = Volume of the rock formation available for CO_2 injection (in cubic meters, m^3).
Ø = Porosity of the formation (fraction, e.g., 0.1 for 10% porosity).
ρm = Rock density (in tons per cubic meter, t/m^3).
MCO_2 = Molar mass of CO_2 (in grams per mole, g/mol) ≈ 44.01 g/mol.
Mm = Molar mass of the reactive mineral (e.g., olivine, $Mg2SiO4$, with Mm ≈ 140 g/mol).
η = Efficiency of the carbonation reaction (fraction, e.g., between 0.5 and 1.0, depending on the rate and efficiency of mineralization).

6.4.2.1 Zone 1 Antioquia: characterization and potential for CO_2 storage

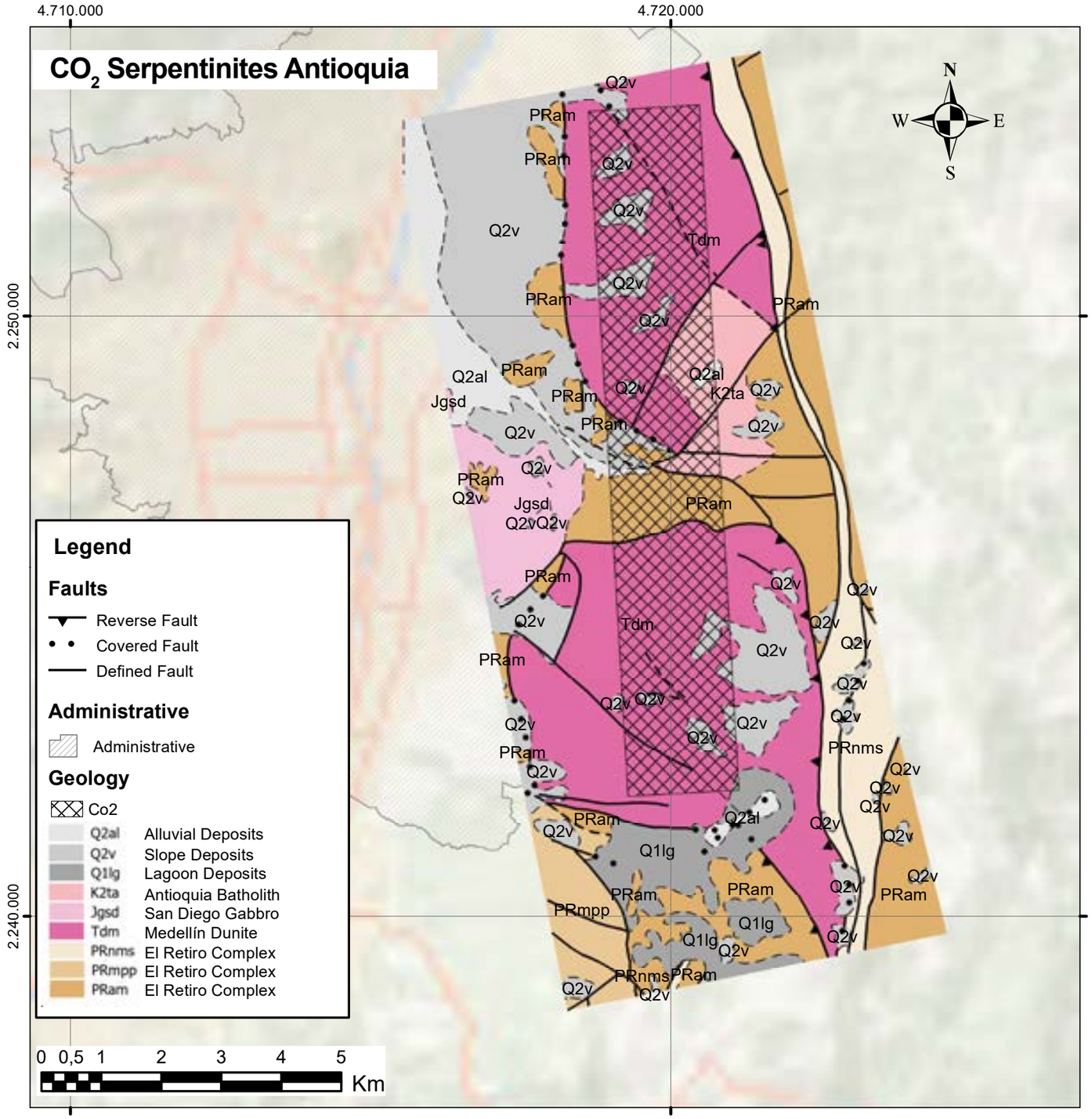

Figure 60. Location Map and Block Diagram of the Area with Potential for CO_2 Storage in Medellín.

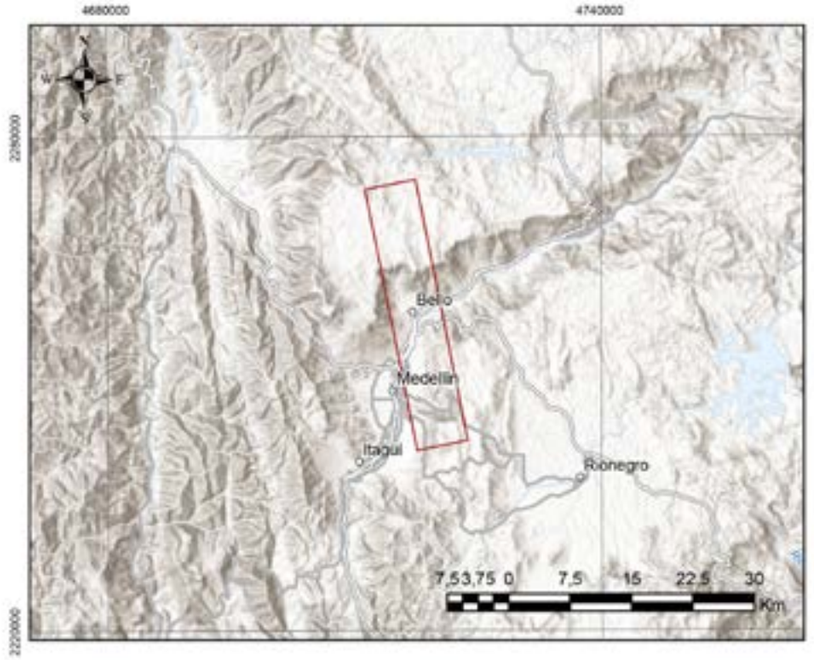

Figure 61. Location Map of the Area with Potential for CO_2 Storage in Serpentinite in the Medellín Area.

This region corresponds to outcropping units located on the eastern flank of the Western Mountain Range (left bank of the Cauca River) and the western flank of the Central Mountain Range, covering the departments of Caldas and Antioquia.

Medellín Dunite

It is a solid rock of olive green color, with a homogeneous appearance and fine-grained texture. It is predominantly composed of olivine, with no presence of pyroxenes, and exhibits variable transformations towards serpentinite, amphibole, talc, chlorite, and magnetite. The minerals of serpentinite are the result of the alteration of the rock, with antigorite being the most common mineral, and smaller amounts of lizardite and chrysotile (Rodríguez, 2005). This rock body has an elongated shape with a NW direction and shows a deformational texture transitioning into mosaic textures with elongated olivine crystals. This structure becomes more evident as the serpentinization process advances.

The CO_2 storage capacity calculation for the Medellín Dunite is obtained using equation :

Parameters

Antioquia (Medellín Dunite)	
Area m^2	21183200
Thickness m	750
Formation Volume (m^3)	1.58x10^10
Porosity (theoretical)	0.1
Rock Density (t/m^3)	2.7
MCO_2	44
Mm	140
n	0.5
Q (ton)	670372428.6

The geochemical characterization of the Medellín Dunite (Rodríguez, 2005) was carried out through chemical analysis of major elements and some trace elements. The dunitic rocks with a lower degree of serpentinization show higher values of MgO, SiO_2, and CaO compared to rocks that have undergone metamorphism or with a higher degree of serpentinization. In contrast, the contents of Al_2O_3 and Fe_2O_3 are lower in these dunitic rocks.

Rocks containing talc and chlorite show lower values of MgO and SiO_2, while the content of Al_2O_3 increases, with no significant variations in CaO. These rocks, particularly those containing talc, were formed through metasomatic processes that introduced SiO_2 from serpentinites and serpentinized dunitic rocks.

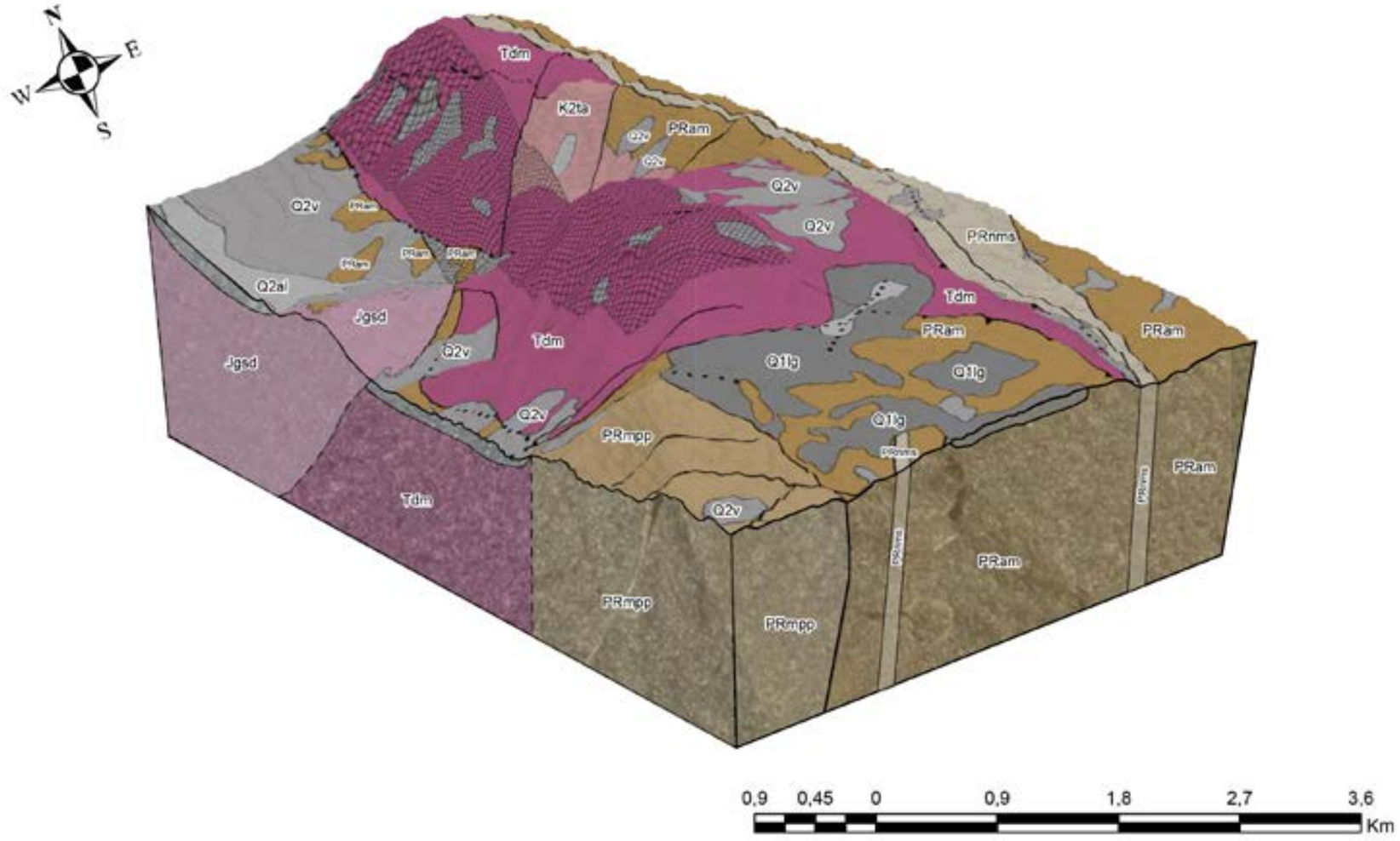

Figure 62. Block Diagram of the Medellín Dunite.

The Medellín Dunite is a geological unit that does not outcrop continuously (Figure 62). It is fragmented into three main bodies (Rodríguez, 2005):

- **South:** Extends from the municipality of Envigado to the Santa Elena stream, with an approximate length of 10 km and an average width of 4.5 km.
- **Center:** Covers the area from the Santa Elena stream to the Medellín River, with a length of 11 km and an average width of 2.5 km.
- **North:** Spans from the municipality of Bello to near San Pedro, in the 146 Medellín Occidental sheet.

6.4.2.2 Zone 2: Cauca - characterization and potential for CO_2 storage

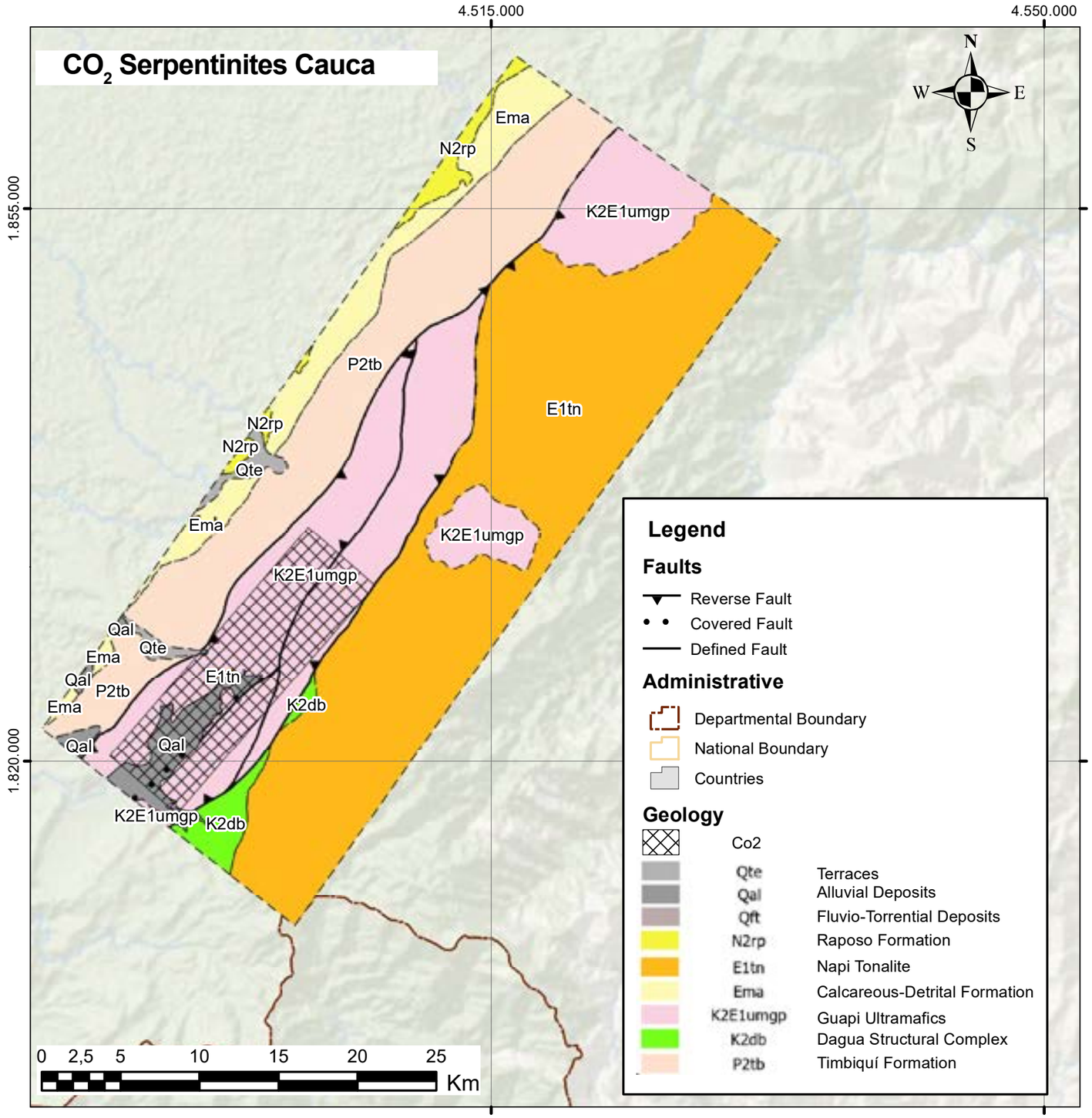

Figure 63. Location map and block diagram for the Cauca area (Guapi Ultramafic Complex). Note. The shaded area is the region used for the CO_2 storage capacity calculation.

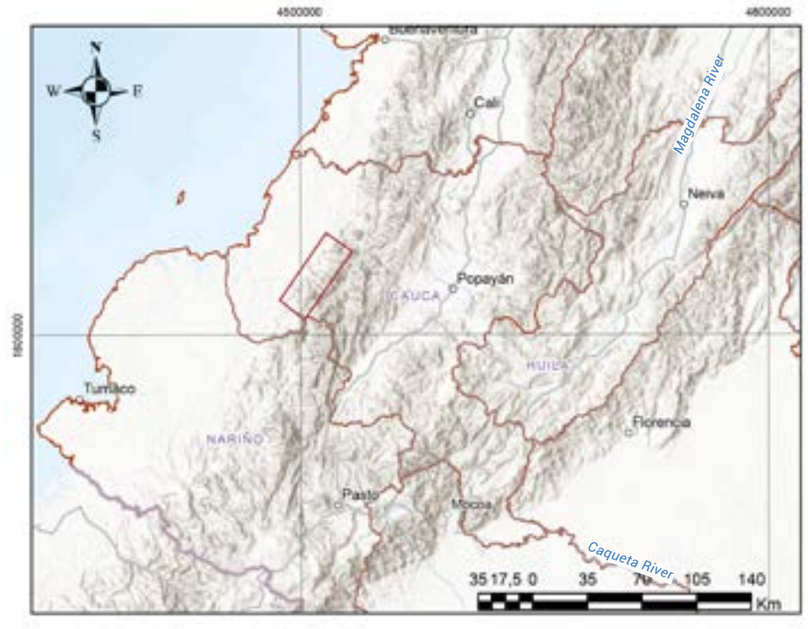

Figure 64. Location Map of the Area with Potential for CO_2 Storage in Serpentinite in Cauca.

Ultramafic rock outcrops are located in the central-eastern part of the department of Nariño. The Guapi Ultramafic Complex is a body that outcrops on the western flank of the Western Mountain Range, in the upper parts of the Guapi River and its tributaries, the Pilpe and Napi rivers (Barbosa, 2003).

The ultramafic and mafic rocks, highly sheared, correspond to "floating" blocks composed of serpentinites, hornblendites, and highly weathered peridotites. Additionally, pale greenish-gray rocks rich in tremolite-actinolite and occasionally antigorite are found. Fresh, undeformed cumulate-type blocks, such as medium-grained harzburgites and fine-grained basalts, are observed along the tectonized ultramafic "floating" block (Barbosa, 2003).

Microscopically, the ultramafic rocks correspond to dunitic rocks, serpentinized dunitas, and harzburgites (ANH, 2014). In the serpentinized dunitas, the predominant serpentine mineral is antigorite, which develops as a pseudomorph of olivine. It forms along fractures and edges of the original crystals, leaving these as islands. Locally, chrysotile develops along reticulated fractures, with short fibrous growth perpendicular to them. Chrysotile is colorless and has low birefringence, with first-order gray interference colors.

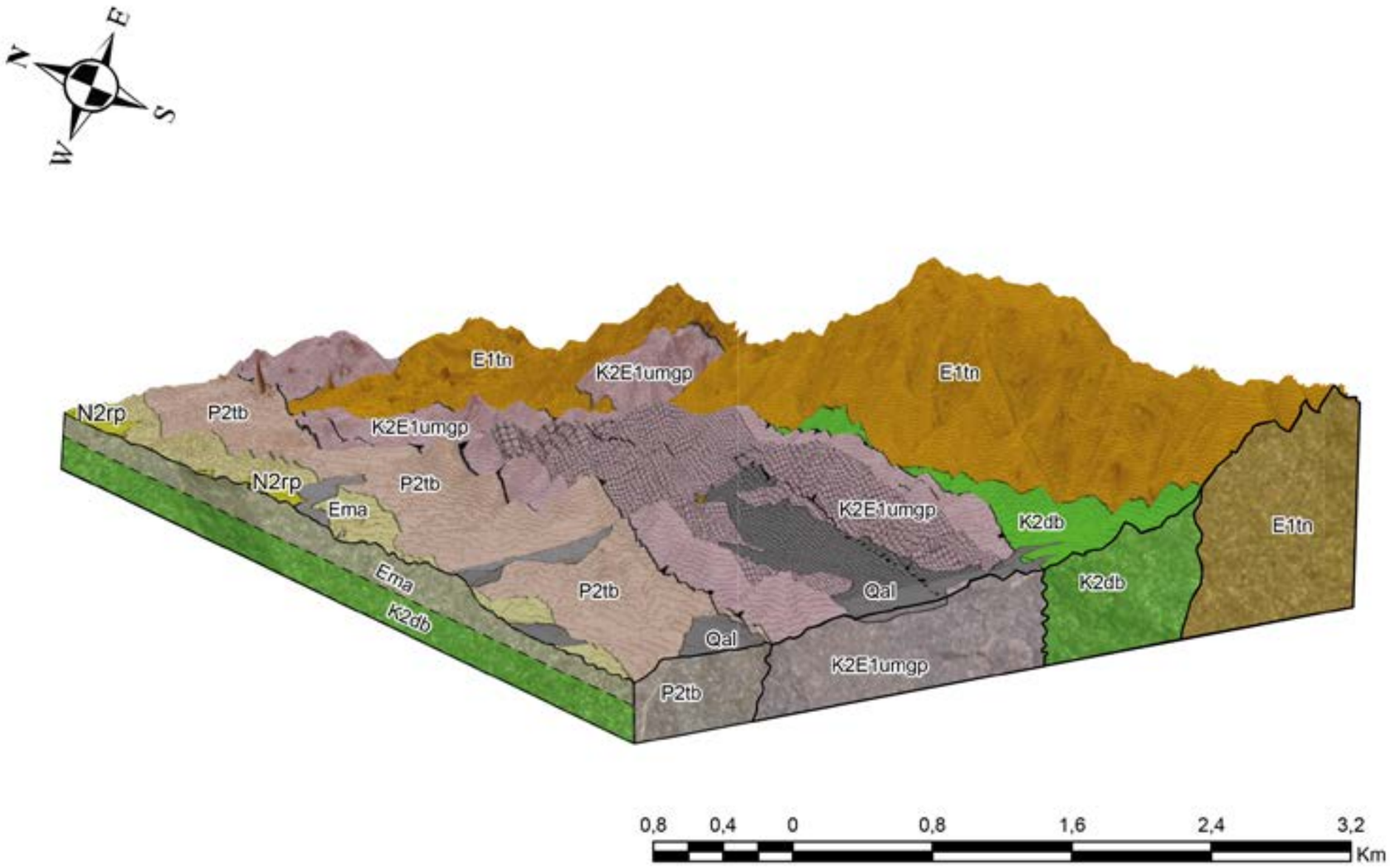

Figure 65. Block Diagram for the Cauca Zone (Guapi Ultramafic Complex).

Since this complex is part of the basement of the Western Mountain Range, it can be inferred that its depth could reach scales of tens of kilometers.

The CO_2 storage capacity calculation for the Guapi Ultramafic rocks is obtained using equation.

Parameters	
Cauca (Guapi)	
Area m2	107299000
Thickness m	1685
Formation Volume (m³)	1.81x10^12
Porosity (theoretical)	0.1
Rock Density (t/m³)	2.7
MCO_2	44
Mm	140
n	0.5
Q (ton)	7.67x10^10

The Guapi Ultramafic rocks are elongated bodies of tectonically emplaced ultramafic rocks that form part of the basement of the Western Mountain Range. These units have an approximate northeast (NE) strike and a length of 45 km, forming a strip of mountain slopes (ANH, 2014).

The Guapi Ultramafic Complex extends from the southernmost part of the Cauca department as an elongated and narrow body with a NE direction. Its approximate area is 145,766 km² (figure 65). This complex is spatially associated to the east with the tonalitic intrusive body of Napi. Locally, it is bounded to the west by basic to intermediate volcanic rocks of the Timbiquí Formation and to the east by the Piedramadura Fault, which separates it from the metasediments of the Dagua Structural Complex and from oceanic basic volcanic rocks of the Diabase Group (ANH, 2014).

6.4.3 CO_2 in geothermal zones of Colombia

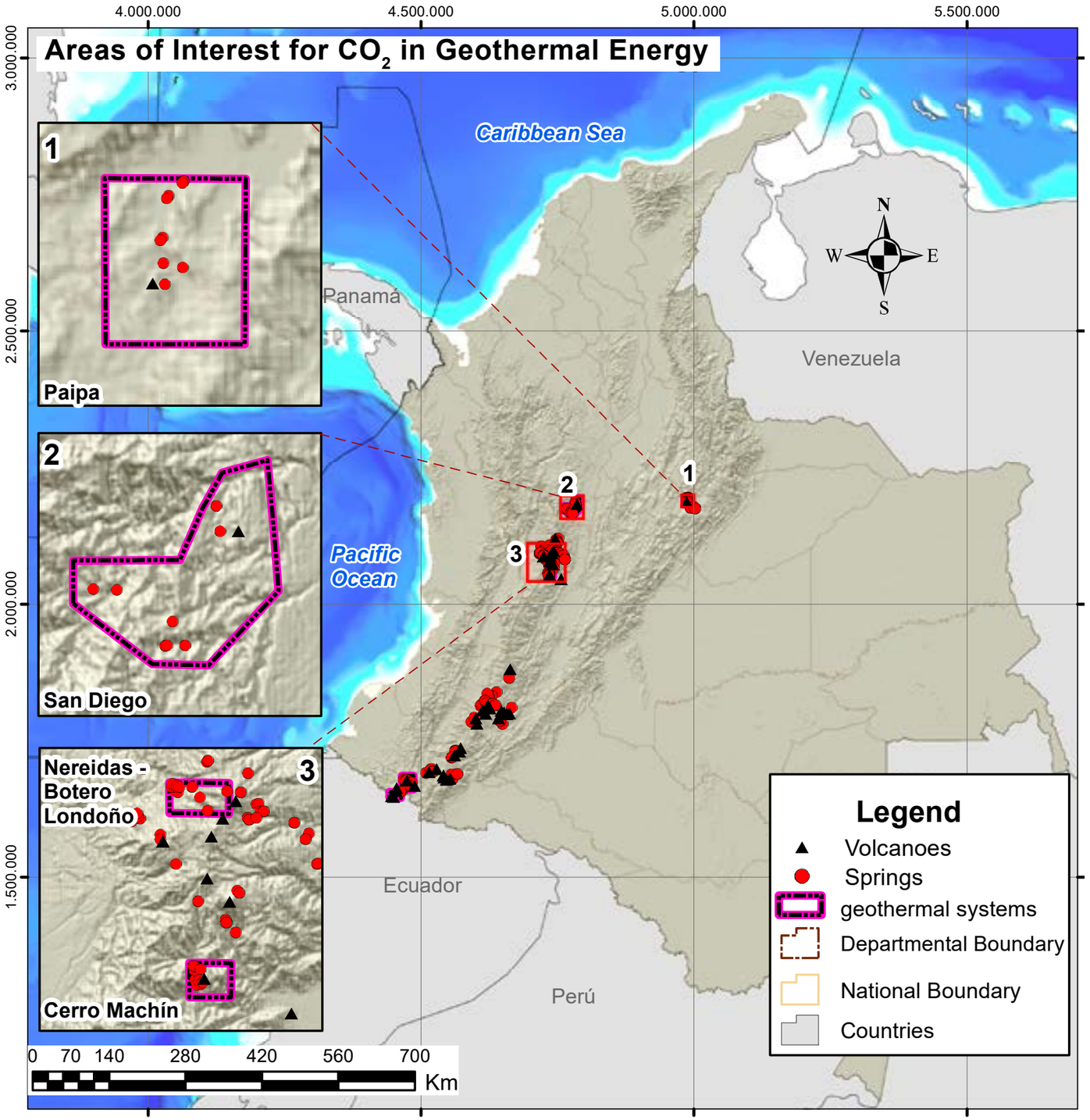

Figure 66. Location Map of the Area with Potential for CO_2 Storage in Geothermal Reservoirs in Colombia.

This work adapted the use of CO_2 as a heat-carrying fluid in geothermal systems, a technology initially proposed in Japan. It was determined that CO_2 must be in a supercritical state, which implies injecting it from a depth of 800 m below the surface. This criterion is the first and most important for evaluating the systems where this technology should be implemented.

To calculate the amount of CO_2 that can be injected into each system, Calhoun's (1982) equation was adopted, which estimates the CO_2 storage volume in saline aquifers, along with the CO_2 storage efficiency factor defined by Bachu (2008). The percentiles used were P10 (1.86%), P50 (2.7%), and P90 (6%), applied to clastic reservoirs.

Four of the 21 volcanic geothermal systems defined by the SGC in Alfaro et al. (2020) were selected, prioritizing those with a conceptual geothermal model and proximity to CO_2 emission sources. The evaluated systems were Paipa, San Diego, Cerro Machín, and Nereidas-Botero Londoño. The evaluation considered the following parameters for CO_2 injection:

- Geothermal reservoir thickness (below 800 m)
- Reservoir area.
- Porosity.
-
- Seal and pH (as secondary criteria).

These systems are located in the following regions:

- Central Mountain Range: Paipa block and San Diego block.
- Cerro Bravo-Cerro Machín: area defined according to the work of Alfaro et al. (2020).

The calculations presented represent an initial approximation for determining the amount of CO_2 that can be injected into these geothermal systems. These values can be refined as the conceptual models are calibrated.

6.4.3.1 Cerro Machín geothermal area

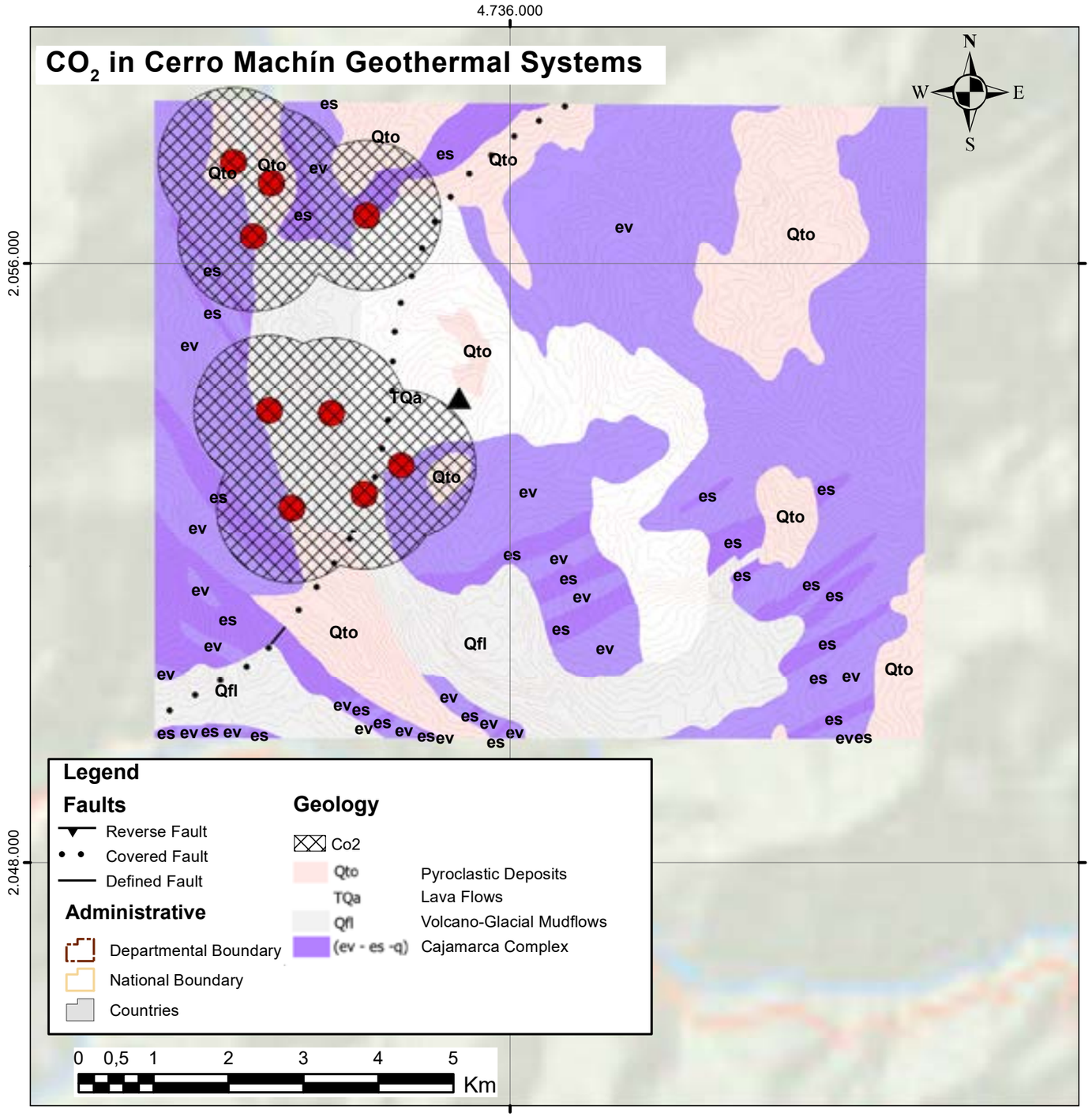

Figure 67. Geological Map of the Cerro Machín Geothermal Area. Note: Red Dots Identify Hydrothermal Springs. The Highlighted Areas Indicate the Impact Zones of the Geothermal Reservoir.

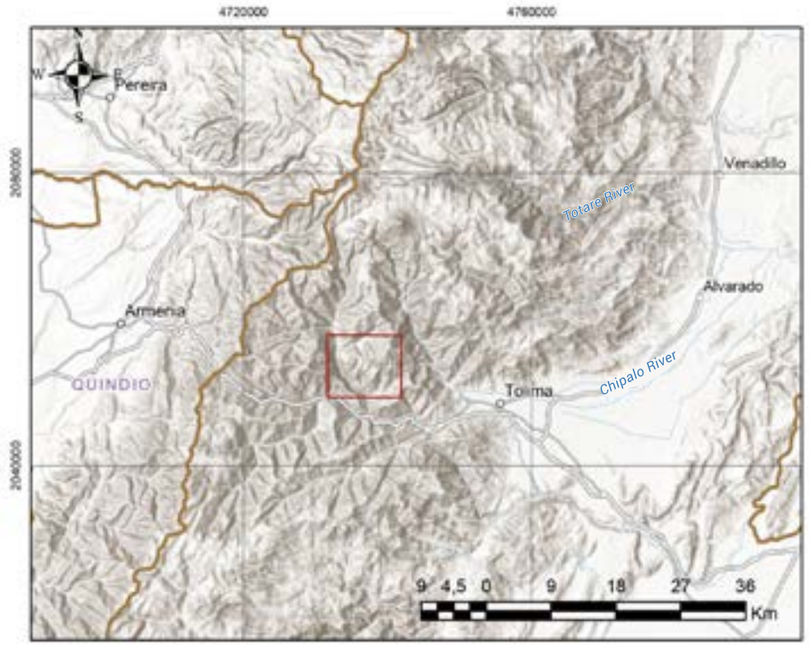

Figure 68. Location Map of the Area With Potential For CO_2 Storage in Geothermal Reservoirs in Cerro Machín.

The Cerro Machín geothermal area is located to the northwest of the Tolima department, near Cajamarca and the corregimientos (rural districts) of Toche and Tapias in Ibagué. In this region, 14 thermal springs are identified, grouped into two zones:

- **Northern Zone:** Near the Toche corregimiento, associated with the Toche River and the San
- **Southern Zone:** Near the crater of the volcano and the Aguacaliente stream.

In the northern zone, calcium bicarbonate waters predominate, while in the southern zone, sodium bicarbonate-chloride waters are more common. The pH values are neutral, ranging from 6.17 to 8.30. The electrical conductivity ranges from 1100 to 3233 µS/cm, and temperatures vary from 32 to 94 °C. The thermal springs in the south emerge from the Cajamarca Metamorphic Complex, while those in the north are related to the deposits of the Toche River and volcanic materials (Alfaro et al., 2020).

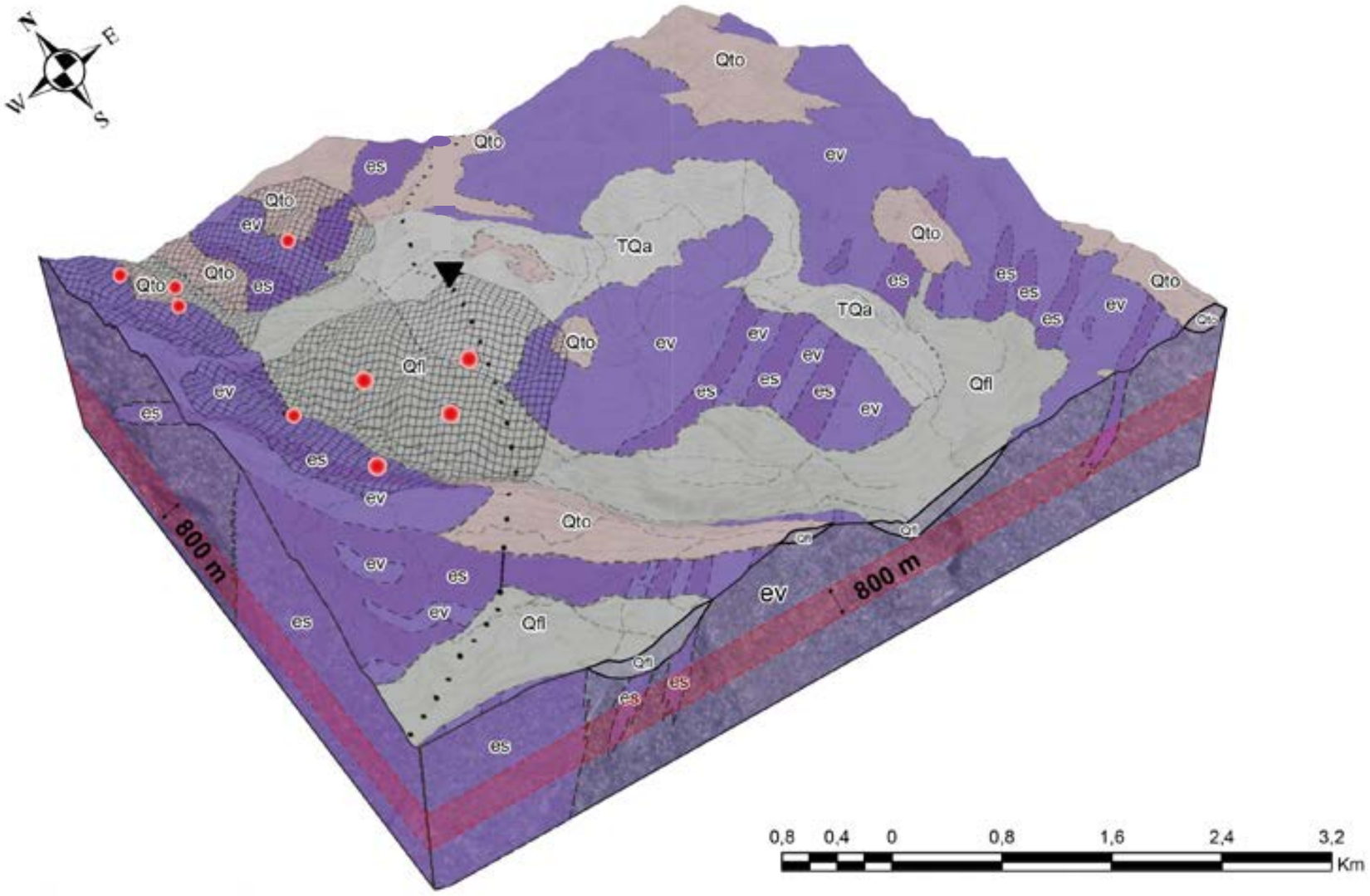

Figure 69. Geological Block Diagram of the Cerro Machín Geothermal Area.

The Cajamarca Metamorphic Complex constitutes the geological basement of the region, overlain by Quaternary pyroclastic deposits. The most prominent structure is the Cajamarca Fault, with a northeast (NE) orientation.

According to Cerpa (2017), the heat source for this geothermal system is related to young magma in the Central Mountain Range, controlled by the subduction of the Nazca and South American plates. The potential reservoir would be the Cajamarca Complex (Mosquera et al., 1982), at an estimated depth of 1.5 km (Alfaro et al., 2020); the lower volcanic layers (Geoconsul, 1992); or the recent lava flows with secondary permeability (Cerpa, 2018).

Rojas et al. (2014) propose a mixed recharge for the thermal springs, composed of water from the Toche River and rainwater that percolates and is heated by the geothermal gradient. Additionally, endogenic waters associated with the Cerro Machín volcano are reported.

The calculation of injectable CO_2 considered the following equation:

$GCO_2 = A*h*\Phi*p*E.$

- Area (A): It was determined as the sum of the expected areas of the northern and southern clusters from the work of Alfaro et al. (2020), resulting in a total of 13.1 km².
- Thickness (h): Based on the profiles of the block diagram, an approximate thickness of 700 m was estimated for the Cajamarca Complex reservoir below 800 m depth.
- Density (ρ): The density of CO_2 at 800 m depth is approximately 750 kg/m³, according to CIEMAT (2006).
- Porosity (Φ): A secondary porosity of 10% was considered, based on the nature and diagenesis of the basement.
- Efficiency Factor (E): The percentiles defined by Bachu (2008) for clastic reservoirs were applied:

- P10 = 1,86%
- P50 = 2,7%
- P90 = 6%

The estimated injectable CO_2 volume for the geothermal system was:

- P10: 12.792.150 tons of CO_2.
- P50: 18.569.250 tons of CO_2.
- P90: 41.265.000 tons of CO_2.

6.4.3.2 Paipa geothermal area

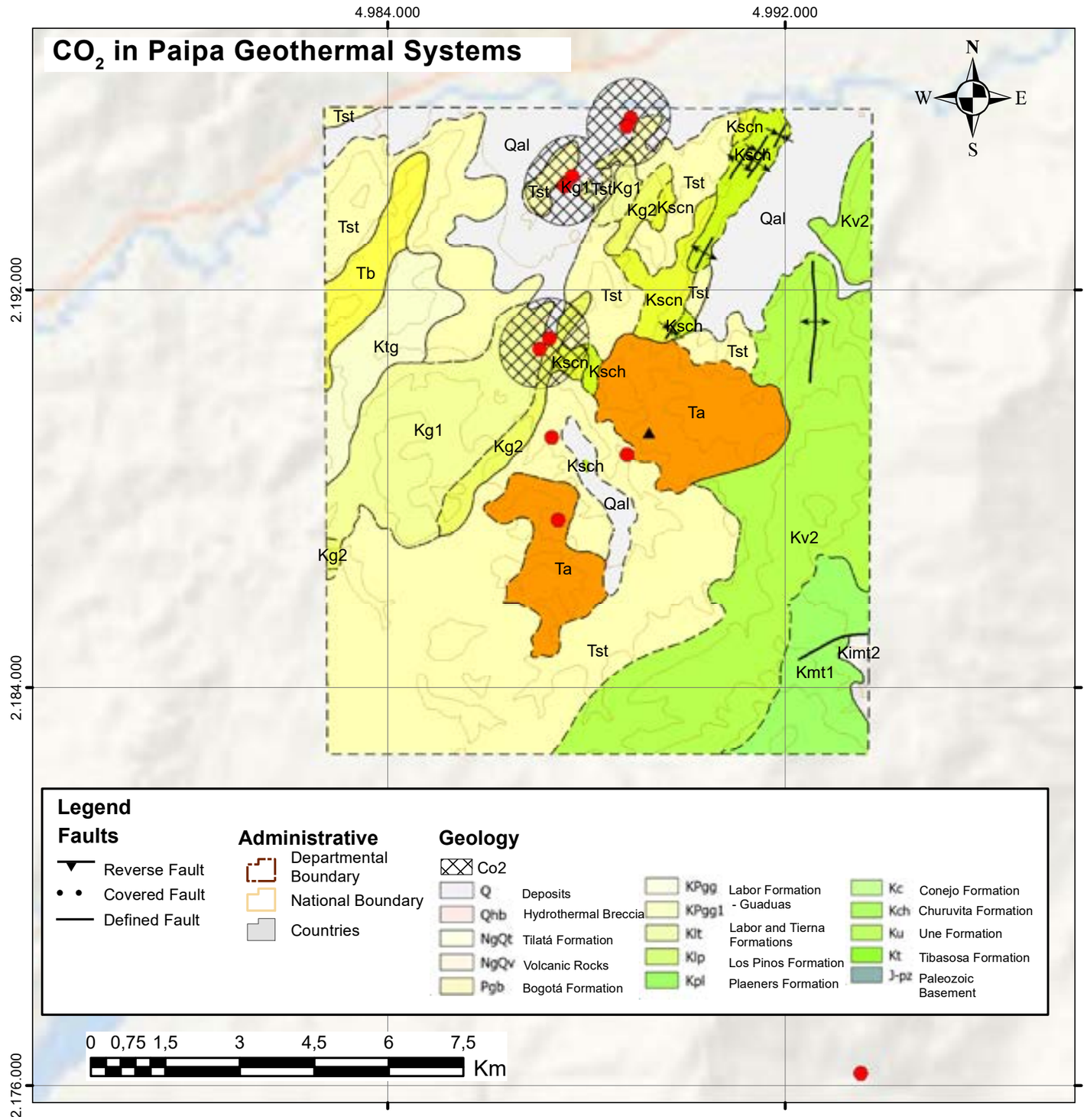

Figure 70. Geological Map of the Paipa Geothermal Area. Note: Red Dots Identify Hydrothermal Springs, and the Highlighted Areas indicate the Impact Zones of the Geothermal Reservoir.

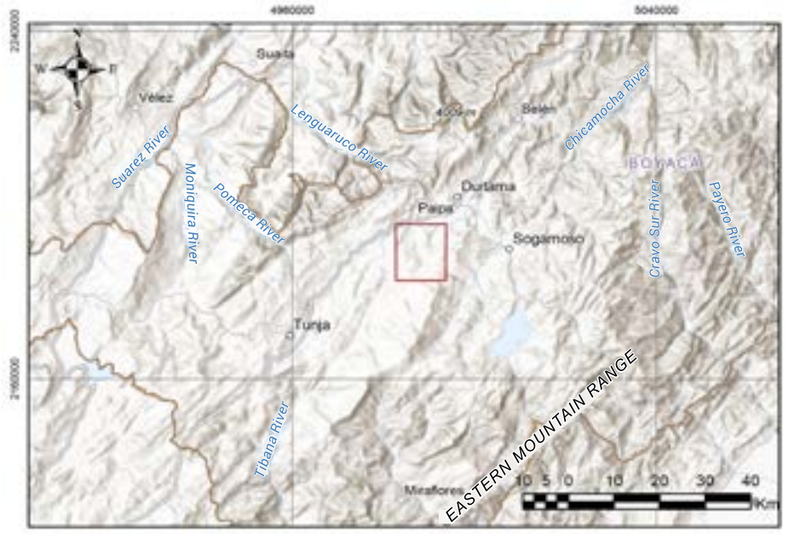

Figure 71. Location Map of the Area with Potential for CO_2 Storage in Geothermal Reservoirs in Paipa.

It is located to the south of the municipality of the same name, in the department of Boyacá. The 14 thermal springs are grouped into four main clusters:

- **Cluster 1:** Located to the north, it includes nine springs from the ITP-Lanceros sectors, with temperatures ranging from 21°C to 74°C.
- **Cluster 2:** Located in the La Playa sector, with temperatures ranging from 50°C to 76°C.
- **Cluster 3:** Comprised of two springs with temperatures of 21°C and 23°C.
- **Cluster 4:** Located in the Olitas stream, it includes one spring with a temperature of 23°C.

Geologically, the area is dominated by Cretaceous sedimentary formations including Tibasosa, Une, Conejo, Plaeners Los Pinos, Labor, and Tierna, as well as Cenozoic formations such as Guaduas, Bogotá, and Tilatá. Also present are volcanic rocks from the Paipa volcano, alluvial deposits, and a Quaternary hydrothermal breccia (Velandia, 2003; Cepeda and Pardo, 2004). The basement is composed of the Floresta Massif, sedimentary rocks from the Cuche, Floresta, and Tíbet formations, Paleozoic igneous intrusions, and Jurassic-Paleozoic igneous-metamorphic rocks.

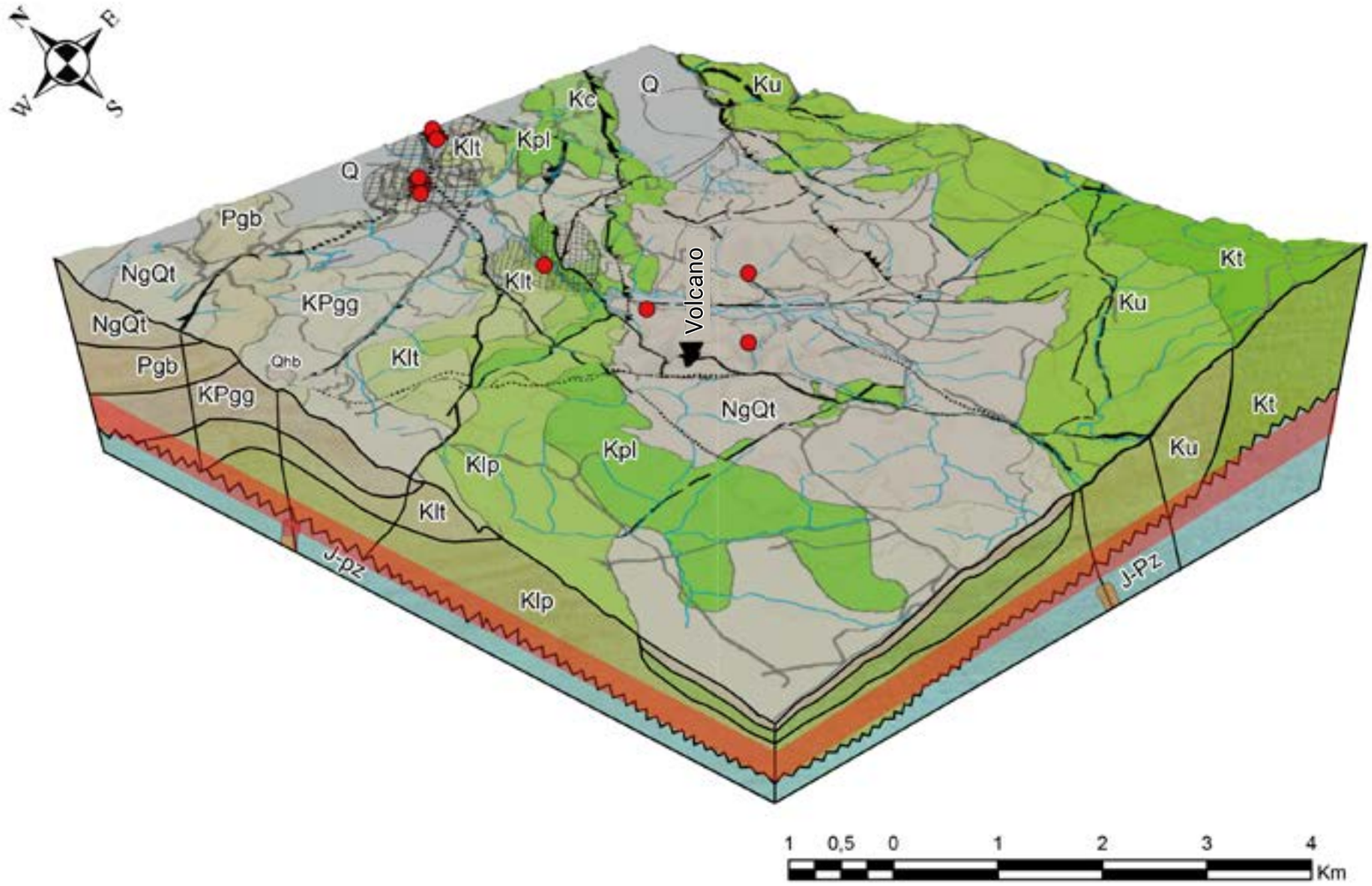

Figure 72. Geological Block Diagram of the Paipa Geothermal Area.

Potential heat sources include:

1. esidual heat from recent magmatism, with an approximate age of 1 million years (Ma).
2. Radiogenic heat associated with igneous intrusions.
3. Geothermal gradient, which increases the temperatures of infiltrations to depths of at least 2 km, reaching up to 76°C (Alfaro et al., 2017).

The potential reservoirs correspond to the Une, Tibasosa, Cuche, and Tíbet formations, as well as the sedimentary and igneous-metamorphic basement (Velandia and Cepeda, 2004). The recharge area is located to the south and southeast (Tibasosa Anticline), through outcrops of the Une Formation (Alfaro et al., 2017).

The seal of the system would consist of claystones and volcanic deposits covering much of the geothermal area.(Alfaro et al., 2017).

The calculation of injectable CO_2 considered the equation:

$GCO_2 = A*h*\Phi*\rho*E$

Where:

- A: Area of the reservoir.
- h: Thickness of the reservoir units.
- Φ: Effective porosity.
- ρ: Density of CO_2 at depth
- E: Storage efficiency factor.

To determine the area (A) of 7.3 km², the expected areas from Alfaro et al. (2020) were considered, summing clusters 1 and 2 and excluding clusters 3 and 4 due to their low temperatures.

Since a minimum depth of 800 m from the topographic surface is required, the profiles of the block diagram were analyzed. In these profiles, it was identified that the reservoir units of the sedimentary and metamorphic basement have a thickness (h) of 700 m until the contact with the intrusives, which are the source of heat (determined through geophysical and seismic studies).

The density (ρ) of CO_2 at 800 m depth was estimated to be approximately 750 kg/m³, according to CIEMAT (2006). Due to the nature of the basement, a secondary porosity (Φ) of 10% was considered.

The efficiency factor (E) for CO_2 storage was estimated according to the percentiles reported by Bachu (2008) for clastic reservoirs.

- P10: 1,86%.
- P50: 2,7%.
- P90: 6%.

With these parameters, the injectable CO_2 volume in the system was calculated as follows:

- P10: 7'128.450 tons of CO_2.
- P50: 10'347.750 tons of e CO_2.
- P90: 22'995.000 tons of CO_2.

6.4.3.3 Geothermal zones – San Diego

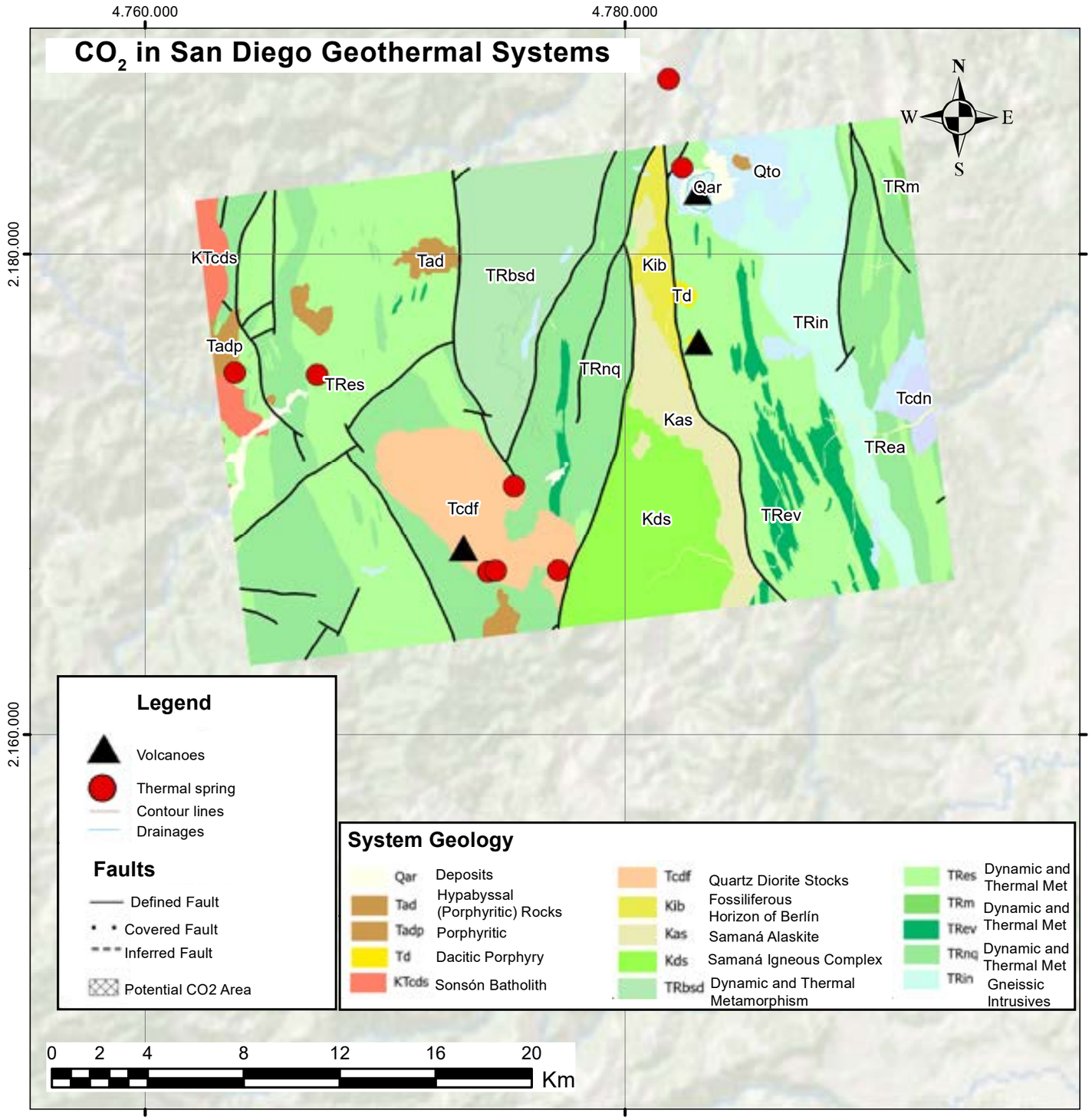

Figure 73. Geological Map of the San Diego Geothermal Area. Note. Red Dots Identify Hydrothermal Springs, and the Highlighted Areas Indicate the Impact Zones of the Geothermal Reservoir.

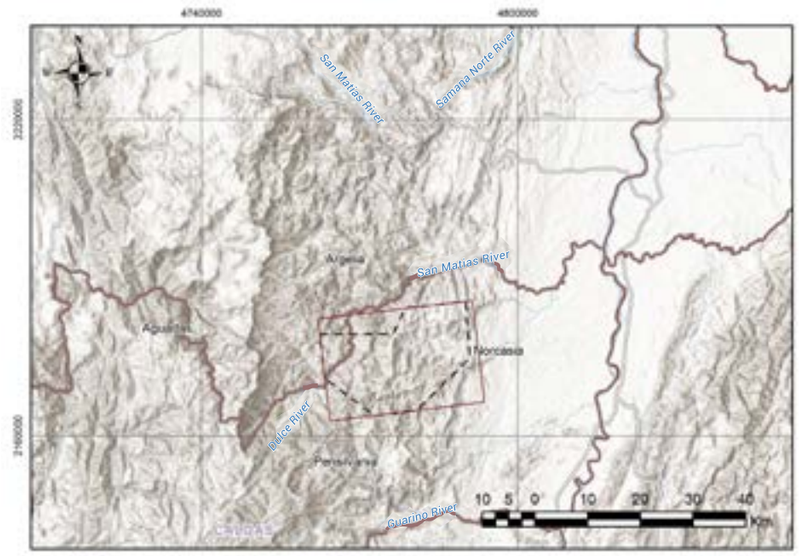

Figure 74. Location Map of the San Diego Geothermal Area.

The San Diego geothermal area, located between the municipalities of Samaná and Norcasia, in the north of Caldas and south of Antioquia, is known for its 15 thermal springs distributed across three main sectors:

1. **NE:** San Diego Maar.
2. **South:** El Escondido Volcano of Florencia.
3. **West:** Puente Linda Igneous Intrusion (or El Espíritu Santo).

This region has significant potential for CO_2 storage in its geothermal reservoirs. The reservoir impact areas are outlined on the maps, and the red points identify the hydrothermal springs.

These springs exhibit distinctive characteristics, such as neutral pH (6.1 to 6.7), high electrical conductivity (2000 to 12,500 µS/cm), and temperatures ranging from 32 to 44°C. According to Alfaro et al. (2020), each sector shows a specific chemical type of water:

- Sodium bicarbonate in the Maar de San Diego.
- Sodium chloride in the El Escondido Volcano.
- Sodium chloride-bicarbonate in Puente Linda.

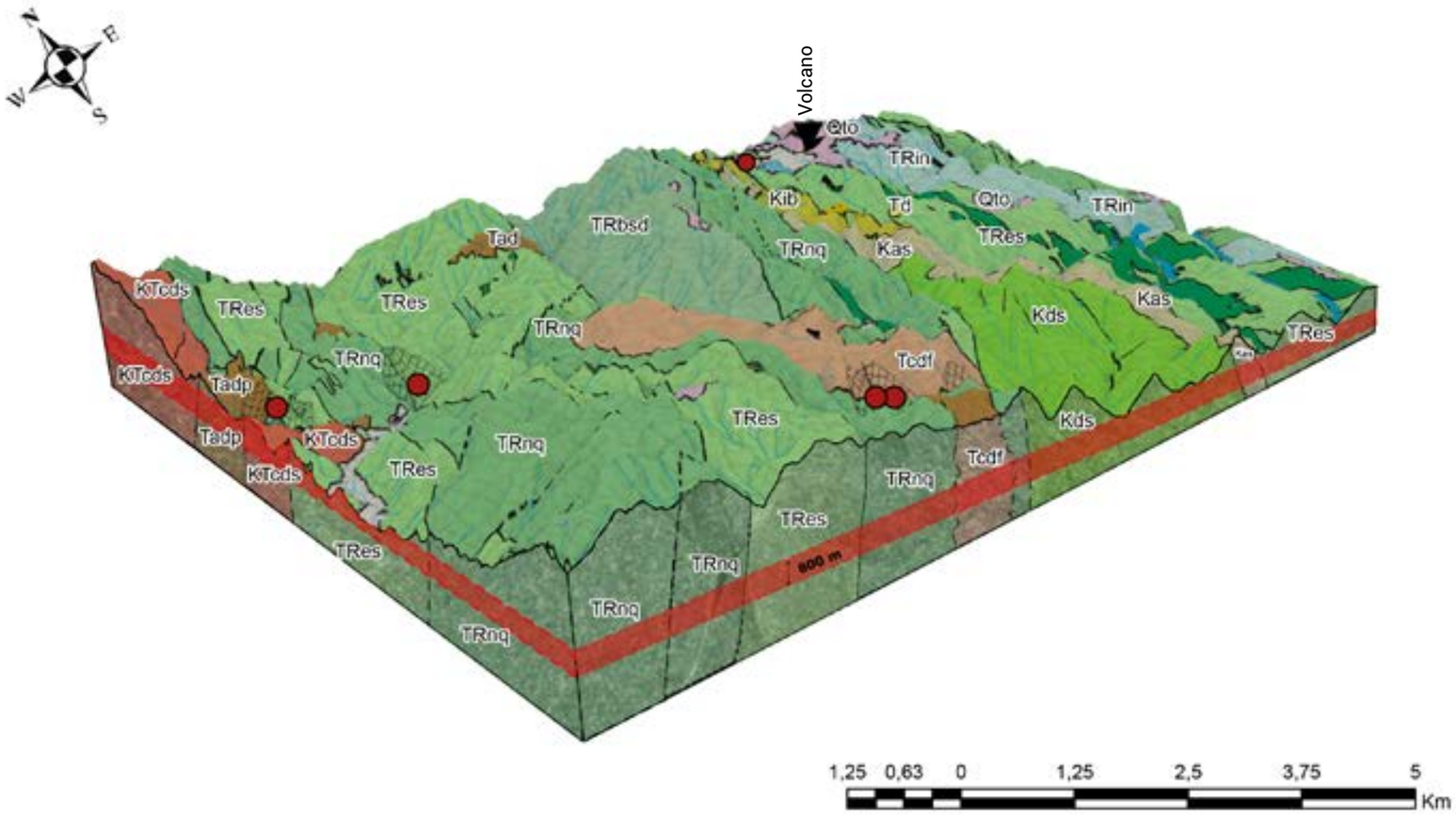

Figure 75. Geological Block Diagram of the San Diego Geothermal Area.

The geology of the area is dominated by the Cajamarca Complex (Paleozoic), which is cut by various geological units:

- Permian-Triassic: Néisic Intrusive.
- Jurassic: Sonsón Batholith.
- Mesozoic: Alaskite Formations and Samaná Complex.
- Cenozoic: Florencia Stock.

Additionally, Miocene-Pliocene andesitic porphyries, Quaternary alluvial and pyroclastic deposits, as well as Cretaceous Berlin Formation sedimentites, are present (Alfaro et al., 2020). The heat source is associated with the recent activity of the volcanoes and the intrusion of igneous bodies, including:

- El Escondido Volcano of Florencia: 153.7 ± 38.5 ka and 55 ± 23 ka.
- Maar de San Diego: 89 ± 4.4 ka (Ar-Ar dating).
- Puente Linda porphyry intrusion: 2.1 ± 1.9 Ma (U-Pb dating, according to Rueda and Rodríguez, 2016).

The proposed reservoirs correspond to the Sonsón Batholith, Florencia Stock, Samaná Complex, Gneissic Intrusive, and the Cajamarca Complex, due to fractures (Rueda and Rodríguez, 2016). Meteoric recharge occurs in Puente Linda and El Escondido, with a carbonate contribution from the Cajamarca Complex.

In addition, in Puente Linda, there is a mixture of chloride and sulfate waters (Rueda and Rodríguez, 2016).

The calculation of injectable CO_2 considered the equation:

$GCO_2 = A * h * \Phi * \rho * E$

Where:

- A: Reservoir area.
- h: Thickness of the reservoir units.
- Φ: Effective porosity.
- ρ: CO_2 density at depth.
- E: Storage efficiency factor.

To determine the area (A) of 7.3 km², the expected areas from Alfaro et al. (2020) were considered, summing clusters 1 and 2 and excluding clusters 3 and 4 due to their low temperatures.

Since a minimum depth of 800 m from the topographic surface is required, the block diagram profiles were analyzed. These profiles identified that the reservoir units of the sedimentary and metamorphic basement have a thickness (h) of 700 m down to the contact with the intrusives, which are the heat source (determined through geophysical and seismic studies).

The density (ρ) of CO_2 at 800 m depth was estimated to be approximately 750 kg/m³, according to CIEMAT (2006). Due to the nature of the basement, a secondary porosity (Φ) of 10% was considered.

The efficiency factor (E) for CO_2 storage was estimated based on the percentiles reported by Bachu (2008) for clastic reservoirs:

- P10: 1,86%.
- P50: 2,7%.
- P90: 6%.

With these parameters, the injectable CO_2 volume in the system was calculated as:

- P10: 7'128.450 toneladas de CO_2.
- P50: 10'347.750 toneladas de CO_2.
- P90: 22'995.000 toneladas de CO_2.

6.4.3.4 Geothermal zones – Nereidas

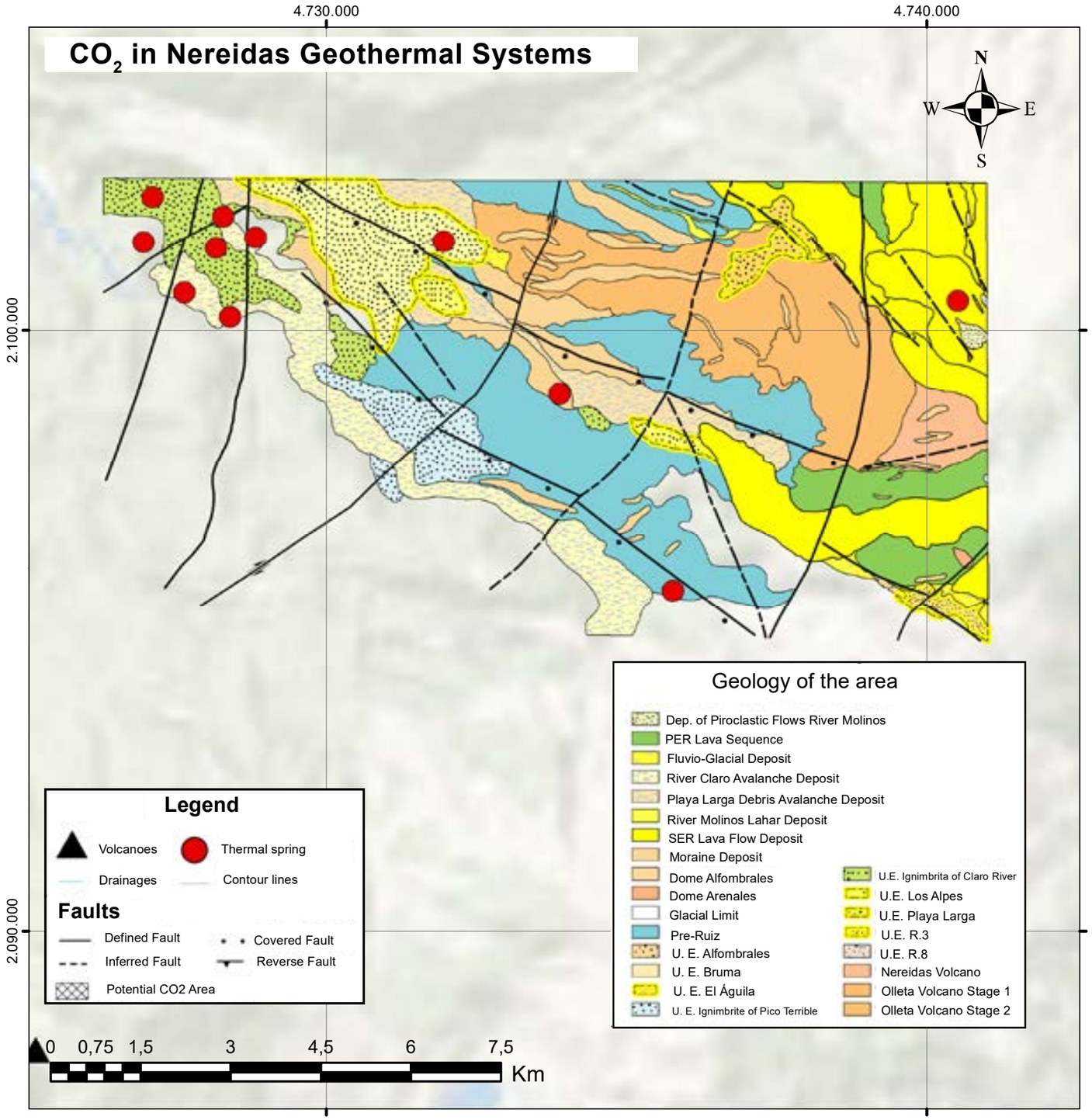

Figure 76. Geological Map of the Nereidas Geothermal Area.

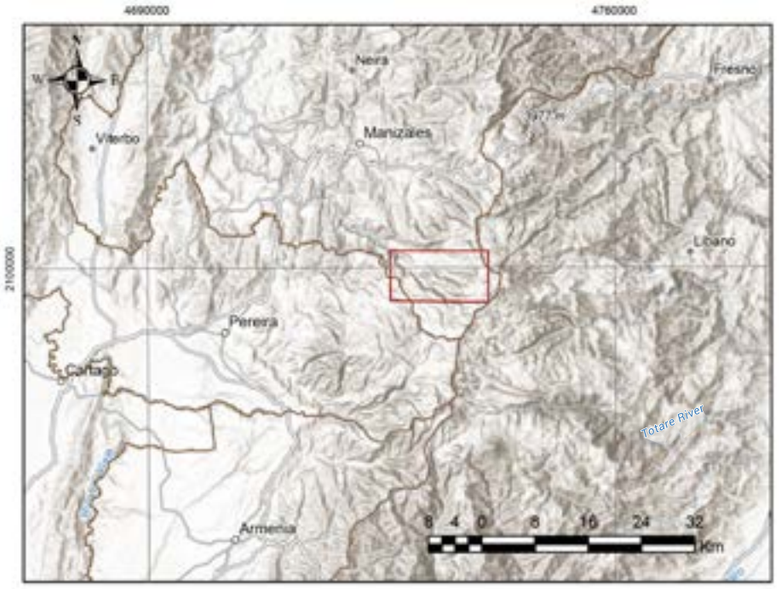

Figure 77. Location Map of the Area with Potential for CO_2 Storage in Geothermal Reservoirs in the Nereidas Area.

Located in the Central Mountain Range, south of the department of Caldas and northwest of the Nevado del Ruiz Volcano (VNR), this geothermal system is situated near the municipalities of Manizales and Villamaría. It is characterized by the presence of 14 thermal springs grouped into five clusters, located to the west of the VNR in the basins of the Claro and Gualí rivers, as well as in the Las Nereidas and Hojas Anchas streams, within the department of Caldas. The chemical composition of the thermal waters varies between the clusters:

- Cluster 1: Sodium chloride water.
- Cluster 2: Magnesium-calcium bicarbonate water.
- Cluster 3: Calcium sulfate water.
- Cluster 4: Calcium-sodium bicarbonate water.
- Cluster 5: Sodium sulfate water.

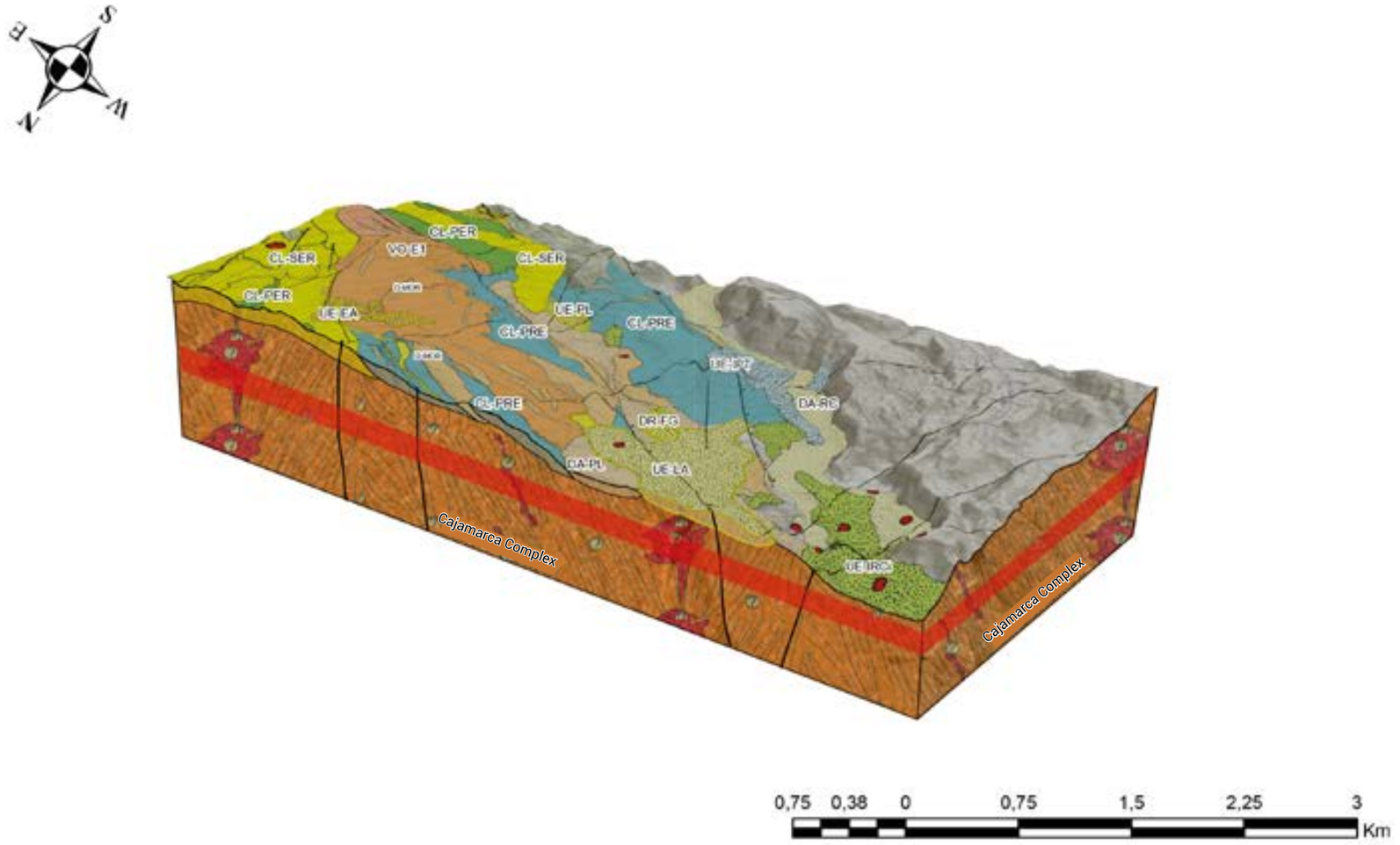

Figure 78. Geological Block Diagram of the Nereidas Geothermal Area.

The springs exhibit a pH range between 2.7 and 8.1, electrical conductivity ranging from 139 to 4900 µS/cm, and discharge temperatures between 27 and 95°C. These springs emerge in schists of the Cajamarca Complex and in overlying Quaternary volcanic deposits, associated with geological faults in the area (Alfaro et al., 2020).

Geologically, the system includes an overlap of lava flows from the Nereidas Volcano, associated with the Pre-Ruíz Eruptive Period, the First and Second Eruptive Periods of the VNR, as well as the La Olleta Volcano. Volcanic matrix-supported deposits are also identified. The predominant lavas are andesitic to dacitic (Martínez et al., 2014).

The heat source of the system is related to large volumes of magma undergoing cooling beneath the geothermal area. This is associated with a deposit of magmatic gases originating from the intrusions responsible for the volcanic edifice of the VNR (Giggenbach et al., 1990; Herrera, 2021).

According to the 1:25,000 scale geological mapping by Martínez et al. (2014), the possible reservoirs include the andesites from the lavas of the First Eruptive Period of Ruíz or the Pre-Ruíz period, as well as the metamorphic rocks of the Cajamarca Complex (Alfaro et al., 2020). Additionally, it is estimated that the cap rock is located at shallow depths in the subsurface (Giggenbach et al., 1990).

The calculation of injectable CO_2 was carried out using the following equation:

$$GCO_2 = A * h * \Phi * \rho * E$$

The magnetotelluric model of Herrera (2021) confirmed the presence of magma bodies cooling at both shallow and greater depths within the system. By projecting the five clusters of thermal springs onto the MT profiles P1 and P3, it was determined that only cluster 5 reaches a depth of 1,050 m from the surface to the heat source. This cluster meets the minimum 800 m depth requirement, leaving a 250 m thickness (h) available for CO_2 injection. The other clusters do not meet this requirement, as their heat sources are too close to the surface.

According to Alfaro et al. (2020), the expected area (A) for cluster 5 was calculated at 2 km². The density (ρ) of CO_2 at 800 m depth is estimated at 750 kg/m³, according to CIEMAT (2006). Due to the characteristics of the basement, a secondary porosity (Φ) of 10% was considered. Additionally, the CO_2 storage efficiency factor (E) was applied according to the percentiles defined by Bachu (2008) for clastic reservoirs.

- P10 = 1,86%
- P50 = 2,7%
- P90 = 6%

The calculation of the injectable CO_2 volume in this system yielded the following results:

- P10: 697.500 tons of CO_2
- P50: 1'012.500 tons of CO_2
- P90: 2'250.000 tons of CO_2

7. ECONOMIC ESTIMATION OF CO_2 IN COLOMBIA

7.1 Colombia

In the economic analysis for the Colombian territory, nine key clusters were identified to advance the cost estimation related to CO_2 capture, transport, and storage. These clusters were selected considering the specific conditions of emissions, transport, and storage, as well as social costs and the mitigation and adaptation policies led by the Ministry of Environment.

Terrestrial 1 scenarios

Five terrestrial scenarios were defined, where the selected emission sources are common for all cases. The identified sources were determined from the conclusions of Activity 1, selecting the industrial clusters of Medellín and Cartagena as the main sources.

Cost estimation for capture

For the cost estimation associated with CO_2 capture, the following processes and values are considered:

1. **Initial CO2 capture:** 15 USD per-ton of CO_2.
2. **CO_2 purification:** 25 USD per-ton of CO_2.
3. **Compression of CO_2 to supercritical state:** 15 USD per-ton of CO_2, optimizing its transport.

Transport systeme

The selected mode of transport is the CO_2 pipeline, specifically designed for the transport of CO_2. In all scenarios, whether using existing networks or building dedicated pipelines, the connection between the emission sources and the storage areas is ensured. According to the reviewed literature, the estimated cost for transportation via pipeline is:

- 4 USD per-ton of CO_2 for every 250 km of distance.
- For greater distances, the cost increases proportionally with the increase in kilometers.

The proposed networks to connect the emission sources with the storage areas are represented in the corresponding (figura 79).

Storage proposals

In the case of Geological Storage, two main technical alternatives were evaluated:

1. Overexploited oil or gas reservoirs

- This alternative considers only the minimum injection costs, as the wells required for the operation have already been drilled.
- Costs associated with well remediation are not included.
- The estimated cost for storage in this option is 2 USD per-ton of CO_2.

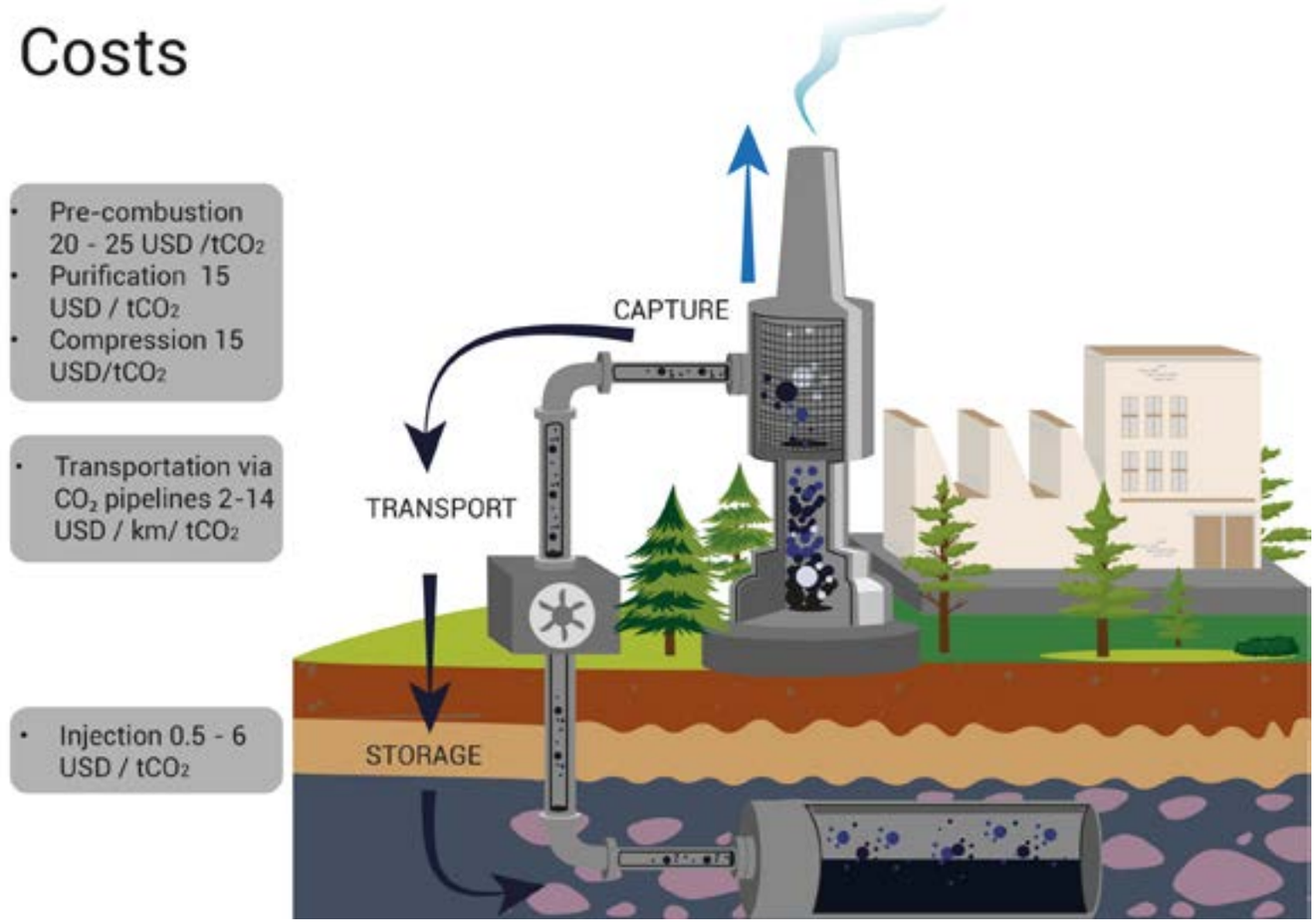

Figure 79. Cost Diagram of CCS Processes in Colombia.

2. Geological storage in basalts and coal beds

- The number of wells required for injecting the available annual CO_2 volume was calculated using the following equation:

$$\text{Number of Wells} = \frac{\text{source } CO_2(\text{ton/year})}{365(\text{days}) \times 50(\text{ton/days}) \times 5(\text{KPSCD/wells})}$$

The estimated cost for the construction of each well and the injection process for one year is 1.5 million USD per well.

The cost of each storage (escSw) *io will vary depending on:

- The amount of CO_2 available annually for each source.
- The type of storage.
- The required transportation distance.

7.1.1 Scenario 1 - caribbean coast to basalt storage

In this scenario, total emissions equivalent to 5,328,430 tons of CO_2 per year are considered, originating from the cities of Santa Marta, Barranquilla, and Cartagena. The cost of the capture, purification, and compression process, directly linked to the emission volume, has been estimated at approximately USD $290 million, as detailed in table 3.

Currently, there is no CO_2 pipeline connecting the emission sources to the injection area, located in basalt formations near Montelíbano in the Córdoba department. Therefore, the construction of this infrastructure would be necessary. The estimated distance for transportation via pipeline is 164 km, with a projected cost of USD $21.3 million.

The selected storage area corresponds to basalt formations identified within the polygon indicated on the map. This zone lacks injection infrastructure. Given the available CO_2 volume, 58 wells are estimated to be required for injection. The associated cost for drilling and installation is calculated at approximately USD $111 million.

For this scenario, the total estimated cost amounts to USD $420 million.

PROCESS	CLUSTER COAST TO BASALTS
CO_2 SOURCE (Mton/y)	5.328.430
CAPTURE (USD$)	79.926.453
PURIFICATION (USD$)	133.210.755
COMPRESSION (USD$)	9.926.453
LONGITUDE (m)	164.091
TRANSPORT (USD$)	21.313.721
STORAGE (USD$)	23.977.936
NEW WELLS	58
COST WELLS (USD$)	87.590.633
STORAGE O&G (USD$)	10.656.860

Table 3. Summary Table of Costs for Capture, Transport, and Injection in Scenario 1.

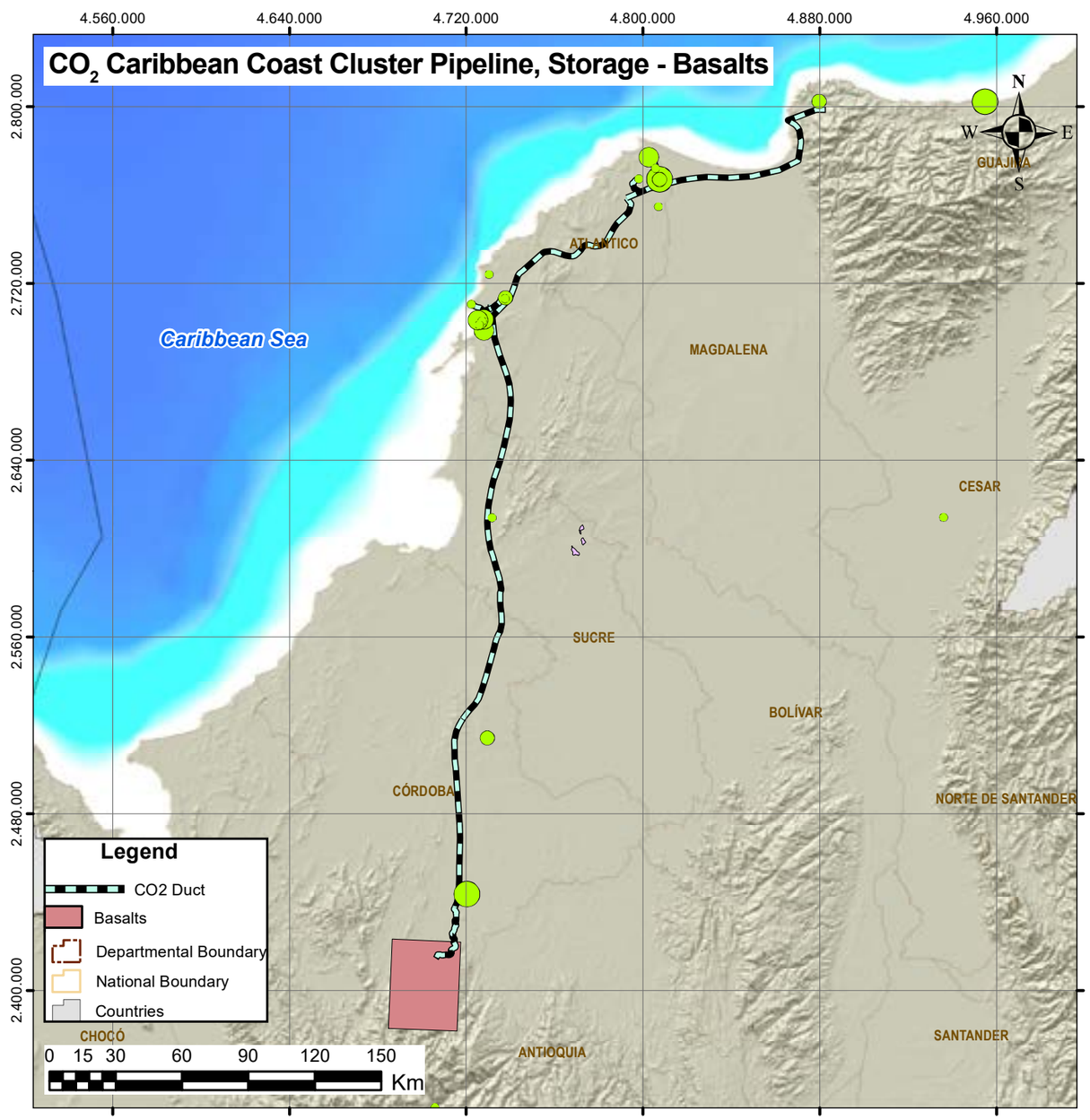

Figure 80. Co_2 Transportation Map, Cluster Caribbean Coast Pipeline, Storage - Basalt.

7.1.2. Scenario 2: caribbean coast to coal bed storage

In this scenario, a total emission of 6,245,420 tons of CO_2 per year is considered, originating from the cities of Santa Marta, Barranquilla, and Cartagena. The cost of the capture, purification, and compression process, directly linked to the emission volume, has been calculated at approximately USD $343 million, as detailed in Table 4.

Currently, there is no pipeline connecting the emission sources to the injection area located in the coal beds near Fonseca, La Guajira. Therefore, it would be necessary to construct this infrastructure. The estimated transport distance via pipeline is 736 km, with a projected cost of USD $73.6 million.

The selected storage area corresponds to coal beds identified within the polygon highlighted on the map. This area lacks injection infrastructure. Given the available CO_2 volume, it is estimated that 68 wells will need to be drilled. The cost associated with well drilling and injection infrastructure is approximately USD $102.6 million.

For this scenario, the total estimated cost amounts to USD $543 million.

PROCESS	CLUSTER COAST TO BASALTS
CO_2 SOURCE (Mton/y)	6.245.420
CAPTURE (USD$)	93.681.300
PURIFICATION (USD$)	156.135.500
COMPRESSION (USD$)	93.681.300
LONGITUDE (m)	736.591
TRANSPORT (USD$)	73.605.123
STORAGE (USD$)	28.104.390
NEW WELLS	68
COST WELLS (USD$)	102.664.438
STORAGE O&G (USD$)	12.490.840

Table 4. Summary Table of Costs for Capture, Transport, and Injection in Scenario 2.

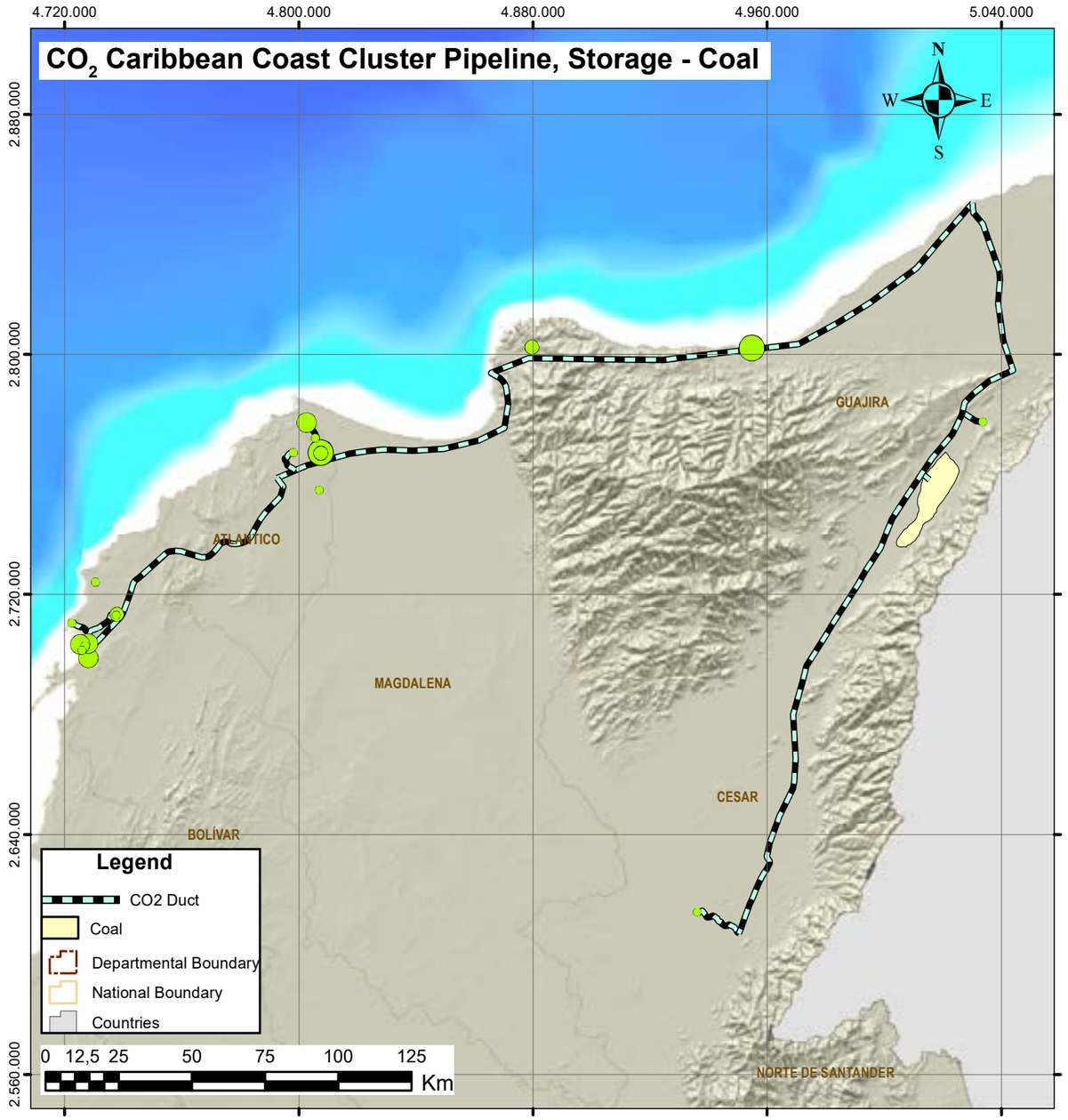

Figure 81. CO_2 Transportation Map, Clúster Caribbean Coast pipeline, Storage - Coal Seams, Fonseca, La Guajira.

7.1.3 Scenario 3: caribbean coast to storage in the MMV Basin

In this scenario, a total emission of 7,284,235 tons of CO_2 per year is considered, originating from the cities of Santa Marta, Barranquilla, and Cartagena. The cost of the capture, purification, and compression process, directly associated with the emission volume, has been calculated at approximately USD $400 million, as detailed in Table 5.

Currently, there is no pipeline connecting the emission sources to the injection area located in the oil reservoir basins near Barrancabermeja, Santander. Consequently, the construction of this infrastructure would be necessary. The estimated transportation distance via pipeline is 860 km, with a projected cost of USD $100 million.

The selected storage area corresponds to oil reservoir basins identified within the polygon shown on the map. This area lacks injection infrastructure. Given the available CO_2volume, it is estimated that existing wells in the oil fields will be used, with a total of 68 wells required. The cost of injection is estimated at approximately USD $14.6 million.

For this scenario, the total estimated cost amounts to USD $540 million. Additionally, this scenario offers economic advantages derived from enhanced oil recovery that can result from CO_2 injection.

PROCESO	CLUSTER COSTA A BASALTOS
CO_2 SOURCE (Mton/y)	7.284.235
CAPTURE (USD$)	109.263.522
PURIFICATION (USD$)	182.105.870
COMPRESSION (USD$)	109.263.522
LONGITUDE (m)	859.530
TRANSPORT (USD$)	100.176.334
STORAGE (USD$)	32.779.057
NEW WELLS	80
COST WELLS (USD$)	119.740.846
STORAGE O&G (USD$)	14.568.470

Table 5. Cost Summary for Capture, Transportation, and Injection in Scenario 3.

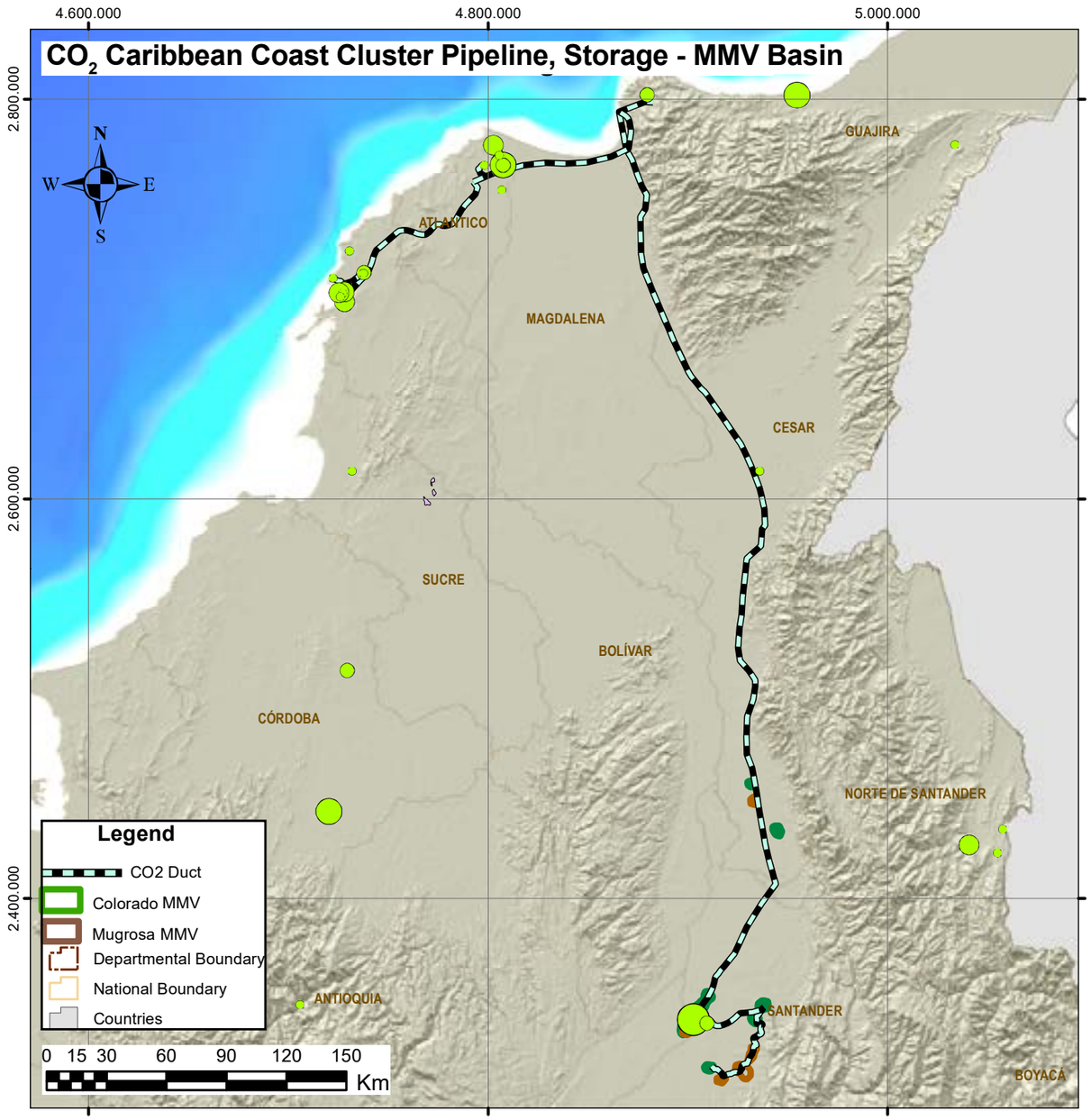

Figure 82. CO_2 Transportation Map, Clúster Costa Caribe Pipeline, Storage - Middle Magdalena Valley.

7.1.4 Scenario 4 - LMV gas fields for EOR

In this scenario, a total emission of 2,383,361 tons of CO_2 per year is considered, originating from the city of Cartagena. The cost of the capture, purification, and compression process, directly associated with the emission volume, has been calculated at approximately USD $131 million, as detailed in Table 6.

Currently, there is no pipeline connecting the emission sources to the injection area located in the Lower Magdalena Valley gas fields, in the Sucre department. Therefore, the construction of this infrastructure would be required. The estimated transportation distance via pipeline is 194 km, with a projected cost of USD $9.5 million.

The selected storage area corresponds to the Lower Magdalena Valley gas fields, identified within the polygon shown on the map. This area lacks injection infrastructure. Given the available CO_2 volume, it is estimated that 26 wells will need to be drilled. The cost associated with injection is estimated at approximately USD $4.7 million.

For this scenario, the total estimated cost amounts to USD $154 million. Additionally, this scenario offers economic advantages derived from enhanced gas recovery that could result from CO_2 injection.

PROCESS	CLUSTER COAST TO BASALTS
CO_2 SOURCE (Mton/y)	2.383.361
CAPTURE (USD$)	35.750.421
PURIFICATION (USD$)	59.584.035
COMPRESSION (USD$)	35.750.421
LONGITUDE (m)	194.255
TRANSPORT (USD$)	9.533.446
STORAGE (USD$)	10.725.126
NEW WELLS	26
STORAGE O&G (USD$)	4.766.723

Table 6. Cost Summary for Capture, Transportation, and Injection in Scenario 4.

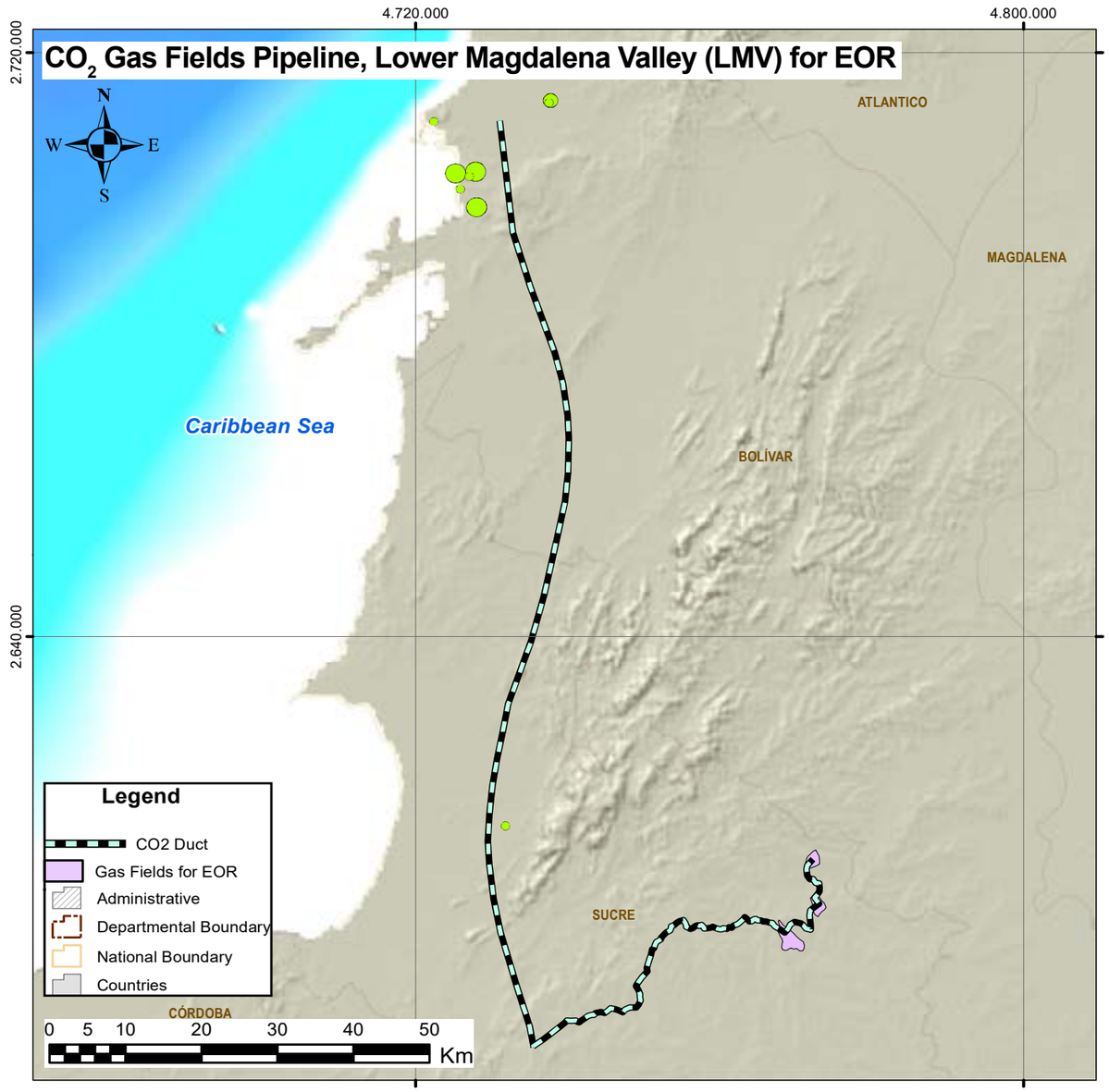

Figure 83. CO_2 Reficar Pipeline, Gas Fields, LMV for EOR.

7.1.5 Scenario 5 - Antioquia to coal beds storage

In this scenario, total emissions equivalent to 2,395,302 tons of CO_2 per year from the area near the city of Medellín are considered. The cost of the capture, purification, and compression process, directly related to the emission volume, has been calculated, as detailed in Table 7, at approximately USD $132 million.

Currently, there is no CO_2 pipeline connecting the emission sources to the injection area located in coal beds near Cimitarra, in the department of Santander. Therefore, the construction of such infrastructure would be necessary. The estimated distance for transportation via the CO_2 pipeline is 361 km, with a projected cost of USD $13.8 million.

The selected storage area corresponds to coal beds near Cimitarra, identified within the polygon shown on the map. This zone lacks injection infrastructure. Given the available CO_2 volume, it is estimated that 26 wells will need to be drilled. The associated cost for well drilling and injection is calculated at approximately USD $44 million.

For this scenario, the total estimated cost amounts to USD $198 million.

PROCESS	CLUSTER COAST TO BASALTS
CO_2 SOURCE (Mton/y)	2.395.302
CAPTURE (USD$)	35.929.524
PURIFICATION (USD$)	59.882.540
COMPRESSION (USD$)	35.929.524
LONGITUDE (m)	360.800
TRANSPORT (USD$)	13.827.597
STORAGE (USD$)	10.778.857
NEW WELLS	26
COST WELLS (USD$)	39.374.821
STORAGE O&G (USD$)	4.790.603

Table 7. Cost Summary for Capture, Transportation, and Injection in Scenario 5.

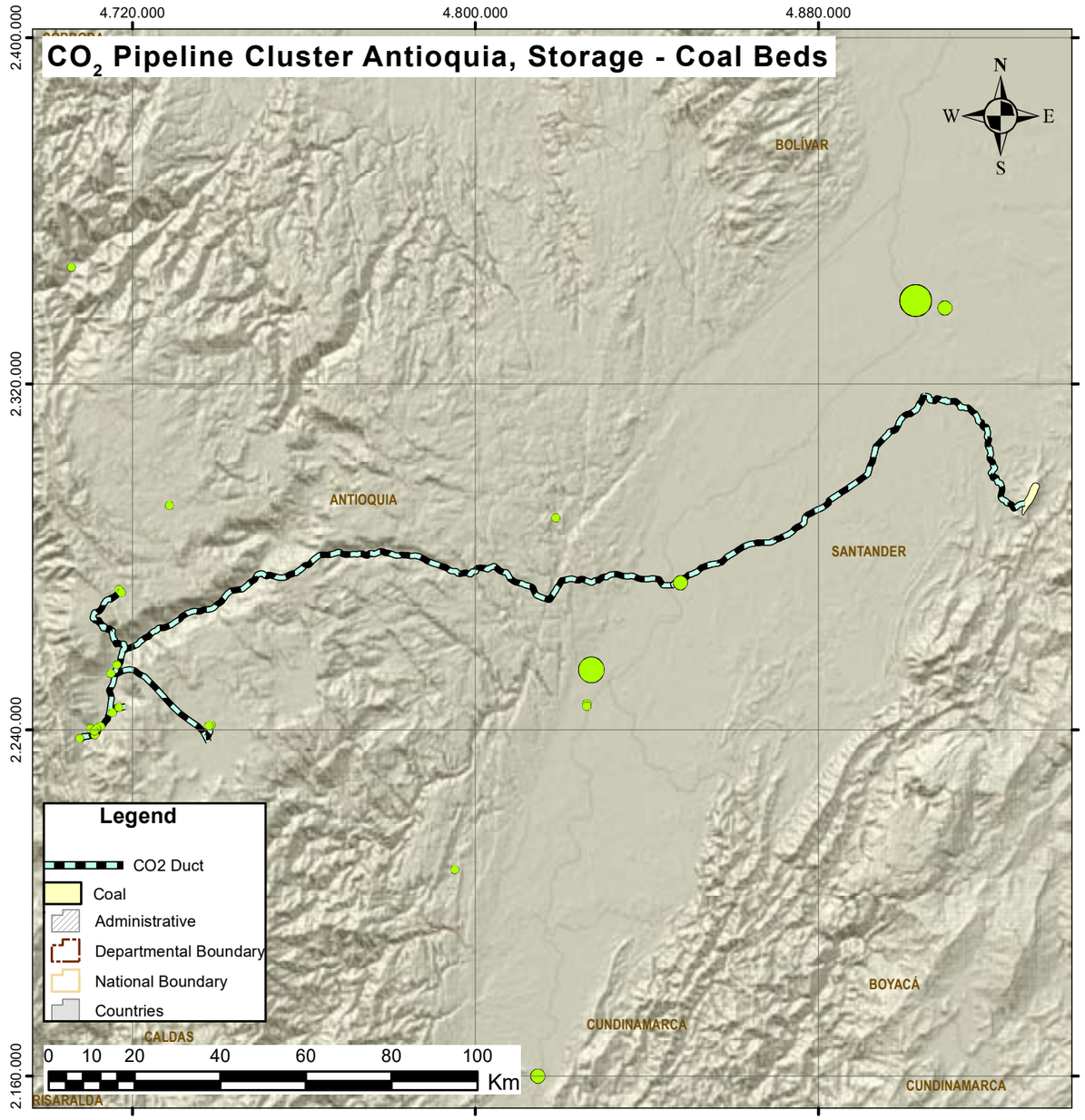

Figure 84. CO_2 Antioquia Cluster Pipeline, Coal Seams.

7.1.6 Scenario 6 – Antioquia to MMV basin storage

In this scenario, total emissions equivalent to 6,313,782 tons of CO_2 per year from the area near the city of Medellín are considered. The cost of the capture, purification, and compression process, directly related to the emission volume, has been calculated, as detailed in Table 8, at approximately USD $347 million.

Currently, there is no CO_2 pipeline connecting the emission sources to the injection area located in oil reservoirs near Barrancabermeja, in the department of Santander. Therefore, the construction of such infrastructure would be necessary. The estimated distance for transportation via the CO_2 pipeline is 736 km, with a projected cost of USD $73.6 million.

The selected storage area corresponds to oil reservoirs identified within the polygon shown on the map. This zone lacks injection infrastructure. Given the available CO_2 volume, it is estimated that injections will need to be made into 69 existing wells. The associated cost for injection is calculated at approximately USD $12.6 million.

For this scenario, the total estimated cost amounts to USD $440 million.

PROCESS	CLUSTER COAST TO BASALTS
CO_2 SOURCE (Mton/y)	6.313.782
CAPTURE (USD$)	94.706.723
PURIFICATION (USD$)	157.844.538
COMPRESSION (USD$)	94.706.723
LONGITUD (m)	560.667
TRANSPORT (USD$)	56.638.863
STORAGE (USD$)	28.412.017
NEW WELLS	69
STORAGE O&G (USD$)	12.627.563

Table 8. Cost Summary for Capture, Transportation, and Injection in Scenario 6.

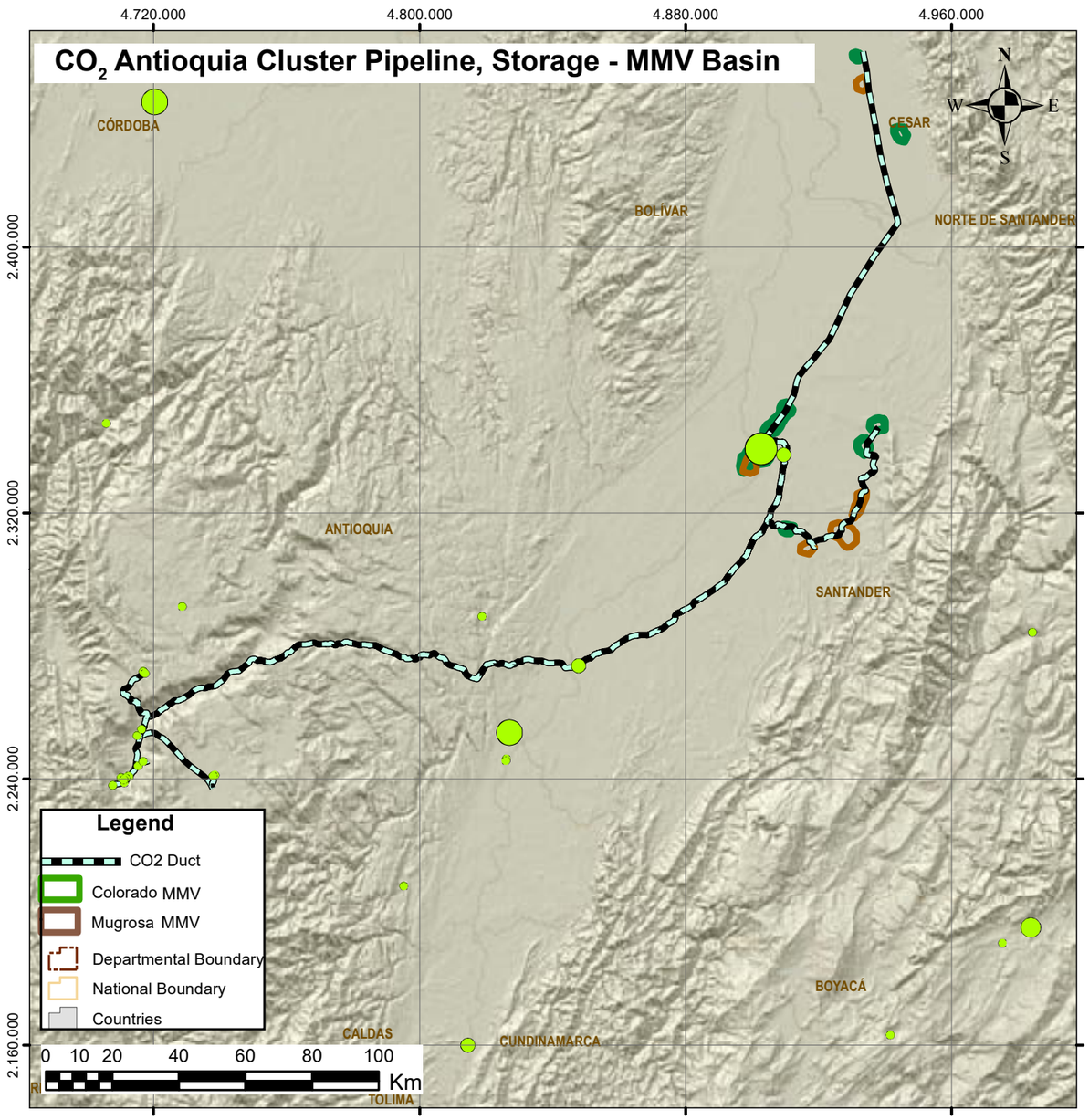

Figure 85. CO_2 Antioquia Cluster Pipeline, MMV Basin.

7.1.7 Scenario 7 - Barrancabermeja refinery to MMV basin

In this scenario, total emissions equivalent to 3,557,569 tons of CO_2 per year from the Barrancabermeja Refinery are considered. The cost of the capture, purification, and compression process, directly related to the emission volume, has been calculated, as detailed in Table 9, at approximately USD $196 million.

Currently, there is no CO_2 pipeline connecting the emission sources to the injection area located in oil reservoirs near Barrancabermeja, in the department of Santander. Therefore, the construction of such infrastructure would be necessary. The estimated distance for transportation via the CO_2 pipeline is 19 km, with a projected cost of USD $14.2 million.

The selected storage area corresponds to oil reservoirs identified within the polygon shown on the map. This zone lacks injection infrastructure. Given the available CO_2 volume, it is estimated that injections will need to be made into 39 existing wells. The associated cost for injection is calculated at approximately USD $7.2 million.

For this scenario, the total estimated cost amounts to USD $230 million. It is important to note that the pipeline connecting oil fields to the department of Cesar was not analyzed in this study.

Additionally, this scenario offers economic advantages derived from enhanced oil recovery that could result from CO_2 injection.

PROCESS	CLUSTER COAST TO BASALTS
CO_2 SOURCE(Mton/y)	3.557.569
CAPTURE (USD$)	53.363.534
PURIFICATION (USD$)	88.939.223
COMPRESSION (USD$)	53.363.534
LONGITUDE (m)	19.404
TRANSPORT (USD$)	14.230.276
STORAGE (USD$)	16.009.060
NEW WELLS	39
STORAGE O&G (USD$)	7.115.138

Table 9. Cost Summary for Capture, Transportation, and Injection in Scenario 7.

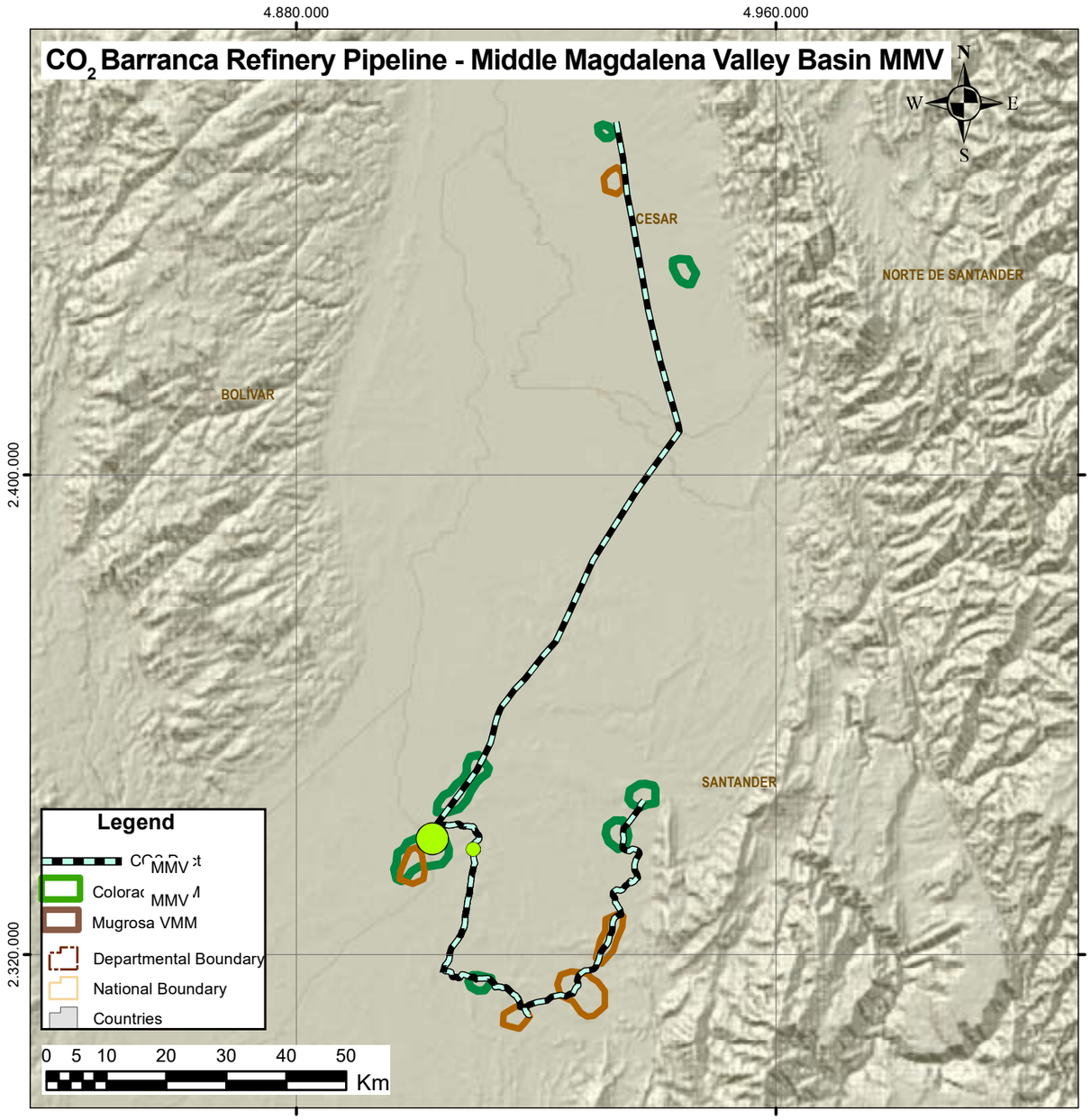

Figure 86. CO_2 Pipeline Barranca Refinery - Basin.

7.1.8 Scenario 8 - Antioquia to geothermal storage

In this scenario, total emissions equivalent to 2,000,000 tons of CO_2 per year from the area near the city of Medellín are considered. The cost of the capture, purification, and compression process, directly related to the emission volume, has been calculated, as detailed in Table 10, at approximately USD $110 million.

Currently, there is no CO_2 pipeline connecting the emission sources to the injection area located in geothermal reservoirs near the municipality of Argelia, in the department of Antioquia. Therefore, the construction of such infrastructure would be necessary. The estimated distance for transportation via the CO_2 pipeline is 162 km, with a projected cost of USD $8 million.

The selected storage area corresponds to geothermal reservoirs identified within the polygon shown on the map. This zone lacks injection infrastructure. Given the available CO_2 volume, it is estimated that 22 wells will need to be drilled. The associated cost for drilling and injection is calculated at approximately USD $32.8 million.

For this scenario, the total estimated cost amounts to USD $158 million.

PROCESS	CLUSTER COAST TO BASALTS
CO_2 SOURCE (Mton/y)	2.000.000
CAPTURE (USD$)	30.000.000
PURIFICATION (USD$)	50.000.000
COMPRESSION (USD$)	30.000.000
LONGITUDE (m)	162.024
TRANSPORT (USD$)	8.000.000
STORAGE (USD$)	9.000.000
NEW WELLS	22
STORAGE O&G (USD$)	32.876.712

Table 10. Cost Summary for Capture, Transportation, and Injection in Scenario 8.

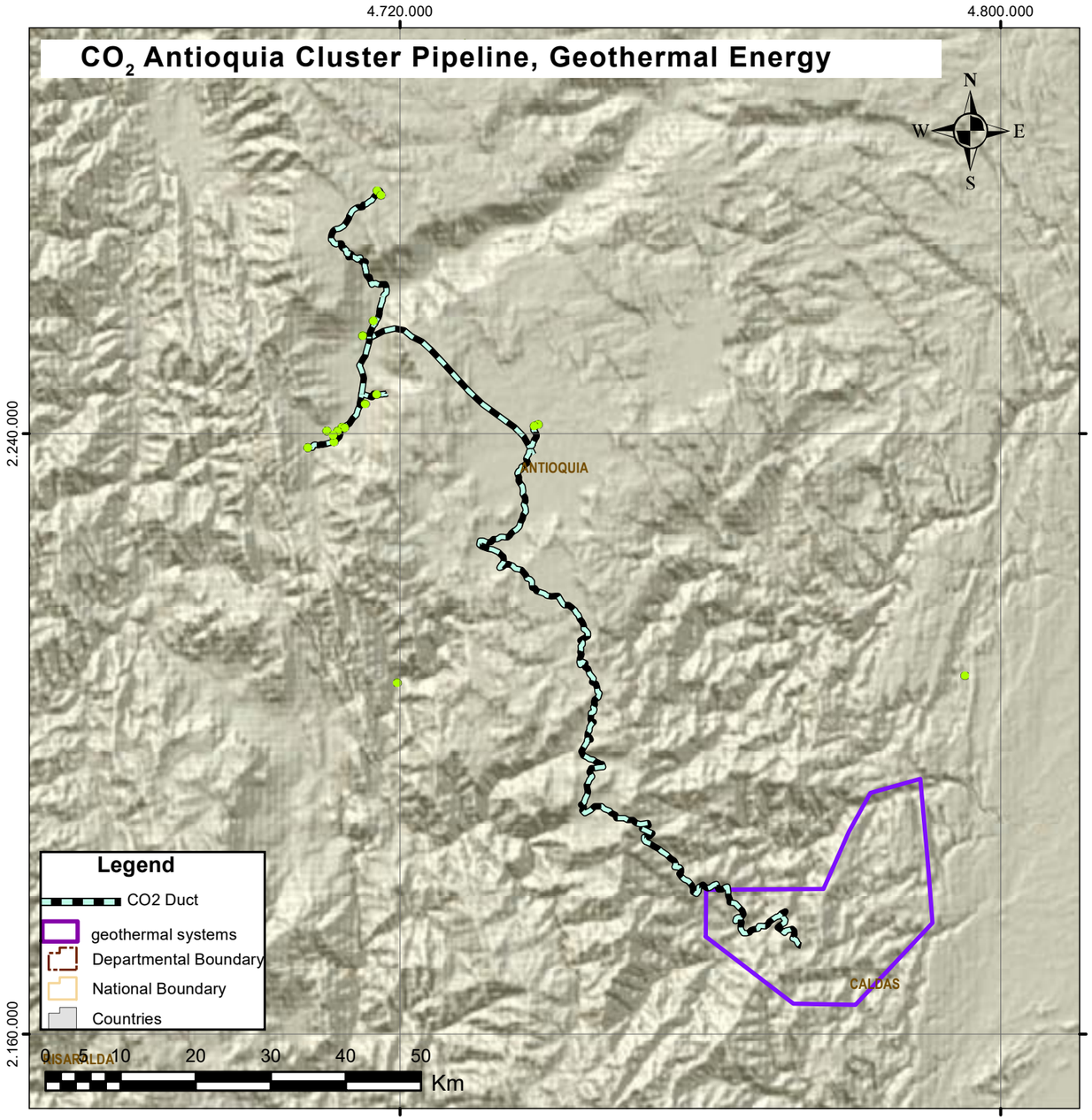

Figure 87. CO_2 Antioquia Cluster Pipeline, Geothermal Energy.

7.1.9 Scenario 9 - Antioquia to serpentinas storage

In this scenario, total emissions equivalent to 2,000,000 tons of CO_2 per year from the area near the city of Medellín are considered. The cost of the capture, purification, and compression process, directly related to the emission volume, has been calculated, as detailed in Table 11, at approximately USD $110 million.

Currently, there is no CO_2 pipeline connecting the emission sources to the injection area located in the Serpentinas reservoirs near Medellín, in the department of Antioquia. Therefore, the construction of such infrastructure would be necessary. The estimated distance for transportation via the CO_2 pipeline is 84 km, with a projected cost of USD $8 million.

The selected storage area corresponds to the Serpentinas reservoirs, marked within the polygon on the map. This zone lacks injection infrastructure. Given the available CO_2 pipeline connecting the emission sources to the injection area located in the Serpentina volume, it is estimated that 22 wells will need to be drilled. The associated cost for drilling and injection is calculated at approximately USD $32.8 million.

For this scenario, the total estimated cost amounts to USD $158 million.

PROCESS	CLUSTER COAST TO BASALTS
CO_2 SOURCE (Mton/y)	2.000.000
CAPTURE (USD$)	30.000.000
PURIFICATION (USD$)	50.000.000
COMPRESSION (USD$)	30.000.000
LONGITUDE (m)	162.024
TRANSPORT (USD$)	8.000.000
STORAGE (USD$)	9.000.000
NEW WELLS	22
STORAGE O&G (USD$)	32.876.712

Table 11. Cost Summary for Capture, Transportation, and Injection in Scenario 9.

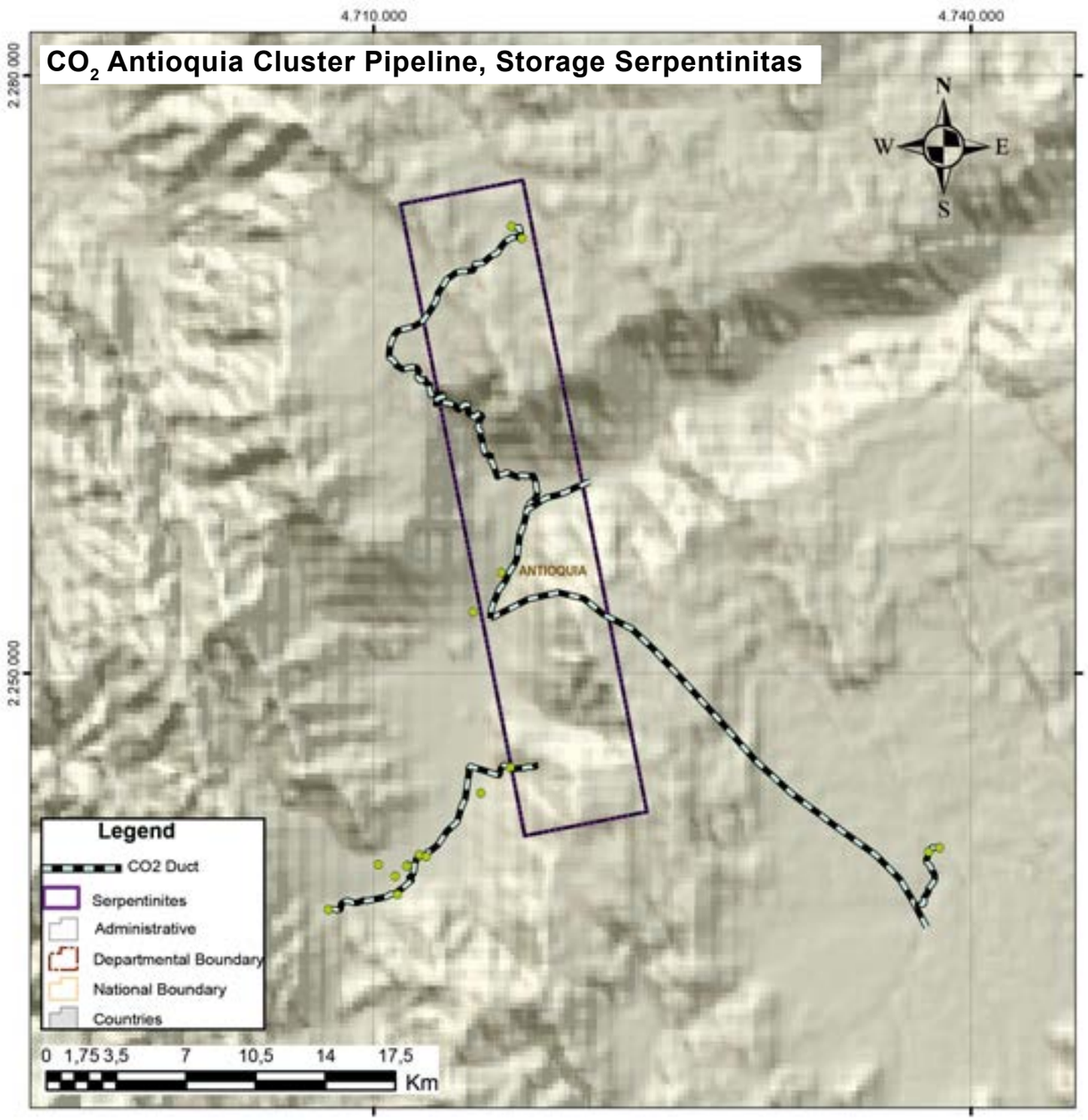

Figure 88. CO_2 Antioquia Cluster Pipeline, Geothermal Energy.

8. CONCLUSIONS

8. CONCLUSIONS

Worldwide, CO_2 CCS projects have experienced significant growth over the past decade. However, the amount of CO_2 captured still represents only a small fraction of global emissions, highlighting the need for broader and accelerated implementation of this technology. To date, 844 CCS projects have been identified in various stages of development. The main challenges and causes of failure in current projects are as follows:

1. **Economic Feasibility:** High operational and maintenance costs, combined with the volatility of oil prices that affect EOR revenues, can undermine the economic viability of projects.

2. **Public Acceptance:** Public opposition, driven by environmental concerns, may hinder the development of CO_2 CCS projects. Transparent communication and community engagement are essential to gaining public support and acceptance.

3. **Technical and Logistical Issues:** Technical failures, challenges related to geological characterization, and logistical obstacles—such as the risk of CO_2 leaks and the complexity of long-distance transportation—represent significant barriers. Effective risk management and the design of robust engineering solutions are crucial to overcoming these challenges (Ampomah, 2024).

The implementation of CCUS technologies in Colombia represents a promising strategy to mitigate GHG emissions. By capturing CO_2 generated from industrial and energy activities, these technologies not only reduce the amount of carbon released into the atmosphere but also allow industries to continue operating while moving toward a more sustainable future. This approach is particularly relevant in a country like Colombia, where key sectors such as mining and energy production are essential to the economy and are in the process of transitioning to a cleaner energy matrix.

The integration of CCUS technologies within the national climate strategy can strengthen Colombia's international commitments in the fight against climate change. By investing in these solutions, the country would not only make progress toward its emission reduction goals but also fulfill global agreements and solidify its firm commitment to sustainable development.

According to the review of global projects, it is considered essential to evaluate several key factors to ensure the effectiveness of carbon capture and storage initiatives. One of the most important aspects is the proper selection of capture methods, such as pre-combustion, post-combustion, and oxy-combustion. This evaluation should be carried out comprehensively, allowing for an accurate estimation of emission volumes, the specific characteristics of emission points, and the particularities of local industries, such as mining, hydrocarbon processing, and energy generation.

Fotografía: Jair Ramírez Cadena

8. CONCLUSIONS

Regarding transportation, it is crucial to consider that Colombia has a diverse geography, including mountains, valleys, plains, and jungles. These features condition the transportation of captured CO_2 outside of established routes, such as pipelines, and significantly increase costs (for example, road transportation).

The Andes mountain range, which runs north to south through the country, presents logistical challenges due to its slopes and altitudes, raising both costs and the complexity of transportation routes. While the large rivers and valleys may facilitate river transport, their vulnerability to phenomena such as floods and erosion could affect the infrastructure needed for CO_2 transportation. The economic feasibility of CCS projects is impacted by these high transportation costs. Therefore, it is essential to design an efficient transportation strategy that minimizes distances and optimizes operational costs.

Despite the limitations arising from the transportation/cost relationship, CO_2 reservoirs are natural geological structures that must maintain specific characteristics over long geological periods. One of the key features of a suitable reservoir is its tectonic stability. Geological stability is crucial to ensure that CO_2 is stored safely, without the risk of leaks or contamination.

Successful CO_2 storage projects have shown that selecting suitable geological formations, such as deep saline aquifers or depleted oil and gas reservoirs, is essential to ensure the integrity of long-term storage. In contrast, projects that failed to advance into execution were typically found in areas with inadequate geological characteristics, compromising their viability. Therefore, prioritizing geologically stable areas with suitable formations can significantly increase the success rate of CO_2 storage projects, maximizing both environmental safety and the economic feasibility of these initiatives.

Given that the high costs associated with CO_2 capture and storage projects require a perspective that ensures investment recovery, it is recommended to consider implementing EOR projects.

These projects not only allow the captured CO_2 to be used to increase oil production but also provide a financial return that can make investment in storage infrastructure more attractive, thus contributing to the economic viability of CCUS initiatives.

Fotografía: Jair Ramírez Cadena

This underscores the need for the national government to establish clear policies and precise guidelines to address the country's specific needs in the development of CCUS projects. These policies should include a regulatory framework that defines clear requirements and standards for the implementation of CCUS technologies, as well as economic incentives to stimulate investment in these technologies.

Furthermore, it is essential to promote the creation of consortia that bring together government entities, private and public sector industries, and universities, with the goal of generating innovative solutions. This collaborative approach will facilitate research and development, while also contributing to the implementation of evaluation and monitoring procedures for environmental impacts, ensuring that negative effects on local ecosystems are minimized. It is also important to proactively address potential social concerns to guarantee public acceptance and support for these initiatives.

The training of professionals in the management of CO_2 capture and storage technologies, along with the involvement of local communities in the planning and execution of projects, are essential to ensure the success of CCUS initiatives. Moreover, it is crucial to align these policies with national strategies for climate change, sustainable development, and energy and industrial transition, ensuring that the projects effectively contribute to the country's long-term sustainability and emissions reduction goals.

Finally, establishing mechanisms for monitoring and reporting on the performance of the projects is vital to ensure their effectiveness in reducing emissions and maintaining the commitment to a more sustainable and climate-resilient future. Internationally, there are recognized best practices in industrial control processes and monitoring during the planning, development, and injection phases of CCUS projects. However, the phase after the industrial phase, particularly concerning the abandonment of infrastructure and the lack of environmental monitoring by companies, has been a recurring source of conflicts and social concerns.

Therefore, it is essential to implement measures to ensure continuous monitoring, transparency, and accountability in the long-term management of these projects, thus protecting both the environment and the affected communities.

Interdisciplinary collaboration between the private, academic, and government sectors is crucial for the success of CCUS projects in Colombia. This coordination will enable the exchange of knowledge, resources, and experiences, facilitating the development of innovative solutions adapted to the Colombian context. Within the framework of these collaborations, it is essential to conduct an exhaustive analysis of the economic feasibility of carbon capture, utilization, and storage technologies, considering the following key aspects:

- **Long-term benefits:** Assess how these technologies contribute to sustainability and the achievement of national and international climate goals.
- **Implementation and maintenance costs:** Establish a clear projection of the costs associated with the implementation of these technologies and their long-term maintenance, allowing for adequate financial planning.
- **Education and awareness:** Promote education and awareness of the population regarding the importance of CCUS technologies, ensuring social acceptance and support at the local and national levels.
- **Research and innovation:** Invest in research to identify technological gaps and opportunities, promoting the development of new solutions and improving existing ones.

At the national level, CCUS represents a strategic opportunity to integrate new technologies into Colombia's future energy landscape, aligning with sustainable development goals and contributing to a low-carbon economy.

Fotografía: Jair Ramírez Cadena

REFERENCES

Agencia Internacional de Energía. (Agosto de 2024). Emisiones de gases de efecto invernadero de la energía Aspectos destacados . Obtenido de Greenhouse Gas Emissions from Energy Highlights Free version of the IEA's annual time series of GHG Emissions from Energy: Emisiones de gases de efecto invernadero de la energía Aspectos destacados.

Agencia Nacional de Hidrocarburos (ANH). (2010). Geología del petróleo: Cuenca Cesar-Ranchería [Informe de la Ronda Colombia].

Agencia Nacional de Hidrocarburos (ANH). (2010). Geología del petróleo: Cuenca Sinú - San Jacinto - Valle Inferior del Magdalena. Ronda Colombia 2010.

Agencia Nacional de Hidrocarburos (ANH). (2011). Valoración del potencial exploratorio de CBM en la cuenca Carbonífera Amagá. Coordinado por G. Bedoya, F. Cediel, y C. Cáceres.

Agencia Nacional de Hidrocarburos (ANH). (2021). Anexo 18.1 y 18.2: Campos con producción comercial de gas y condiciones de calidad. Vicepresidencia de Operaciones, Regalías y Participaciones.

Agencia Nacional de Hidrocarburos (ANH). (2021, agosto 6). Ronda Colombia 2021: Cesar-Ranchería [Presentación PowerPoint].

Agencia Nacional de Hidrocarburos. (2012). Cuenca Catatumbo: Integración geológica de la digitalización y análisis de núcleos.

Alfaro, C., Matiz, J., Rueda, J., Rodríguez, G. F., González, C., Beltrán, M., Rodríguez, G. Z. y Malo, J. (2017). Actualización del modelo conceptual del área geotérmica de Paipa. Bogotá: Servicio Geológico Colombiano.

Alfaro, C. M., Rueda Gutiérrez, J. B., Casallas Y. P., Rodríguez G. Z., y Malo J. E. (2020)a. Estimación Preliminar del Potencial Geotérmico de Colombia. Bogotá: Servicio Geológico Colombiano.

Alfaro–Valero, C.M., Rueda–Gutiérrez, J.B., Matiz–León, J.C., Beltrán–Luque, M.A., Rodríguez–Rodríguez, G.F., Rodríguez–Ospina, G.Z., González–Idárraga, C.E. & Malo–Lázaro, J.E. 2020b. Paipa geothermal system, Boyacá: Review of exploration studies and conceptual model. In: Gómez, J. & Pinilla–Pachon, A.O. (editors), The Geology of Colombia, Volume 4 Quaternary. Servicio Geológico Colombiano, Publicaciones Geológicas Especiales 38, p. 161–196. Bogotá. https://doi.org/10.32685/pub.esp.38.2019.04

Bachu, S. (2000). Sequestration of CO2 in geological media: criteria and approach for site selection in response to climate change. . Energy Conversion & Management, 953–970.

Barbero Blanco, L. (2012). Propuesta de secuestro de CO2 atmosférico mediante la carbonatación de serpentinitas. BARBOSA, C. G., 2003. Memoria explicativa Mapa Geológico del Departamento del Cauca. 221p. Cali.Bermúdez, José & Mejía, María & García, Gabriel & G., Gilberto & Barbosa Camacho, G. (2003). Mapa geológico del departamento del Cauca: Memoria explicativa. Instituto Colombiano de Geología y Minería, INGEOMINAS.

Boyd et al., 2017; Public perceptions of carbon capture and storage in Canada: Results of a national survey. International Journal of Greenhouse Gas Control
Volume 67, December 2017, Pages 1-9

Cepeda, H. y Pardo, N. (2004). Vulcanismo de Paipa. Bogotá: Ingeominas.

Cerpa, A. (2018). Caracterización del potencial geotérmico a partir de análisis geoquímicos de fuentes termales en el volcán Cerro Machin, Colombia. Universidad EIA, Trabajo de pregrado.

Cossio, U. (2002). Geología de las Planchas 127 Cupica, 128 Murrí, 143 Bahía Solano y 144 Río Tagachí. Departamentos del Chocó y Antioquia. INGEOMINAS, 101p. Bogotá.

INGEOMINAS (2002). GEOLOGÍA DE LA PLANCHA 112 BIS JURADÓ

Dusar y Verkaeren, 1992 Influence of geologic and economic parameters on the (E)CBM-development in the Campine Basin (Belgium) . Polish Geological Institute Special Papers, 7 (2002): 271–280Proceedings of the IV European Coal Conference

Dusseault et al., 2002. Sequestration of CO2 in Salt Caverns. Canadian international petroleum conference.PAPER 2002-237

Ennis-King, J., & Paterson, L. I. N. C. O. L. N. (2001, April). Reservoir engineering issues in the geological disposal of carbon dioxide. In Fifth international conference on greenhouse gas control technologies, Cairns (Vol. 1, pp. 290-295).

European Environment Agency. (10 de Junio de 2024). Industrial pollutant releases to air in Europe. Obtenido de Industrial pollutant releases to air in Europe: https://www.eea.europa.eu/en/analysis/indicators/industrial-pollutant-releases-to-air

Global Carbon Project. (2011-2021). Global Carbon Budget Archive. Obtenido de Global Carbon Budget Archive: https://www.globalcarbonproject.org/carbonbudget/archive.htm

Hefny et al., 2020 Synchrotron-based pore-network modeling of two-phase flow in Nubian Sandstone and implications for capillary trapping of carbon dioxide. International Journal of Greenhouse Gas Control, Volume 103, December 2020.

Herrera, J. (2021). Modelado magnetotelúrico de las áreas geotérmicas de Nereidas Botero Londoño y Nevado del Ruíz. Bogotá: Servicio Geológico Colombiano.

International Energy Agency. (15 de marzo de 2024). CCUS Projects Explorer. Obtenido de CCUS Projects Explorer: https://www.iea.org/data-and-statistics/data-tools/ccus-projects-explorer

IPCC. (2022). IPCC Sixth Assessment Report. Obtenido de IPCC Sixth Assessment Report: https://www.ipcc.ch/report/ar6/wg1/

IPCC. (2023). Intergovernmental Panel on Climate Change. Obtenido de AR6 Synthesis Report: https://www.ipcc.ch/report/ar6/syr/figures/summary-for-policymakers/figure-spm-7/

IPCC, 2005, Special Report on Carbon dioxide Capture and Storage, Final Draft.

ANH
AGENCIA NACIONAL DE **HIDROCARBUROS**

Uptc®
Universidad Pedagógica y Tecnológica de Colombia

HOME

CO_2 STORAGE ATLAS IN COLOMBIA